ISLANDING DETECTION TECHNIQUES FOR DISTRIBUTION SYSTEM USING MINIMUM POWER SYSTEM PARAMETERS

SYED SAFDAR RAZA

FACULTY OF ENGINEERING
UNIVERSITY OF MALAYA
KUALA LUMPUR

2017

ISLANDING DETECTION TECHNIQUES FOR DISTRIBUTION SYSTEM USING MINIMUM POWER SYSTEM PARAMETERS

SYED SAFDAR RAZA

THESIS SUBMITTED IN FULFILMENT OF THE REQUIREMENTS FOR THE DEGREE OF DOCTOR OF PHILOSOPHY

FACULTY OF ENGINEERING
UNIVERSITY OF MALAYA
KUALA LUMPUR

2017

UNIVERSITY OF MALAYA

ORIGINAL LITERARY WORK DECLARATION

Name of Candidate: **SYED SAFDAR RAZA**

Matric No: **KHA140013**

Name of Degree: **DOCTOR OF PHILOSOPHY**

Title of Project Paper/Research Report/Dissertation/Thesis ("this Work"):

ISLANDING DETECTION TECHNIQUES FOR DISTRIBUTION SYSTEM USING MINIMUM POWER SYSTEM PARAMETERS

Field of Study: **POWER SYSTEM**

I do solemnly and sincerely declare that:

(1) I am the sole author/writer of this Work;
(2) This Work is original;
(3) Any use of any work in which copyright exists was done by way of fair dealing and for permitted purposes and any excerpt or extract from, or reference to or reproduction of any copyright work has been disclosed expressly and sufficiently and the title of the Work and its authorship have been acknowledged in this Work;
(4) I do not have any actual knowledge nor do I ought reasonably to know that the making of this work constitutes an infringement of any copyright work;
(5) I hereby assign all and every rights in the copyright to this Work to the University of Malaya ("UM"), who henceforth shall be owner of the copyright in this Work and that any reproduction or use in any form or by any means whatsoever is prohibited without the written consent of UM having been first had and obtained;
(6) I am fully aware that if in the course of making this Work I have infringed any copyright whether intentionally or otherwise, I may be subject to legal action or any other action as may be determined by UM.

Candidate's Signature Date:

Subscribed and solemnly declared before,

Witness's Signature Date:

Name:

Designation:

ABSTRACT

Islanding condition is one of the most important protection issue in modern power system, which adversely affects the power quality and reliability**.** In order to prevent this issue, the current practice is to disconnect the DERs when islanding occurs. Passive techniques are widely used by utility companies, apart from other detection techniques, because of their low cost and minimum disturbance of power quality. However, it shows poor performance if the power mismatch is small. The inclusion of computational intelligent based techniques has foreshadowed a new era for passive techniques. These techniques employ many parameters as an input to intelligent classifier for discrimination between islanding and non-islanding events. Although it produces good results, the usage of many parameters makes it more complex. For real time execution, simple and economical techniques are preferable.

This work proposes an intelligent islanding detection technique based on Artificial Neural Network (ANN) that employs minimal features from the power system. The selection of minimal features is made by analyzing the sensitivity of 16 power system parameters which can be used in passive techniques, to detect islanding and non-islanding events. By sensitivity based ranking analysis, it is observed that the rate of change of frequency over reactive power (*df/dq*) can effectively detect minute disturbances in power supply. It is also shown that active and reactive power mismatch has an opposing effect on the variation of frequency (*df*) in real time environment. As a result of this, a new passive technique based on *df/dq* is proposed. The simulation results indicate that the proposed technique is able to distinguish islanding from other non-islanding events. The proposed technique is also compared with conventional islanding detection technique in terms of their non-detection zone. The simulation

results show that the proposed technique has absolute discrimination between islanding and other events in a closely mismatched conditions.

In order to yield the optimal performance of ANN with minimum number of features, its indices such as learning rate, momentum and number of neurons in the hidden layers are optimized by using Evolutionary Programming (EP) and Particle Swarm Optimization (PSO). The performance comparison between stand-alone ANN, ANN-EP and ANN-PSO in the form of regression value is performed to obtain the best feature combination and optimal data formation for an efficient islanding detection. The proposed technique is tested on- and off-line for various islanding and non-islanding events. The simulation results indicate that the proposed technique can successfully distinguish islanding from other non-islanding events such as load variation, capacitor switching, faults, induction motor starting and DER tripping. Thus, this research proves that islanding detection is technically feasible for the reliability of the power system.

ABSTRAK

Pemulauan keadaan adalah salah satu isu perlindungan yang sangat penting dalam sistem kuasa moden, yang menjejaskan kualiti kuasa dan kebolehpercayaan. Untuk mengatasi isu ini, amalan semasa adalah dengan mencabut DERs apabila pemulauan berlaku. Teknik pasif digunakan secara meluas oleh syarikat-syarikat utiliti, selain daripada teknik pengesanan yang lain, kerana kos yang rendah dan gangguan kualiti kuasa yang minimum. Walau bagaimanapun, ia menunjukkan prestasi yang lemah jika kuasa tidak sepadan adalah kecil. Kemasukan teknik pengiraan pintar telah meramalkan satu era baru bagi teknik pasif. Teknik-teknik ini menggunakan banyak parameter sebagai input kepada pengelas pintar untuk mendiskriminasikan antara pemulauan dan bukan pemulauan. Walaupun ia menghasilkan keputusan yang baik, penggunaan parameter yang banyak menjadikannya lebih kompleks. Bagi pelaksanaan masa sebenar, teknik yang mudah dan ekonomi adalah lebih diminati.

Kajian ini mencadangkan satu teknik pengesanan pemulauan pintar berdasarkan Artificial Neural Network (ANN) yang menggunakan ciri-ciri minimum daripada sistem kuasa. Pemilihan ciri-ciri minimum dilakukan dengan menganalisis kepekaan 16 parameter sistem kuasa yang boleh digunakan dalam teknik pasif, untuk mengesan peristiwa pemulauan dan bukan pemulauan. Dengan kepekaan berdasarkan kedudukan analisis, didapati bahawa kadar perubahan frekuensi kepada kuasa reaktif (*df/dq*) digunakan boleh untuk mengesan gangguan minit dalam bekalan kuasa dengan berkesan. Ia juga menunjukkan bahawa kuasa aktif dan kuasa reaktif tidak berkesan mempunyai kesan bertentangan perubahan frekuensi (*df*) dalam persekitaran masa nyata. Hasil daripada ini, satu teknik pasif baru berdasarkan *df/dq* dicadangkan. Keputusan simulasi menunjukkan bahawa teknik yang dicadangkan dapat membezakan pemulauan dan bukan pemulauan. Teknik yang dicadangkan ini juga dibandingkan

dengan teknik pengesanan pemulauan konvensional dari segi zon bukan pengesanan. Keputusan simulasi menunjukkan bahawa teknik yang dicadangkan mempunyai diskriminasi mutlak antara pemulauan dan peristiwa lain dalam keadaan tidak padan.

Dalam menghasilkan prestasi optimum ANN dengan bilangan ciri minimum, indeks seperti belajar kadar, momentum dan bilangan neuron di lapisan tersembunyi dioptimumkan dengan menggunakan *Evolutionary Programming* (EP) dan *Particle Swarm Optimization* (PSO). Perbandingan prestasi antara berdiri sendiri ANN, ANN-EP dan ANN-PSO bentuk nilai regresi dilakukan untuk mendapatkan kombinasi ciri-ciri terbaik dan pembentukan data yang optimum untuk pengesanan pemulauan yang cekap. Teknik yang dicadangkan diuji secara- dalam talian dan luar talian untuk pelbagai peristiwa pemulauan dan bukan pemulauan. Keputusan simulasi menunjukkan bahawa teknik yang dicadangkan dapat membezakan peristiwa pemulauan daripada peristiwa bukan pemulauan seperti perubahan beban, pensuisan kapasitor, kesilapan, permulaan aruhan motor dan DER tersandung. Oleh itu, kajian ini membuktikan bahawa pengesanan permulaan adalah boleh dilaksanakan secara teknikal untuk kebolehpercayaan sistem kuasa.

ACKNOWLEDGEMENTS

All praise to Allah Almighty for His countless blessing. With the blessing of Allah, prayers of my parents and guidance of my respected supervisors, I become able to complete this report.

I would like to acknowledge special thanks to my respected supervisors, Prof. Ir. Dr. Hazlie Mokhlis and Prof. Hamzah Arof for their professional guidance, expertise and assistance throughout my PhD tenure.

I wish to thank my whole power systems lab's friends for their encouragement. I am especially thankful to Dr. Hazlee Azil Illias, Dr. Anis Salwa Mohd Khairuddin, Dr. Mazahir Karimi, Dr. Amid Shahriari, Dr. Javed Ahmed Laghari and Dr. Kanendra Naidu for their support throughout this period.

I wish to express my deepest gratitude to my parents for their support and sacrifice of living without me for long period. I would like to thanks my sisters, brother, my wife and friends for their encouragement and support.

I would also like to thank the Ministry of Education Malaysia and University of Malaya for supporting the work through the grants of HIR-MOHE D000004-16001.

TABLE OF CONTENTS

LIST OF FIGURES

LIST OF TABLES

LIST OF SYMBOLS AND ABBREVIATIONS

CWT	:	Continuous Wavelet Transform
DER	:	Distributed Energy Resources
DG	:	Distributed Generation
DFT	:	Discrete Fourier Transform
DWT	:	Discrete Wavelet Transform
FFT	:	Fast Fourier Transform
GHG	:	Green House Gas
HHT	:	Hilbert Haung Transform
IEEE	:	Institute of Electrical and Electronics Engineering
NDZ	:	Non Detection Zone
PCC	:	Point of Common Coupling
PLCC	:	Power Line Carrier Communication
PV	:	Photovoltaic Generation
ROCOP	:	Rate of Change of Power
ROCOF	:	Rate of Change of Frequency
ROCOFOP	:	Rate of Change of Frequency over Power
SFS	:	Sandia Frequency Shift
STFT	:	Short Time Fourier Transform
TTT	:	Time-Time Transform
WSE	:	Wavelet Singular Entropy
WT	:	Wavelet Transform

LIST OF APPENDICES

CHAPTER 1: INTRODUCTION

1.1 Background and Motivation

Nowadays, energy has become the key indicator for both national and international economic development and sustainability. However, fossil fuel based power generating units has resulted in the production and emission of green-house gases (GHG), which adversely affects the global environment. In power generation system, improvement in energy efficiency is very important because electrical power industry emits one-third of the world GHG (Pan, Xu, Li, Shieh, & Jang, 2013; Sheen, Tsai, & Wu, 2013; Yaniktepe, Savrun, & Koroglu). Furthermore, utility companies are also facing major challenges, as the demand of electrical power is rising exponentially. The existing transmission line infra-structure is incapable of meeting such a huge demand for power. Thus, the global concern regarding environmental pollution and deregulation in the electrical power industry has driven the application of distributed energy resources (DERs) as a mean of producing electrical energy (Silva, Morais, & Vale, 2012).

Distributed energy resource (DER) is the power generating unit placed in the vicinity of load to avoid the extension of current network. A distribution network can be considered as a set of circuits being supplied from a common bus (Gómez-González, López, & Jurado, 2013; Urbanetz, Braun, & Rüther, 2012). A DERs may be any small type of electrical power generations installed in a distribution system bearing capacity of less than 10MW (Barker & De Mello, 2000). It consists of any renewable energy sources such as wind turbine, micro turbine, fuel cells, photovoltaic array, conventional diesel and natural gas reciprocating engines. DERs based on water, wind, and solar resources provide pollutant-free energy, thus, environment friendly. Furthermore, the usage of DER is advantageous for all stake holders (power generating units, DER proprietors, and consumers) in terms of power reliability, quality, efficiency and economics (Bayod-Rújula, 2009; Hasmaini Mohamad, Mokhlis, Bakar, & Ping, 2011).

Some of the advantages of DERs are summarized below (Rekik, Abdelkafi, & Krichen, 2013; Rivarolo, Greco, & Massardo, 2013):

(1) With the utilization of DERs, the cost of transmission and distribution reduces almost 30%.

(2) It enhances the energy efficiency.

(3) DER reduces the capital cost, thus have shorter construction time.

(4) The usage of DER results in the reduction of transmission power loss, as generation is capable of supplying load without transmission.

(5) The use of DER may improve the voltage profile and ensures power quality.

(6) The use of DER significantly reduces the emission of GHG.

Due to these advantages, the interconnection of DERs into distribution network is undergoing a rapid global expansion.

1.2 Problem Statement

Despite all these advantages, the increasing trend of DER penetration in power system requires system configuration to be changed. Hence, to attain the maximum advantage of DERs, certain technical issues such as state (islanded or grid connected) detection, control of voltage and frequency require acute attention. Among them, the principle concern is islanding condition. In the islanding condition, the distribution system that is connected with the DER is electrically isolated from the main grid, yet continues to be energized by the DER connected to it (IEEE Std 929, 2000; IEEE Std 1547, 2003). When islanding occurs in a distribution network, voltage and frequency are severely disturbed because of the unevenness of generation and load. (Walling & Miller, 2002). Furthermore, islanding adversely effects the existing equipment, utility liability, reduction of power reliability and quality.

Due to the above severe consequences of islanding, (IEEE Std 929, 2000), and (IEEE Std 1547, 2003) state that islanding should be prevented and in case of islanding, the DER should detect and disconnect itself from the distribution network within 2 seconds (100 cycles).

Over the years, many islanding detection techniques have been proposed, such as passive-, active-, and communication-based techniques (Mahat, Zhe, & Bak-Jensen, 2011). Passive techniques isolate the DERs by monitoring the systems' parameters at the point of common coupling, while active techniques introduce perturbations into the power system and analyze the responses for decision-making. Communication-based techniques, on the other hand, are based on the principle of communication. Currently, signal processing and computational intelligent-based islanding detection techniques are also utilized for islanding detection. Each technique has its own advantages and disadvantages (Khamis, Shareef, Bizkevelci, & Khatib, 2013; Laghari, Mokhlis, Karimi, Bakar, & Mohamad, 2014; S. Mohanty, Kishor, Ray, & Catalao, 2014).

Relays used by the majority of the power supply companies for islanding detection are based on passive methods, mostly due to low cost and minimum disturbance of power quality. However, they do not perform well if the power mismatch is small, resulting in a large non-detection zone (Xuancai, Chengrui, Guoqiao, Min, & Dehong, 2009). The introduction of signal processing- and computational intelligent-based techniques heralded a new era for passive islanding detection methods. They render improvements in cost, accuracy, computational time, and reliability (Laghari et al., 2014). These techniques proposed by researchers employ many features as inputs to classifier for efficient discrimination between islanding and non-islanding events. The intelligent classifiers commonly employed for decision making are fuzzy logic, decision tree, support vector machine, adaptive neuro fuzzy inference system and artificial neural network (Laghari et al., 2014).

Artificial neural network (ANN) is one of the commonly used classifiers for islanding detection. It can learn from the given data directly with minimum computation complexity. It is also adaptive, able to handle various nonlinear relationships and can generalize solutions for new data set (Hammerstrom, 1993). Many researchers have implemented ANN and its modified forms such as self-organizing map (SOM) neural network (Moeini, Darabi, & Karimi, 2010; Moeini, Darabi, Rafiei, & Karimi, 2011), extension neural network (ENN) (Chao, Chiu, Li, & Chang, 2011; Meng Hui, Mei-Ling, & Kang-Jian, 2015), probabilistic neural network (PNN) (Lidula & Rajapakse, 2009), and modular probabilistic neural network (MPNN) (Soumya R. Mohanty, Ray, Kishor, & Panigrahi, 2013) for islanding detection.

It is observed that a high detection accuracy is obtainable by ANN based islanding detection techniques using many parameters/features. However, when more parameters are used, the algorithms become more complex, computationally heavier and require more data storage. It also increases the time to process the reference data which is ultimately used for discrimination of islanding events from that of non-islanding events. Furthermore, the selection of these power system parameters for classifier input does not consider/follow any proper guideline. The earlier techniques are either proposed for inverter- or synchronous-based systems without considering all three types of DERs (synchronous, inverter and induction based) in a single system. For practical applications, simple and economical techniques that are suitable for all types of DER's are preferable. It is also advantageous to make use of minimal features as inputs to the classifier while maintaining or improving its accuracy. Moreover, the number of features are selected on the basis of sensing ability to sense the deviations in the power system. This issue is significant, as the inaccuracy in detecting islanding may collapse the distribution network completely.

1.3 Objectives

The primary objective of this research is to address some of the important technical issues in order to make intentional islanding operation of distribution network feasible. Considering the importance of islanding operation of DER, the first and foremost step is to detect the islanding scenario. The main objectives of this research in this context are as follows:

(1) To perform the sensitivity analysis of different power system parameters on islanding detection.

(2) To arrange the different power system parameters on the basis of sensing ability and to analyze the most sensitive parameter analytically.

(3) To develop a passive islanding detection technique by employing the most sensitive parameter for discrimination between islanding and non-islanding events.

(4) To implement a minimum features based intelligent islanding detection technique for the detection of islanded mode.

(5) To enhance the accuracy of the proposed intelligent technique by employing the application of optimization approaches.

1.4 Scopes and Limitations

The scope and limitations of this research are as follows:

(1) This research considers only the major technical issues of islanding detection. Financial issues for implementing the islanding technique is not considered.

(2) This study considers local information to detect islanding detection instead of using latest communication technologies in order to reduce its cost and make islanding operation more economical.

(3) New modules are developed for proposed islanding detection technique. These modules are developed with the PSCAD script through FORTRAN programming codes. A MATLAB programming code is also interfaced to PSCAD to increase the programming flexibility.

1.5 Research Methodology

In order to achieve the above mentioned objectives, following research methodology will be carried out:

(1) Review all existing islanding detection techniques proposed for distribution network.

(2) Model a hybrid distribution network consisting of mini hydro-, induction generator- and inverter-based DERs using PSCAD/EMTDC software v 4.2.1, and also model the same distribution network under IEEE 1547 test frame.

(3) Perform the sensitivity analysis of different power system parameters using the distribution network under IEEE 1547 test frame.

(4) Performance based ranking of different power system parameters is investigated and the most sensitive parameter is analyzed analytically.

(5) Propose a new passive technique for islanding detection by utilizing the most sensitive parameter.

(6) Model islanding detection technique in PSCAD/EMTDC software.

(7) Incorporate the proposed islanding detection technique into the IEEE 1547 test frame and test its performance.

(8) Compare the proposed islanding detection technique with conventional islanding detection technique in terms of their non-detection zones (NDZ).

(9) Propose a new intelligent islanding detection technique by utilizing the minimum number of features/signals from power system parameters and tested on a hybrid distribution system.

(10) The accuracy of the classifier will be enhanced by employing the application of optimization approaches.

1.6 Thesis Outline

This research report comprises of five chapters, wherein each chapter has reported the related topic briefly.

Chapter 1 provides the background and motivation of the proposed research followed by problem statement. The objectives of study are presented followed by scopes and limitations of the research. In the end, research methodology and research report outline are given.

Chapter 2 focuses on overview of DER showing a paradigm shift from central generation with their benefits and its impact on future electricity. It also includes operation modes of DERs and the associated issues. The phenomenon of islanding with their technical issues which restricts its implementation in distribution network is also discussed. The current practice on islanding is also discussed followed by the various islanding detection techniques with their comparison are reviewed.

Chapter 3 presents the modelling of the test system under consideration followed by the sensitivity analysis of different power system parameters under islanding and non-islanding events. The different power system parameters are prioritized on the basis of response analysis. Furthermore, the analytical analysis of the most sensitive parameter is also elaborated in detail.

Chapter 4 presents the methodologies of the proposed islanding detection techniques for DERs. In the start, the procedure of the proposed passive technique is elaborated. Then the method of the proposed intelligent islanding detection technique is explained followed by the detailed analysis on feature selection, training and testing data formation by systematic and inter-systematic selection. Furthermore, the comparative study is made between stand-alone and hybrid ANN on the basis of regression value in order to obtain the best performance of classifier by optimizing its indices.

Chapter 5 presents the simulation results of the proposed passive techniques under all possible islanding and non-islanding conditions followed by comparison between proposed and conventional passive technique on the basis of non-detection zone. Then the simulation results of the intelligent islanding detection techniques are proposed. These results are further categorized into off- and on-line testing. The accuracy analysis by introducing different percentages of error are also investigated.

Chapter 6 concludes this thesis by summarizing the research contributions and presents possible future work for this research

CHAPTER 2: ISLANDING DETECTION TECHNIQUES: A REVIEW

2.1 Introduction

Distributed energy resources (DERs) are mainly used to meet increasing power demands and curb environmental pollution. Normally, a DER system consists of a utility grid, supported by pollutant-free energy resources, such as solar, wind, hydro, and fuel cells.

This chapter starts with an outline of DER highlighting the shift of power generation trend from central to local level. Their benefits, operation modes, issues and its predicted contribution in the future are also highlighted. The phenomenon of islanding will be discussed with their issues and technical difficulties posed to a DER system. Moreover, this chapter provides a review of various islanding detection techniques with their respective advantages and drawbacks.

2.2 Distributed Energy Resources (DER)

Due to the rapid increase of oil and natural gas prices, greenhouse effect, and other environmental issues, the installation of distributed energy resources (DERs) has shed a new light in the field of electric power supply. It attracts industrial and commercial customers by providing a competitive environment with respect to new integrating technologies, environmental benefits, and reduced losses (Gsänger, 2011; K.M. Tsang, 2013). Secondary power sources in DERs, such as mini/micro hydro, wind turbines, photovoltaic and fuel cell increases the efficiency and stability of the distribution network

The concept of DER is as old as the power system itself. In fact, the power system itself started using distributed energy resource. The first power plant bearing named Pearl Steam Power Plant was invented by Thomas Edison in 1882. It was capable of supplying power to 500 customers in New York (Frank Delea, 2010). At that time, there was no concept of utility grid, electric power was generated near the load point (Pepermans, Driesen, Haeseldonckx, Belmans, & D'haeseleer, 2005).

Later on, with the technology advancement, it became feasible to generate power at one place and transmit it to the consumers at far locations by changing the voltage levels. This leads to centralized power generation and its transmission to far places by a large scale transmission network. This centralized power generation reduces the production cost of electricity (cost per kWh). Furthermore, due to this, the reliability of electricity supply was highly enhanced as the failure of one unit in a large interconnected system didn't have greater influence on the whole system. Hence, up to the beginning of twentieth century, the power industry was ruled by the centralized power generation.

In the last decade, DERs have been widely used due to technological innovations, and environmental issues. International Energy Agency (IEA) list five main causes of wide induction of DERs in power system, which are developments in DER, constraints on the construction of new transmission lines, increased customer demand for higher reliable electricity, the electricity market liberalization and concerns about climate change ("Distributed Generation in Liberalized Electricity Market," 2002). All these factors are forcing the power industry to take another shift from centralized generation to distributed generation.

2.3 Impact of Distributed Energy Resources

The acceptance of DERs all over the world is not only due to environmental alarms but also because they offer several other benefits. Some of these are listed below:

(1) The capital cost is less and hence requiring shorter construction time.

(2) According to International Energy Agency (IEA), the transmission and distribution cost can be reduced up to 30% if the DER is located at the most optimal position ("Distributed Generation in Liberalized Electricity Market," 2002).

(3) There is minimal transmission power losses as DERs supply power to the load without transmission network (Acharya, Mahat, & Mithulananthan, 2006).

(4) It enhances the energy efficiency, improves voltage profile and power quality by supporting the central power generation companies to reduce their load in the transmission network.

(5) The DERs gives a competitive environment to the power supply companies which can lead to reduction in the overall price of electricity.

(6) The installation of DERs provides a viable solution in remote areas where extension of grid is not cost-effective. In such areas, it is lucrative to install DERs instead of extending a grid connection.

(7) The DERs can also be used as backup supply for critical loads such as hospitals in case of electricity supply failure from utility.

Many power utility companies across the globe have substantial inclusion of DERs in their distribution networks. Some countries are setting up targets for future DERs installation. The European union had set a target to replace 27% of their electricity generated from fossil fuels with renewable energy sources by 2030 ("European Union Commission Report," 2015). In this regard, Malaysia has also set a target to utilize 5.5% renewable energy by the end of 2015 and 11% by the end of 2020 ("malaysia explores its renewables options," 2015). This increasing interest in renewable energy generation is also supporting the DER penetration in the utility companies in future.

2.4 DG Operating Modes and their Issues

Distributed energy resources can function as following:

1) Grid connected mode.
2) Islanded mode.

The explanations of these modes are given in the following sections:

2.4.1 Grid Connected Mode

In it, DER is attached to a grid or distribution network and becomes part of whole system. However, it should be noted that the integration poses some technical issues that act as challenges in the extensive use of DERs. It needs to be addressed before the DER can be utilized efficiently. The following are the main issues of DER operation with grid connected mode (Ackermann & Knyazkin, 2002; Dugan & McDermott, 2002; J. A. P. Lopes, Hatziargyriou, Mutale, Djapic, & Jenkins, 2007).

(1) The use of DER in the distribution system causes the power flow bidirectional where power is flowing not only from grid, but also from DER. In the absence of DER, the distribution system is traditionally designed as radial systems in which the power is generated and transmitted in a unidirectional from the transmission to distribution level. This leads to simple operation mainly for over current protection system. However, the use of DER in distribution network could create problems, effect the system operation and may necessitate a change in protection strategy.

(2) In the presence of DERs, the short circuit level of the distribution network increases that results in the increased amount of fault current. However, this short circuit level depends on the several factors such as generator type, number of DER in the distribution network. For example, in case of synchronous based DER, the fault current depends upon the total synchronous reactance. Moreover, increase in fault current cause adverse impact on protection system.

(3) One more concern in DER operation is the existence of islanding. Since, this is the topic of interest throughout this thesis, more detailed explanation of this will be discussed in the following section.

2.4.2 Islanded Mode Operation

According to IEEE standard, islanding mode operation is defined as "*A condition in which a portion of utility system that contains both load and distributed resources remains energized while isolated from the remainder of the utility system*" (IEEE Std 929, 2000).

When islanding occurs, distribution network is disconnected from the main grid. The islanding area can be based on substation, one or more distribution feeder and voltage levels. However, this islanding formation will be sustained if there is sufficient generation to meet the islanded load. Figure 2.1 shows the islanding phenomenon of a distribution network connected with three distributed energy resources.

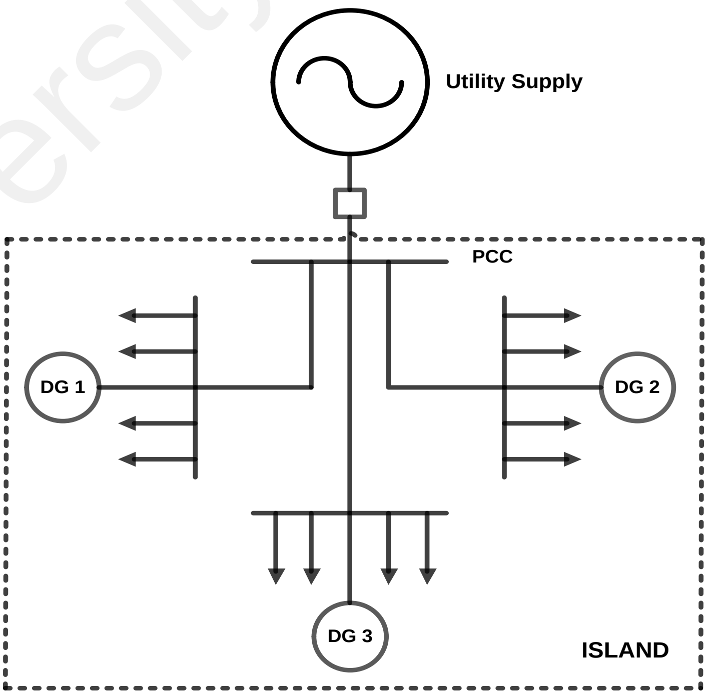

Figure 2.1: Phenomenon of islanding occurrence

After islanding, the DER must maintain the stability, reliability, power quality, voltage and frequency of the islanded system within acceptable range. Otherwise, blackouts may occur in the islanded networks. The islanding operation can be intentional or unintentional. The description of both is discussed as follows:

2.5 Un-intentional Islanding and Associated Issues

The unintentional islanding occurs due to sudden power system imbalance such as severe fault, line and generator outages which ultimately splits the system into islanded networks (Dola & Chowdhury, 2006). These unintentional islands may cause active or reactive power deficiency, which leads to frequency, angle, or voltage instability. These instabilities further trip the other regions if not handled properly. These issues become more severe at large power mismatch conditions to existing equipment. Furthermore, it badly affects the utility liability, power reliability and quality. The key issues of islanding are illustrated below:

2.5.1 Power Quality Issue

The vital obligation of the power supply company is to deliver clean energy. However, the power quality of the distribution system is greatly affected during islanding condition. At large power mismatch condition, the voltage and frequency differ considerably. Therefore, it is necessary to control frequency and voltage of the islanded network swiftly. Controlling these parameters within permissible limits is the utmost technical challenge currently being studied worldwide.

2.5.2 Synchronization Issue

One of the most important issue which requires special consideration during islanding condition is the synchronization issue. The majority of the distribution system are overhead system and they use autorelcosers for protection. The large number of line fault in such system are transient in nature and are likely to disappear if the line is temporarily de-energized. According to utility statistics, the percentage of permanent faults in the distribution systems occurs only at 10% to 15% ("IEEE Guide for Automatic Reclosing of Line Circuit Breakers for AC Distribution and Transmission Lines," 2003). Therefore, service continuity, system stability and availability of power at consumer end can be improved by means of automatically reclosing the circuit breaker.

During islanding, the auto-recloser makes numerous efforts to interconnect with the grid which may end in out of synchronism due to the mismatch of the phase angle, voltage magnitude and frequency. The impact may be less if these values are within nominal range. However, the impact is very high in rotating type DERs in which high mechanical torques and currents are produced due to out of synchronism closure. This can result in damaging the prime movers of the generator (Walling & Miller, 2002).

2.5.3 Grounding Issue

Many power supply companies have single point grounding/earthing wherein the earth/ground connection is situated at the utility side. It works well if there is no DERs in the distribution network. However, if the DERs are installed in the distribution system, a separate grounding/earthing is required at DERs side for safe operation. If the DERs are installed without a separate earthing/grounding point in the distribution system, it may cause adverse impact during islanding. Thus, effective operation of islanded DER requires its own separate earthing/grounding (H. Mohamad & Crossley, 2009). For this purpose, ("IEEE Recommended Practice for Grounding of Industrial and Commercial Power Systems," 2007) advocates to use multiple earthing/grounding for multiple DERs functioning in parallel.

2.5.4 Personnel Safety

The energized islanded section by DERs may endanger the life of line worker during maintenance. This occurs due to the ignorance of system condition. If the maintenance work continues it may result in hazard. However, by taking some proper operational precautions this risk can be prevented.

2.6 Intentional Islanding

In intentional islanding, the grid is split into controllable small regions intentionally (Pahwa, Youssef, Schumm, Scoglio, & Schulz, 2013). In such a state, each region should have significant generation to energize its loads in order to remain active. Intentional islanding may also be used in un-intentional islanding as a precautionary scheme to curtail the losses triggered by unintentional islanding (Aghamohammadi & Shahmohammadi, 2012).

Though, intentional islanding is now proscribed, research efforts are still being undertaken to analyze its operation. Many countries have developed micro grid systems to evaluate the islanding effects and their respective solutions. Figure 2.2 enlists the name and location of these micro grids. (Lidula & Rajapakse, 2011) gives the detail of these practical systems.

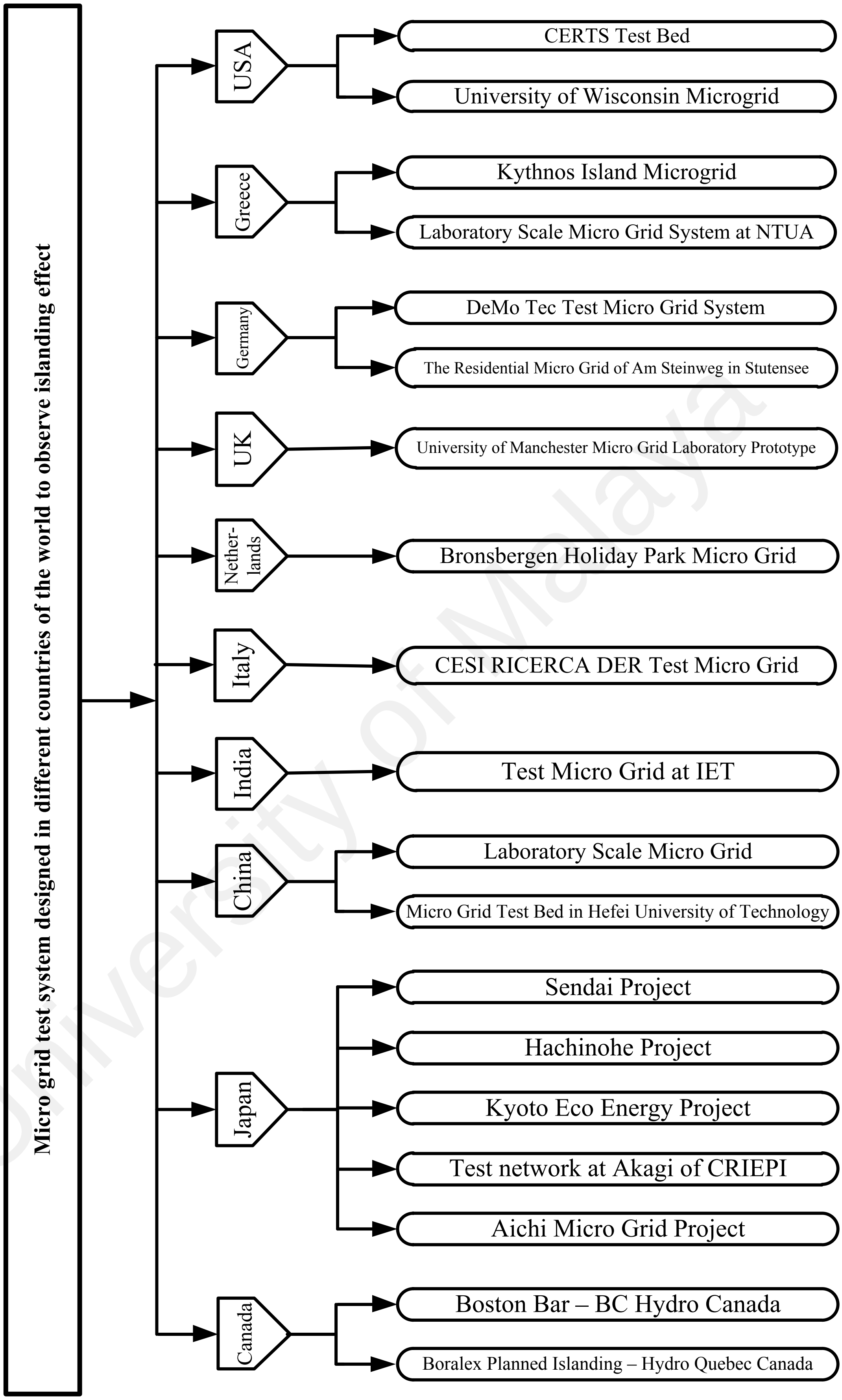

Figure 2.2: Micro grid test system in different countries

Research effort in many countries are under way to make intentional islanding possible. Some of the active countries are United Kingdom (Chowdhury, Chowdhury, Crossley, & Chui Fen, 2008), Carolina (Gooding, Makram, & Hadidi, 2014), Thailand (Fuangfoo, Lee, & Kuo, 2006), India (Joshi & Pindoriya, 2013), Colombia (Quintero et al., 2012), Brazil (Londero, Affonso, Nunes, & Freitas, 2010), and Denmark (C. Yu, Zhao, & Ostergaard, 2008). It is substantiated that the operation of DERs in islanded mode has the potential to bring many benefits to the owner of DERs and consumers. However, few technical issues need to be reviewed regarding equipment and control strategies for successful operation of islanding.

2.7 Standards and Guidelines for Intentional Islanding

The islanding condition has an adverse impact on the electrical appliances and on the life of line workers. To overcome these issues, numerous standards have been established which serve as a guideline for utilities or independent power producers (IPP). The main standards are as follows:

(1) IEEE Standard for Interconnecting Distributed Resources with Electric Power Systems (IEEE Std 1547, 2003).

(2) IEEE Recommended Practice for Utility Interface of Photovoltaic (PV) Systems (IEEE Std 929, 2000).

(3) UL 1741 standard: Inverter, Converter, and Controllers for Use in Independent Power System ("UL1741 Inverter, Converter, and Controllers for Use in Independent Power System," 2001).

(4) IEEE Std C37.95, Guide for Protective Relaying of Utility-Consumer Interconnections ("IEEE Guide for Protective Relaying of Utility-Consumer Interconnections," 2014).

(5) IEEE 242-2001 Recommended Practice for Protection and Coordination of Industrial and Commercial Power Systems ("IEEE Recommended Practice for Protection and Coordination of Industrial and Commercial Power Systems (IEEE Buff Book)," 2001).

These standards help power supply companies to perform an intentional islanding within an electric power system. Table 2.1 recapitulates the standard parameters, such as quality factor, islanding detection time, frequency, and voltage operation range for these standards (Ku Ahmad, Selvaraj, & Rahim, 2013).

Table 2.1: Standards of islanding detection

Standard	**Quality Factor**	**Detection time**	**Frequency limits**	**Voltage limits**
IEC 62116	1	$t < 2\ s$	$(fo\text{-}1.5\ Hz) \leq f\ \&\ f \leq (fo+1.5Hz)$	85 % $\leq V \leq$ 115 %
UL1741	2.5	$t < 2\ s$	59.3 Hz $\leq f \leq$ 60.5 Hz	88 % $\leq V \leq$ 110 %
IEEE 1547	1	$t < 2\ s$	59.3 Hz $\leq f \leq$ 60.5 Hz	88 % $\leq V \leq$ 110 %
Korean standard	1	$t < 0.5\ s$	59.3 Hz $\leq f \leq$ 60.5 Hz	88 % $\leq V \leq$ 110 %
IEEE 929-2000	2.5	$t < 2\ s$	59.3 Hz $\leq f \leq$ 60.5 Hz	88 % $\leq V \leq$ 110 %
VDE 0126-1-1	2	$t < 0.2\ s$	47.5 Hz $\leq f \leq$ 50.5 Hz	88 % $\leq V \leq$ 110 %

2.8 Non Detection Zone (NDZ)

The non-detection zone is a main issue that determines the accuracy and efficiency of an islanding detection technique. It is the range in terms of power difference between generation and load demand wherein islanding detection technique fails to detect the islanding. The islanding detection technique with smallest non detection zone is better than with larger non-detection zone. The non-detection zone can be exemplified in terms of frequency and voltage range as well as in active and reactive power mismatches. The NDZ for active power is illustrated as follows (Hashemi, Ghadimi, & Sobhani, 2013; Zeineldin, El-Saadany, & Salama, 2006):

$$\Delta P = -3V \times \Delta V \times I \tag{2.1}$$

Where,

ΔP = Active power imbalance,

V = Rated voltage,

I = Rated current

ΔV = Variation in voltage (difference of V_{max} and V_{min}).

The non-detection zone (NDZ) for active power upon considering the power factor is as follows:

$$\Delta P = -3V \times \Delta V \times I \times \cos\phi \tag{2.2}$$

The NDZ for reactive power is shown below:

$$\Delta Q = \frac{3V^2}{\omega_n L}\left(1 - \frac{f_n^2}{\left(f_n - \Delta f\right)^2}\right) \tag{2.3}$$

where,

ΔQ = Reactive power imbalance,

V = Rated voltage,

f_n = Nominal frequency,

Δf = Variation in frequency deviation (difference of f_{max} and f_{min}),

$\omega_n = 2\pi f$,

$L = V^2 / \left(2\pi f P Q_f\right)$

Another approach to determine the non-detection zone in terms of active and reactive power mismatch is attained by means of following equations (Zhihong, Kolwalkar, Zhang, Pengwei, & Walling, 2004):

$$\left(\frac{V}{V_{\max}}\right)^2 - 1 \le \frac{\Delta P}{P} \le \left(\frac{V}{V_{\min}}\right)^2 - 1 \tag{2.4}$$

$$Q_f \times \left[1 - \left(\frac{f}{f_{\min}}\right)^2\right] \le \frac{\Delta Q}{Q} \le Q_f \times \left[1 - \left(\frac{f}{f_{\max}}\right)^2\right] \tag{2.5}$$

where,

V_{max} = Maximum over voltage limit,

V_{min} = Minimum under voltage limit,

f_{max} = Maximum over frequency limit,

f_{min} = Minimum under frequency limit,

Q_f = Quality factor,

V = Rated voltage,

f = Rated frequency,

P = Active power,

Q = Reactive Power,

ΔP = Active power mismatch,

ΔQ = Reactive power mismatch.

2.9 Categorization of Islanding Detection Methods

Islanding detection techniques are mainly categorized into remote, local, signal processing and computational intelligence based, as shown in Figure 2.3 (Velasco, Trujillo, Garcerá, & Figueres, 2010; Wei Yee Teoh, 2011; B. Yu, Matsui, & Yu, 2010).

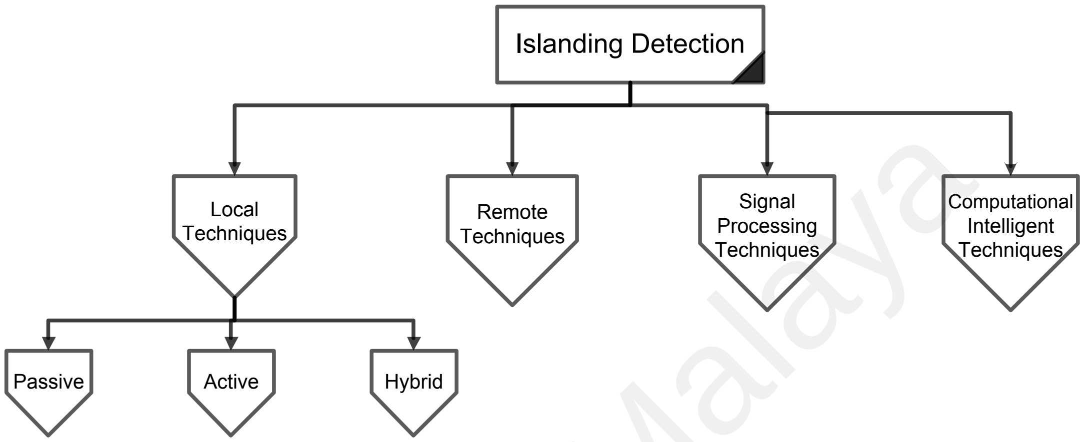

Figure 2.3: Categorization of islanding detection techniques

These methods are further classified into different techniques on the basis of different criteria, such as detection speed, error detection rate, power quality, non-detection zone (NDZ), and efficacy in multiple inverter cases (Li et al., 2014). Comprehensive discussions of these techniques are presented in the following sections.

2.10 Remote Islanding Detection Techniques

Remote islanding detection techniques works on the principle of communication between utility and distributed energy resource. Once islanding occurs, a trip signal is sent to the distributed generation resource. Transfer trip scheme (Balaguer-Álvarez, 2010; Jun Yin; Liuchen Chang; Diduch, 2004) and Power line carrier communication (PLCC) scheme (Wencong et al., 2007; Wilsun et al., 2007) falls under this category. These techniques have zero NDZ, faster response time, zero impact on power quality and system transients, high reliability, and works effectively in multiple DG systems. However, remote techniques are very expensive for implementation on small-scale systems (Barsali, Ceraolo, Pelacchi, & Poli, 2002). Hence, local techniques are preferred for the aforementioned purpose.

2.11 Local Islanding Detection Techniques

As the name indicates, it is based on measuring the variations in system parameters, such as frequency, voltage, impedance, phase angle, active power, reactive power, and harmonic distortion at the DG site for islanding detection. These techniques are further categorized into passive, active, and hybrid techniques. The number of proposed active and passive techniques increases rapidly over the last few years(Khamis et al., 2013).

2.11.1 Passive Islanding Detection Techniques

Passive islanding detection techniques basically monitor the system parameters, such as frequency, voltage, and harmonics at the point of common coupling, or at the DG terminals, and compare it with a predetermined threshold value for islanding detection. Figure 2.4 shows the basic working principle of passive islanding detection techniques.

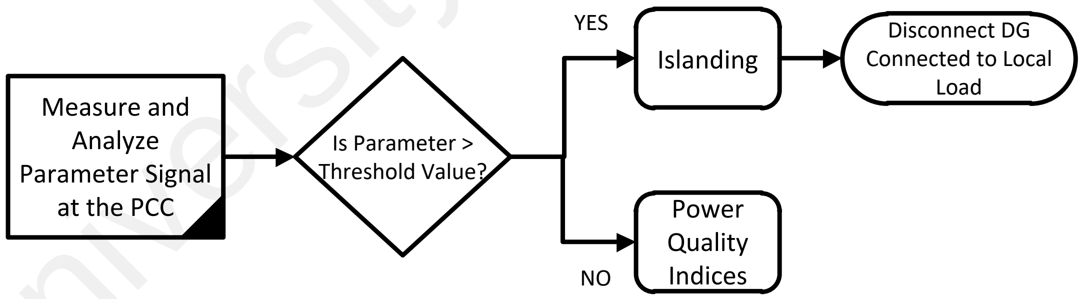

Figure 2.4: Basic working principle of passive islanding detection technique

Some of the most common passive techniques are the rate of change of power (ROCOP) (Ku Ahmad et al., 2013), rate of change of frequency (ROCOF) (Ding & Crossley, 2005; Freitas, Wilsun, Affonso, & Zhenyu, 2005; Jia, Bi, Liu, Thomas, & Goodman, 2014), rate of change of frequency over power (ROCOFOP) (Pai & Huang, 2001), change of impedance (O'Kane & Fox, 1997), voltage unbalance (Sung-Il & Kwang-Ho, 2004), over/under (O/U) voltage and over/under frequency (De Mango, Liserre, Aquila, & Pigazo, 2006), harmonic distortion (voltage and current) (De Mango, Liserre, Aquila, et al., 2006; Sung-Il & Kwang-Ho, 2004), phase jump detection (Singam & Hui, 2006), rate of change of voltage and change in power factor (Salman, King, & Weller, 2001) as shown in Figure 2.5.

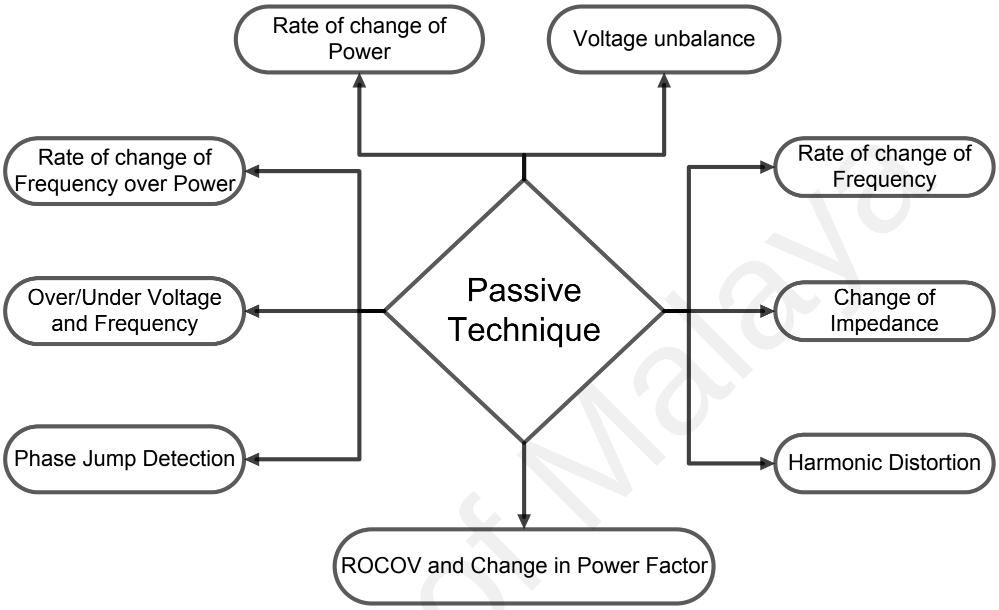

Figure 2.5: Common passive techniques

Cost effectiveness, fast detection speed, and no impact on power quality are some of the major advantages of passive techniques. The characteristics of these techniques are summarized in Table 2.2.

Table 2.2: Characteristics of different passive techniques

Method	Detection Time	Error Detection Rate	Impact on Power Quality	NDZ
ROCOP	24-26 msec	High	No	Small
ROCOF	24 msec	High	No	Small
ROCOFOP	100 msec	Low	No	Smaller than ROCOF
Change of Impedance	10 msec	Low	No	Small
Voltage Unbalance	53 msec	Low	No	Large
O/U voltage and frequency	4 msec to 2 sec	Low	No	Large
Harmonic Distortion	45 msec	High	No	Large for high Q
Phase Jump	10-20 msec	Low	No	Large

A major problem with this technique is that it suffers from large non detection zone (NDZ), and it is very difficult to detect islanding when the generation and load in the islanded system are closely matched. Furthermore, the setting of threshold value requires special consideration. Lower threshold settings may result in nuisance tripping, and if the setting is too high, islanding may not be detected. Hence, error detection rates are high. These drawbacks can be overcome by using signal processing and computational intelligent based techniques. However, these problems can also be overcome by active techniques (Laghari et al., 2014; Li et al., 2014).

2.11.2 Active Islanding Detection Techniques

Active islanding detection techniques interact with the power system by introducing perturbations into the system variables, such as frequency, voltage, currents, and harmonics. Figure 2.6 shows the basic working principle of active islanding detection techniques. The impact of these perturbations is significant if the distributed generation resource is islanded otherwise quite negligible.

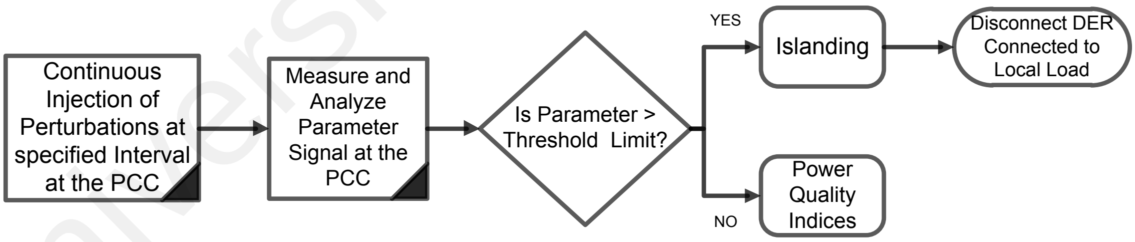

Figure 2.6: Basic working principle of active islanding detection techniques

Some of the most common active techniques are reactive power export error detection (RPEED) (Chowdhury, Chowdhury, & Crossley, 2009), impedance measurement (Ku Ahmad et al., 2013; O'Kane & Fox, 1997), slip mode frequency shift method (SMS) (F. Liu, Kang, Zhang, Duan, & Lin, 2010; L. A. C. Lopes & Huili, 2006), Active frequency drift (AFD) (De Mango, Liserre, & Aquila, 2006), frequency jump (FJ) (Li et al., 2014), Active frequency drift with positive feedback (AFDPF) (Ropp, Begovic, & Rohatgi, 1999), sandia frequency shift (SFS) (Zeineldin & Conti, 2011; Zeineldin & Kennedy, 2009), sandia voltage shift (SVS) (Trujillo, Velasco, Figueres, & Garcerá, 2010), variation of active and reactive power (De Mango, Liserre, & Aquila, 2006; Li et al., 2014; Velasco et al., 2010), negative sequence current injection (H. Karimi, Yazdani, & Iravani, 2008; Tuyen & Fujita, 2011), high frequency signal injection (D. Reigosa, Briz, Blanco, Garcia, & Manuel Guerrero, 2014; D. D. Reigosa, Briz, Charro, Garcia, & Guerrero, 2012), virtual capacitor (Chiang, Jou, & Wu, 2012), virtual inductor (Jou, Chiang, & Wu, 2007) and phase PLL perturbation method (Velasco, Trujillo, Garcera, & Figueres, 2011) as shown in Figure 2.7. Most of these techniques are used for inverter type DGs.

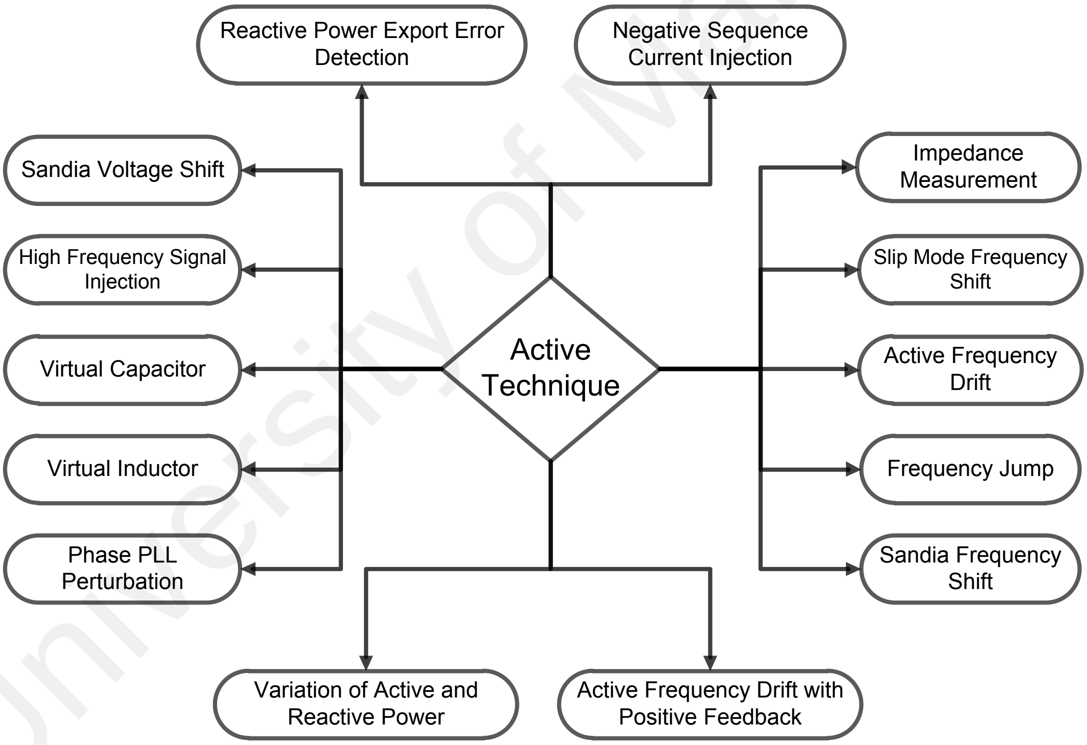

Figure 2.7: Common active techniques

In comparison to passive techniques, active techniques reduce the non-detection zone (NDZ) and decrease the error detection rate. The characteristics of these techniques are summarized in Table 2.3.

Table 2.3: Characteristics of different active techniques

Techniques	Detection Time	Error Detection Rate	Impact on Power Quality	NDZ
RPEED	2 sec	Low	Degrades	Small
Impedance Measurement	0.77-0.95 sec	Low	Degrades	Small
SMS	0.4 sec (approx)	Low	Degrades	Small
AFD	With 2 sec	High	Degrades	Large if value of Q is high
FJ	75 msec	Low	Degrades	Small
AFDPF	1 sec (approx)	Lower than AFD	Slightly degrades	Smaller than AFD
SFS	0.5 sec	Low	Slightly degrades	Smallest
SVS	0.5 sec	Low	Slightly degrades	Smallest
Variation of active and reactive power	0.3-0.75 sec	High	Degrades	Small
Negative sequence current injection	60 msec	Low	Degrades	None
High frequency signal injection	Few msec	Low	Slightly degrades	Smallest
Virtual capacitor	20-51 msec	Low	Slightly degrades	Smallest
Virtual Inductor	13-59 msec	Low	Slightly degrades	Smallest
Phase PLL Perturbation	120 msec	Low	Negligible	Smallest

Furthermore, in order to inject perturbations into the power systems, additional controllers/power electronics equipment is required. This increases the complexity of the system and reduces the power quality. Moreover, additional detection time is required in order to observe the power system response on perturbations. Hence, the system's stability is significantly degraded.

2.11.3 Hybrid Islanding Detection Techniques

Hybrid islanding detection techniques basically works on the combined features of the aforementioned techniques and is effectively applied to complex systems. During islanding detection, the passive technique functions as primary, while the active technique functions as a secondary measure, as shown in Figure 2.8. Hence, the combination of these methods will improve the multiple performance indices.

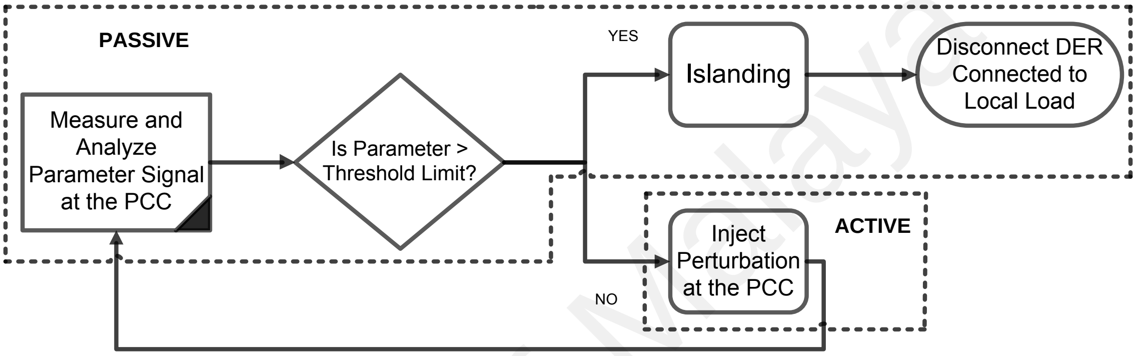

Figure 2.8: Basic working principle of hybrid techniques

Some examples of hybrid islanding detection techniques include voltage unbalance and frequency set point method (Menon & Nehrir, 2007), technique based on voltage and real power shift (Mahat, Zhe, & Bak-Jensen, 2009), voltage fluctuation injection (Wen-Yeau, 2010), hybrid SFS and Q-f technique (Vahedi, Noroozian, Jalilvand, & Gharehpetian, 2010), and the technique based on rate of change of reactive power and load connecting strategy (Laghari, Mokhlis, Bakar, & Karimi, 2013) as shown in Figure 2.9.

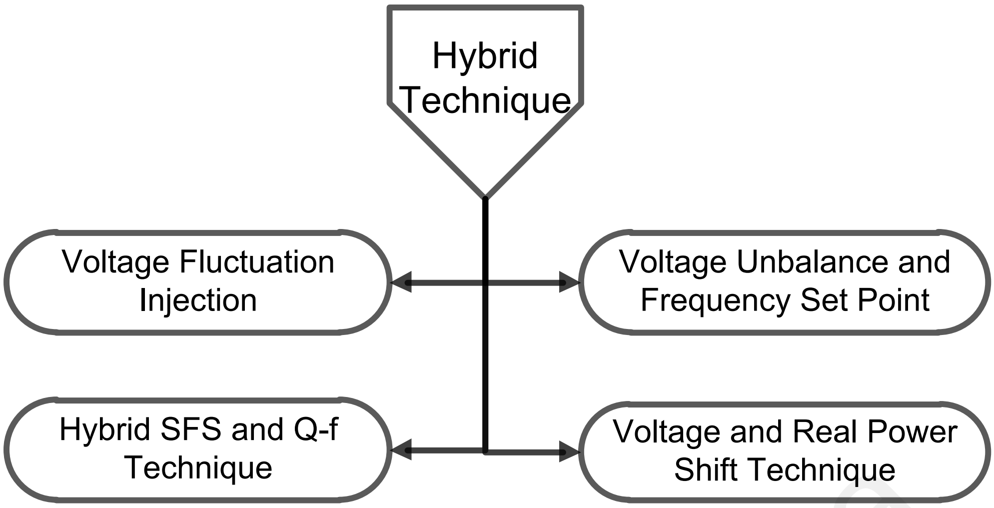

Figure 2.9: Hybrid islanding detection techniques

These techniques possess very small non-detection zone (NDZ), and degradation in power quality is also reduced because perturbations are only introduced when islanding is suspected. However, this combination increases the cost of the system, along with the islanding detection time.

From the above discussion, it is noticed that each islanding detection technique has its own merits and demerits. However, the issues that are still unresolved include accuracy, very high detection speed, and compatibility of detecting islanding in multiple and hybrid DERs environment. In this regard, it can be noted from the aforementioned review that passive islanding detection techniques have the potential to fulfil these requirements, provided that their limitation are solved using some other means. Passive islanding detection techniques have the advantage of not degrading the power quality, capable of detecting islanding quickly, and are compatible for all types of DERs. However, their main limitation is the large non detection zone and threshold settings. Both of these limitations can be addressed by using signal processing and computational intelligent techniques.

2.12 Signal Processing Techniques for Islanding Detection

Signal processing techniques are commonly used to improve the performance of passive islanding detection techniques. Versatility, stability, cost effectiveness, and ease of modification properties of the signal processing techniques help researchers extract the hidden characteristics of the measured signals for islanding detection. On the basis of these extracted features, decision can be made on whether islanding did occur. Figure 2.10 shows the basic steps involved in islanding detection using signal processing techniques.

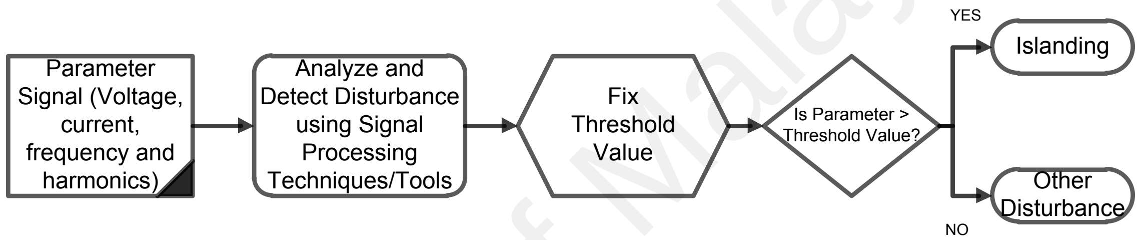

Figure 2.10: Block diagram for signal processing based islanding detection technique

The basic signal processing tools, which are used for islanding detections, are Fourier transform, s-transform, Hilbert Huang transform, wavelet transform, and TT-transform as shown in Figure 2.11.

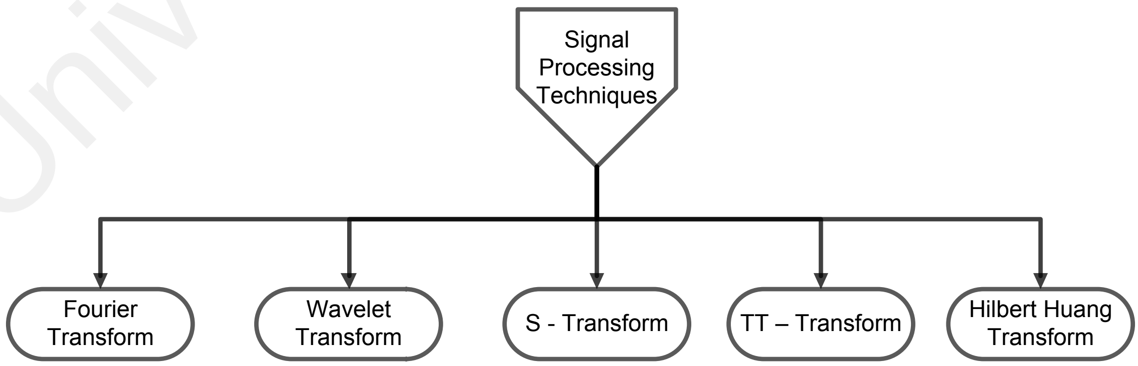

Figure 2.11: Basic signal processing tools for islanding detection

The description of these signal processing tools used in islanding detection techniques are discussed in the following sections.

2.12.1 Fourier Transform based Islanding Detection Techniques

Fourier transform is the most common technique in frequency domain analysis. It basically represents a signal as a summation of sinusoidal terms of different frequencies. It extracts the features of the stationary signal at specific frequencies, but is incapable of detecting the time distribution of different frequencies. It is also unable to resolve any momentary information associated with fluctuations (M. Karimi, Mokhtari, & Iravani, 2000). Hence, the time-frequency analysis is proposed. The short time Fourier transform (STFT) is the modification of Fourier transform. It divides the signal into small frames, where each frame can be assumed to be stationary. These numerous frames of the signal are evaluated by the moving window. This moving window identifies the relation between the time and the change in frequency (Dash, Panigrahi, Sahoo, & Panda, 2003). However, STFT cannot analyse the non-stationary signal due to the limitation of fixed window's width (Gu & Bollen, 2000).

Discrete Fourier transform (DFT) is the de-facto technique used for frequency domain analysis of discrete time signals. It transforms the discrete time sequence of finite length into discrete frequency sequence of finite length. Fast Fourier transform (FFT) also gives similar results as the DFT, although in lesser amounts of time. However, it is not suitable for the analysis of non-stationary signals, due to the fact that it depicts those spectral values that do not exist in the original signal. Kim (Kim, 2012) introduces a new passive technique for islanding detection based on DFT for the extraction of the desired features. Conventional passive techniques misinterpret the grid disturbances, such as sag, swell, and transient conditions. NDZ might also have occurred if the power generated by photovoltaic (PV) and the load matches. The proposed method uses the variations in 2^{nd} harmonic components of grid voltage. The use of harmonic coefficients provides robust control against grid disturbances and also reduces the NDZ. The islanding detection time is around 1msec via the usage of high performance DSP controller.

In order to overcome the problem of slow computation time of DFT, Goertzel algorithm is used. It is basically a type of discrete Fourier transform and a faster pitch detection technique compared to FFT and DFT. It works from the perspective of filtering operation at a specified frequency, or from the perspective of the DFT taken over short time section of the signal. It directly calculates the amplitude and phase of the desired frequency of the input signal, which ultimately reduces the computational time (Gonzalez, Garcia-Retegui, & Benedetti, 2007; Jacobsen & Lyons, 2003; Sozanski, 2006). Jae-Hung et al. (Jae-Hyung, Jun-Gu, Young-Hyok, Yong-Chae, & Chung-Yuen, 2011) uses Goertzel algorithm to reduce the islanding detection time in single phase 2 stage Photovoltaic (PV) system. In the proposed system, the inverter injects the output current with a ninth harmonic component into the grid, and detects the same in voltage at the point of common coupling. NDZ does not exist in this method, even under perfect match of power and load. The impact on the power quality is also negligible, and islanding is detected within 2 cycles.

2.12.2 Wavelet Transform based Islanding Detection Techniques

The wavelet transform (WT) is also used for the analysis of the signal. It is a mathematical model based on square integral and group theory, similar to FT. It decomposes a signal into its constituents at different frequency scales (Chen, 2005; Graps, 1995). It represents a signal in both time and frequency domains. Hence, it is suitable for examining the signals in those applications where time-frequency resolution is considered necessary. It has been widely used in power system applications, such as detection, disturbance transition events in electrical power quality, feature extraction, power system protection, and de-noising (Daubechies, 1990; Santoso, Powers, & Grady, 1997; Santoso, Powers, Grady, & Hofmann, 1996).

The wavelet transform is more advantageous compared to Fourier based transforms (STFT, FFT and DFT). Since, it can vary its window size, the time-frequency resolutions are not compromised. Furthermore, wavelet transform determines the time and frequency information simultaneously for low and high frequencies by long and short windows, respectively (Walid G. Morsi & El-Hawary, 2010). Wavelet transform is categorised into continuous (CWT) and discrete wavelet transforms (DWT). CWT is used in islanding detection by analysing DG voltage. The Mallat decomposition is also used to extract and eliminate the noise from the signal (Yanping, Qiuxia, Junjuan, Dezhong, & Yuexin, 2008). This method reduces the computational efficiency by introducing the numerous coefficients. This problem diverts the attention of the researchers towards DWT.

In (Pigazo, Liserre, Mastromauro, Moreno, & Dell'Aquila, 2009; Pigazo, Moreno, Liserre, & Aquila, 2007), DWT was used to analyse the voltage signal from a single phase PV system. The proposed method uses Bi-orthogonal 1.5 and 5 decomposition levels for islanding detection. The reduction in the number of sensors, minimisation in computational burden and complexity are some of the advantages associated with this technique. Daubechies mother wavelet based DWT is used in (Hsieh, Lin, & Huang, 2008). It examines the variations in voltage and frequency. The salient features of this method are the simplicity in programming, enhancement of islanding detection capability, and simultaneous observation of power quality profiles. The proposed scheme is tested and verified in several scenarios with flexibility, feasibility, and robustness. In (Samantaray, Pujhari, & Subudhi, 2009), negative sequence of current and voltage signals are considered by Daubechies db4 based DWT. The standard deviation and change in energy coefficients discriminates between islanding and other disturbance conditions. In the proposed method, islanding is detected in 1 cycle by using the first level of energy and standard deviations. Researchers benefit from the compactness and localisation properties of the Daubechies db4 in diminishing NDZ. The proposed scheme is compared with the existing passive (over/under voltage and frequency) scheme, and found very efficient and effective in all working conditions (Hanif, Dwivedi, Basu, & Gaughan, 2010).

Karegar et al. (Karegar & Sobhani, 2012) proposed using the DWT for the islanding detection of wind turbines. Voltage profiles were examined by db5. The proposed scheme proves dependability under different load conditions. In (Hanif, Basu, & Gaughan, 2012), db4 DWT-based technique is utilised for grid connected PV DGs. The spectral changes in the higher frequency components of voltage are analysed for islanding detection. The proposed scheme is found to be very effective, and managed to detect islanding conditions within 0.05 seconds. Sharma et al.(Sharma & Singh, 2012) utilised the localisation and compactness property of the Dyadic wavelet transform for islanding detection. It has been found that the proposed scheme discriminates the islanding and non-islanding scenarios for grid connected PV system in more than 1 cycle. Liu et al. (Y. H. Liu, Luor, Huang, & Lin, 2008) introduces the islanding detection scheme based on WT for the stand alone operation of DG system.

The main disadvantages associated with DWT are the integration of the high frequencies and measurement of several electrical quantities. Therefore, wavelet packet transform (WPT) is proposed in (W. G. Morsi, Diduch, & Chang, 2010). This scheme proposes a new index called node rate of change of power index. This index computes the change of the power at each WPT sub band. The base of WPT is db10, because it has a smaller number of wavelet coefficients. In (Shariatinasab & Akbari, 2010), the "Haar" mother wavelet has been used for islanding detection. This type of mother wavelet requires the least decomposition levels, thus, has the least detection time. This method calculates the current signal at the point of common coupling (PCC) and detects the islanding within 5.5ms. The proposed method is also applicable for multi-DG environment.

In (Jiaxin & Caisheng, 2012), a new feature extraction technique is proposed for islanding detection. This work examine the variations in harmonic profiles for inverter based DG system, and is basically an extension of (Pigazo et al., 2009). Wavelet transform-based multi-resolution analysis (WT-based MRA) technique is used for feature extraction. The WT-based MRA decomposes the output voltage into multiple scales. Each scale produces a sequence of wavelet coefficients (WCs) on the bases of frequency bandwidth. The change in the ratio of the WCs is used for islanding detection. The simulation results prove that the proposed scheme is successful for islanding detection under all operating conditions.

Samui and Samantaray in (Samui & Samantaray, 2012, 2013) proposed a new technique for islanding detection based on wavelet singular entropy (WSE). WSE integrates the advantages of wavelet transform, singular value decomposition, and Shanon entropy. In the proposed scheme, the wavelet transform analyses the three phase voltage signal and generates the detailed coefficients. Singular value matrix is calculated from these detailed coefficients in order to determine the WSE for each phase. Finally, WSE index is produced by adding all the phases of WSE. The proposed scheme is compared with the two existing schemes (rate of change of frequency (ROCOF) and rate of change of power (ROCOP)) in a perfectly matching environment, and it has been found that the proposed scheme detects islanding condition effectively within 10 msec.

2.12.3 S-Transform based Islanding Detection Techniques

Wavelet transform extracts the desired features of the signal from both time and frequency domains. However, batch processing and noise sensitivity are the disadvantages associated with this technique. To overcome these problems, Stockwell proposes s-transform in 1996. In this technique, the properties of both STFT and WT are merged. It is a time-frequency technique having a variable window of STFT and an expansion of WT. It is based on a scalable localising Gaussian window, and supplies the frequency dependent resolution (Dash, Panigrahi, & Panda, 2003; Stockwell, Mansinha, & Lowe, 1996; Ventosa, Simon, Schimmel, Danobeitia, & Manuel, 2008). It provides multi-resolution, and keeps the phase of each frequency component unchanged. It transforms the signal from the time domain to two dimensional frequency domains. Local spectral characteristics are examined either by the amplitude time frequency spectrum, or by the phase time frequency spectrum. In this tool, the sinusoid is fixed with respect to the time axis, and localised scalable Gaussian window examined it more comprehensively by dilating and translating the phase frequency (Dehghani, 2009; Mishra, Bhende, & Panigrahi, 2008). S-transform (ST) provides considerable and noteworthy results in the detection and localisation of disturbances due to islanding or any other condition. Thus, it detects the disturbance signal efficiently and accurately.

In (P. K. Ray, Mohanty, Kishor, & Dubeya, 2010), the islanding detection technique using s-transform is proposed for the hybrid system. It clearly shows the domination of s-transform in comparison to wavelet transform for islanding detection on the bases of the simulation results. Ray et al. (P. K. Ray, Kishor, & Mohanty, 2010; Prakash K. Ray, Mohanty, & Kishor, 2011) extracts the negative sequence voltage for islanding detection. They also compared the wavelet transform and s-transform under noisy conditions. On the basis of the simulation results, it has been found that s-transform determine the islanding scenario proficiently, within 26-28 msec. Islanding detection, on the basis of performance indices, was also conducted, which is another contribution to this field. A new technique that relies on s-transform based cumulative sum detector (CUSUM) is proposed in (Samantaray, Samui, & Babu, 2010). In this proposed technique, the spectral energy contents of the negative sequence voltage and current signals are used for computation. It has been verified that the proposed technique detects the islanding condition in 25 msec with an accuracy of more than 92%.

The problem associated with s-transform is that its performance weakens under certain operating situations, such as transients. The s-transform is modified to hyperbolic s-transform to overcome the adverse effect of transients and to realize a superior signal processing technique (Biswal, Dash, & Panigrahi, 2009; Nantian, Dianguo, & Xiaosheng, 2010). Compared to s-transform, the hyperbolic s-transform has a pseudo Gausian hyperbolic window. It has frequency dependence in its shape in integration to its width and height. This asymmetrical window provides better resolution in both time and frequency at high and low frequencies, respectively. In (S. R. Mohanty, Kishor, Ray, & Catalao, 2012), hyperbolic s-transform is used to detect the islanding condition. The change in energy and standard deviation (STD) of the perturbed voltage signal at PCC is resolute, and on the basis of these predicated values; a suitable threshold is finalised in order to detect an islanding event. The results clearly reveal the advantages of the proposed scheme for islanding detection under both noise and noise-free environments.

2.12.4 TT-Transform based Islanding Detection Techniques

Many time varying frequency techniques are used to process non-stationary signals. Some of the most common techniques are STFT, wavelet, and s-transform. However, these transforms introduce redundancy, passing from a 1-D (one-dimensional) time signal to a 2-D time-frequency (or time-scale) signal. In 2003, an incipient technique based on S-transform is proposed, called the time-time transform (TT-transform). It includes redundancy in time passing from a 1-D time signal to a 2-D time-time signal (Pinnegar & Mansinha, 2003; Simon, Schimmel, & Danobeitia, 2008).

Aziah et al. (H. S. Aziah Khamis, M.Z.C Wanik, 2010) proposed a new signal processing tool i.e TT-transform for islanding detection. The results of the proposed scheme were represented; utilizing 2-D TT transformed plots of the original signals. It was confirmed that the technique is capable of detecting the islanding scenario in a more precise and expeditious manner, because each event possess a distinctive/unique patterns. In (S. R. Mohanty et al., 2012), TT-transform is used to extract the desired features for islanding detection. The results obtained are compared with wavelet and s-transform. It is found that the proposed technique is superior for islanding detection in all conditions.

2.12.5 Hilbert Huang Transform based Islanding Detection Techniques

The Hilbert Huang transform (HHT) is a novel signal processing technique. It consists of two different procedures. In the first stage, the signal to be examined is decomposed into intrinsic mode function (IMF) that have consequential instantaneous frequencies and amplitudes, via utilization of the empirical mode decomposition (EMD) process. In the second stage, the IMFs are sorted from the highest frequency to the lowest frequency. The Hilbert transform can then be applied to each IMF, giving the instantaneous amplitude and instantaneous frequency versus time curve. This combination of EMD process and Hilbert transform is known as the HHT (Afroni, Sutanto, & Stirling, 2013; Drummond & Sutanto, 2010). The dominance of this scheme over wavelet transform, STFT, and S-transform has been presented in literature (Ayenu-Prah & Attoh-Okine, 2009; Donnelly, 2006; Peng, Tse, & Chu, 2005).

In (Mohammadzadeh Niaki & Afsharnia, 2014), an incipient passive islanding detection scheme for inverter-based DGs is offered, which utilises HHT for features extraction. The simulation results showed that the proposed scheme can efficaciously detect islanding in less than two cycles. Moreover, the simplicity, efficacy, expeditiousness, and robustness of the technique against noise are verified in multi-DG systems.

2.13 Computational Techniques for Islanding Detection

The computational techniques are those which are based on human intelligence at imitate level. Some of the most commonly used computational techniques are Artificial Neural Networks (ANN), Artificial Immune system (AIS), Fuzzy Logic Control (FLC), Adaptive Neuro-fuzzy Inference System (ANFIS) and Decision Tree (DT) classifiers as shown in Figure 2.12.

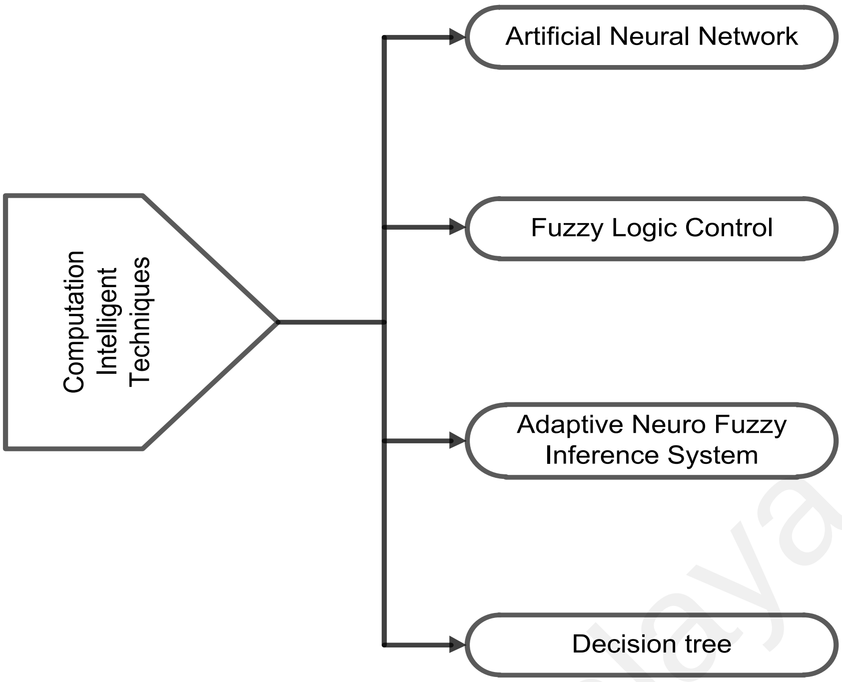

Figure 2.12: Computational intelligent islanding detection techniques

These techniques have been expansively used nowadays and has the ability to resolve nonlinear problems with higher accuracy and speed as compared to conventional techniques. The brief description of these techniques is as follows.

2.13.1 Artificial Neural Network (ANN) based Techniques

Artificial Neural Network (ANN) has been used as an important tool for solving engineering problems (Dias, Antunes, & Mota, 2004). Like the biological system, it also comprises of nodes or neurons. Researchers have been using ANN and its types for islanding detection applications for a long time. For both multiple based (Fayyad & Osman, 2010) and hybrid inverter based DERs (ElNozahy, El-Saadany, & Salama, 2011), ANN based islanding techniques have been presented. The islanding detection parameters are transients in voltage signals (Fayyad & Osman, 2010) and three phase currents (ElNozahy et al., 2011). Both these techniques entail no adverse impact on power quality because of passive nature. By wavelet transform, various features has been extracted from the parameters which are then employed for ANN training. The non-islanding events consist of switching of load, capacitor, single phase, three phase and line-to-line faults at different positions of distribution system. The accuracy obtained by simulations are 97.77% in (Fayyad & Osman, 2010) and 99.1% in (ElNozahy et al., 2011). Moreover, the technique proposed in (ElNozahy et al., 2011) can be executed for real time applications.

(Ghazi & Lotfi, 2010) has proposed ANN based hybrid islanding detection technique for synchronous based DER which combines the passive and active techniques for higher reliability and accuracy. Six parameters such as $\Delta v/dt$,$\Delta f/dt$, $\Delta f/\Delta p$, $\Delta p/dt$, $\Delta Q/dt$, and total harmonic distortion (THD) of current are used for passive technique. While the positive feedback of active/reactive power is utilized in active technique. In active power approach, the change in frequency whereas in reactive power approach, the change in voltage is applied to the compensator which adjusts the reference active power to the DER. This positive feedback intensifies the voltage or frequency limits that results in the islanding detection bearing no negative impact during normal operation. The technique is tested on two distribution networks, and compared with another technique proposed in (El-Arroudi, Joos, Kamwa, & McGillis, 2007). The simulated technique has an accuracy of 88.9%, whereas the proposed technique in (El-Arroudi et al., 2007) was 83.33% accurate. The technique used 6 parameters, whereas the technique proposed in (El-Arroudi et al., 2007) uses 11 parameters (Δf, ΔV, $\Delta f/\Delta t$, $\Delta V/\Delta t$, $\Delta p/\Delta t$, $\Delta f/\Delta p$, CTHD, VTHD, power factor deviation, the absolute value of phase voltage times power factor, the gradient of the voltage times power factor). Hence, the accuracy is improved (Ghazi & Lotfi, 2010).

Another ANN based passive technique for DFIG wind turbines is proposed in (Abd-Elkader, Allam, & Tageldin, 2014). It uses the symmetrical components of the second order harmonics of voltage and current signals. These signals are processed by using

Fourier transform and then fed to ANN for islanding detection. The results validate its ability to discriminate between islanding and other events.

Apart from ANN, its types, such as self-organizing map (SOM) neural network, extension neural network (ENN), probabilistic neural network (PNN), and modular probabilistic neural network (MPNN) have also been used for islanding detection. (Moeini et al., 2010) and (Moeini et al., 2011) has proposed the application of SOM neural network for islanding detection. These techniques use automatic load frequency control signal to direct islanding detection. The accuracy obtained is 97.92% (Moeini et al., 2010) and 98.19% (Moeini et al., 2011), respectively.

(Chao et al., 2011) has proposed an ENN based hybrid islanding technique for PV-based DER. Since it is hybrid technique, wherein voltage, frequency, and phase difference are used as passive parameters, while the active technique utilizes the voltage drift method. The ENN was used to distinguish islanding event and power quality disturbances (voltage swell, voltage dip, power harmonic, and voltage flicker). The simulation results show that islanding can be distinguished from other power quality disturbances properly by using ENN based technique.

In (Lidula & Rajapakse, 2009) the application of PNN for islanding detection was proposed. Using the PSCAD/EMTDC software, the technique is tested on a CIGRE medium voltage distribution system. The overall accuracy obtained by PNN was 90%. The MPNN based islanding detection technique for hybrid DERs (fuel cell, PV, and Wind) was proposed in (Soumya R. Mohanty et al., 2013). This technique has used S-transform for feature extraction and MPNN for classification. It has been tested with noise and diverse power quality signals on experimental prototypes, ultimately, 97.4% accuracy been achieved.

2.13.2 Fuzzy Logic Control (FLC) based Techniques

Fuzzy Logic Control (FLC) models a system with the aid of fuzzy rules which are difficult to be represented by mathematical equations. (Rosolowski Eugeniusz, 2007) used three passive parameters such as voltage, *df/dt*, *dp/dt,* to propose Fuzzy based islanding detection techniques for rotating type DER. The changes are examining in these three parameters using algorithm and fuzzy logic rules are used to detect islanding. Radial distribution system validates this technique and found it proficient to discriminate islanding from non-islanding events.

Another FLC based technique is proposed in (Samantaray, El-Arroudi, Joos, & Kamwa, 2010) and (Kumarswamy, Sandipamu, & Prasanth, 2013) which considers 11 parameters (Δf, ΔV, $\Delta f/\Delta t$, $\Delta V/\Delta t$, $\Delta p/\Delta t$, $\Delta f/\Delta p$, CTHD, VTHD, $\Delta p.f$, absolute ($V/p.f$), gradient ($V/p.f$)) for islanding detection. Initial classification has been made by decision tree (DT). Then, fuzzy membership function and corresponding rules for islanding detection are generated. The technique is verified with and without noise, resulting 100% accuracy.

In (Dash, Padhee, & Panigrahi, 2012), a combination of FLC and S-transform based islanding detection technique is proposed which uses negative sequence voltage and current as input parameters. FLC has been used in order to differentiate between islanding and non-islanding events. This technique is passed under several test cases, and found highly accurate in detecting islanding events with the detection time less than a cycle.

In (Shi & Wu, 2013), an active FLC based technique compatible for photovoltaic systems is proposed. The inverter current tries to regulate the difference in phase at the PCC as it is active technique. Upon disconnection of grid, the frequency deviates from its nominal value results islanding detection. It has shorter detection time (6–20 cycles), and zero NDZ. Aguiar et al. (Aguiar, Bastos, Neves, Reis, & Machado, 2013) uses two active techniques; voltage positive feedback and frequency positive feedback in d_q synchronous frame in FLC based islanding technique. Here, no injection has been made once the DER is coupled with grid. Therefore, islanding can be detected with reduced power quality degradation issues.

An active islanding detection technique Sandia Frequency Shift (SFS) is another technique which has very small NDZ. Taking its advantage, it is widely used for inverter-based DERs. However, NDZ in this technique depends on its design parameters whose improper tuning may results in the failure of this technique. In order to find solution to this problem, Vahedi and Karrari (Vahedi & Karrari, 2013) proposed FLC based technique. This technique regulates the load parameters (R, L, and C) online and adaptively tune the SFS parameter to diminish NDZ in the SFS technique. Here, load quality factor is determined by FLC on the basis of R, L, and C values. Then, positive feedback in SFS is set using that load quality factor in order to avoid failure of islanding detection technique. This technique can be instigated in real time applications as it tunes SFS gain factor on real-time basis.

2.13.3 Adaptive Neuro Fuzzy Inference System (ANFIS) based Techniques

ANFIS classifier is designed to model nonlinear and complex systems bearing less number of training data where ANN and FLC capabilities are combined. ANFIS is also practiced for islanding detection problems. In (Bitaraf, Sheikholeslamzadeh, Ranjbar, & Mozafari, 2012), an ANFIS-based islanding detection technique was proposed wherein five parameters (v, f, I, P, and f/p) are utilized. The accuracy obtained from results were 100% with zero NDZ. It is easy to implement, fast, and is applicable for both multiple and hybrid DERs.

(F. J. Lin, Kuang-Hsiung, & Jian-Hsing, 2012) and (F. J. Lin, Huang, Tan, Chiu, & Chang, 2013) proposed modified ANFIS with wavelet transform for islanding detection. In these techniques, current signal has been injected which diverges the frequency during islanding. These techniques also substitute the conventional PI controller with wavelet fuzzy neural network controller to enhance the accuracy. Results proved that PI controller took 1.06 s, whereas wavelet fuzzy neural network technique took 0.68 s. The merits of this technique are trivial detection time, small NDZs and minimum power quality degradation.

ANFIS based technique for inverter based DER has been presented in (Hashemi et al., 2013) in which the *dp/dt* is used as an input parameter. On the basis of simulation results, it has been found that NDZ reduced to zero without effecting the threshold. ANFIS is also combined with DWT for islanding detection of inverter based DG as proposed in (Shayeghi & Sobhani, 2014), which is based on energy analysis of wavelet coefficients and ANFIS. By the results, it is obtained that in proposed technique NDZ reduced to zero. Furthermore, ANFIS overcomes the need of threshold maintenance.

2.13.4 Decision Tree Classifier based Techniques

Decision Tree (DT) classifier provides a practical solution for all possible inputs by considering their statistical variations. It is useful to figure out unsolved analytical methods. It alters the complex decision-making processes into a combination of simpler decisions (Rovnyak, 2004). The basic DT structure is shown in Figure 2.13 (Lidula & Rajapakse, 2009).

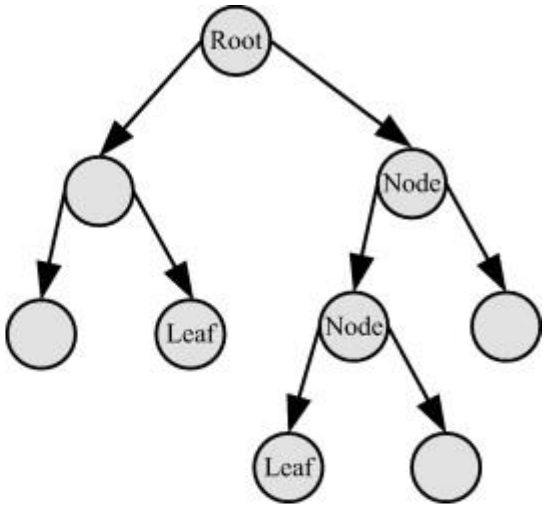

Figure 2.13: Decision tree classifier basic structure

In DT classification, the entire space is considered as a root node. In principle, it works by splitting a root node into child nodes on the basis of predictor variable. A child node can be further divided into other child nodes or a leaf node where no more splits are possible (Rokach & Maimon, 2005). Predictions are made based on the make-up of leaf nodes. To use a decision tree to make a prediction, the split decisions are followed until a leaf node is reached (Madani, Abbaspour, Beiraghi, Dehkordi, & Ranjbar, 2012).

The DT classifier has also been applied for islanding detection techniques. A DT based islanding detection technique is proposed in (Heidari, Seifossadat, & Razaz, 2013b) wherein DWT is used to extract the features from both voltage and current. These features are then processed by DT for islanding detection. The simulation results showed that the technique based on voltage signal has a quick detection, simpler, and cheap as compared to the other techniques. It is 98% accurate and has detection time of one cycle.

(Lidula & Rajapakse, 2010) proposed a DT based islanding detection technique utilizing DWT for feature extraction from both voltage and current transient signals. These extracted signals are used as an input by DT classifier for discrimination. This technique has been validated on CIGRE medium voltage distribution system with multiple DGs using PSCAD/EMTDC software. This technique is 96.43% accurate with detection time of two cycles. The assessment of this technique is presented in another paper, considered as part-II (Lidula & Rajapakse, 2012) where the test system consists of VSC based DC source. This technique is also validated with the other passive techniques and found 96.11 ± 1.405% accurate. The detection time for this technique is two cycles for synchronous generator based DG, and three cycles for VSC based DC source and the induction generator. As compared to other passive techniques, it is more accurate, has fast detection time and zero NDZ.

Pham et al. (Pham, Denboer, Lidula, Perera, & Rajapakse, 2011) works on the hardware implementation of the proposed technique wherein the analogue electronics replaces the feature extraction methodology. With the help of digital signal processing (DSP) kit, hardware implementation is performed easily. Furthermore, DT approach is also compared with two other pattern recognition techniques (support vector machine and modular probabilistic neural network) (Lidula & Rajapakse, 2009). On average, the accuracy achieved by decision tree, modular probabilistic neural network, and support vector machine was 99.61%, 90%, and 78%, respectively. The detection time by using DT was 0.0223 sec. Consequently, DT-based technique surpasses those of MPNN and SVM based techniques.

(El-Arroudi et al., 2007) has proposed decision tree based islanding detection technique, utilizing 11 parameters (Δf, ΔV, $\Delta f/\Delta t$, $\Delta V/\Delta t$, $\Delta p/\Delta t$, $\Delta f/\Delta p$, CTHD, VTHD, power factor deviation, the absolute value of phase voltage times power factor, the gradient of the voltage times power factor) to detect islanding. Mainly the emphasis was to design a technique that can detect islanding for broader network topology. Using data mining approach, the information was gathered and is supplied to DT based classifier for islanding detection. It was tested on multiple DG resources. Through the simulation results it is obtained that the detection time for this technique is 45-50 ms without upsetting threshold. Another application of DT for threshold setting of islanding detection relays is proposed in (El-Arroudi & Joos, 2007). It uses decision tree data mining technology to extract threshold settings of islanding relays from the analyses of system parameters (voltage, current, power, power factor, frequency). The approach is tested on a multiple DG resources, and the result indicates that this approach can be used to optimize the detection threshold settings of the existing islanding detection techniques (El-Arroudi & Joos, 2007).

The DT classifier has also been combined with other tools to enhance the accuracy for islanding detection. Its application in combination with adaptive boosting (AdaBoost) is proposed in (Madani et al., 2012). The technique is suitable for PV, Doubly Fed Induction Generator (DFIG) units, and synchronous generator based DGs. AdaBoost algorithm linearly combines the set of weak classifiers in order to generate a strong classifier. On the basis of simulation results, it has been found that this technique bears trivial NDZ. DT is also combined with FLC for islanding detection that considers 11 parameters as presented in (Samantaray, El-Arroudi, et al., 2010) and (Kumarswamy et al., 2013). Results have shown 100% efficiency with and without noise and therefore, could be utilized for real time applications.

2.14 Signal Processing based Techniques with Intelligent Classifier

Until now, the islanding detection techniques relying solely on the signal processing and computational tools are discussed. In signal processing based islanding detection techniques, the desired features are extracted from the input signal and compared to a threshold value. The selection of threshold value is quite a difficult task. If its value is set high, then islanding will not be detected, while if it is set very low, then it trips the

DG even for the case of disturbances. To overcome this issue, intelligent classifiers have been combined with signal processing based islanding detection techniques. Intelligent classifiers commonly used in signal processing based islanding detection techniques are decision tree (DT), artificial neural network (ANN), probabilistic neural network (PNN), adaptive neuro fuzzy inference system (ANFIS), random forest (RF), support vector machine (SVM) and Fuzzy logic control. These intelligent classifiers enhanced the efficiency, speed, accuracy, and can detect islanding without using any threshold settings, as in the case of common signal processing-based passive techniques. The basic theme of this scheme is shown in Figure 2.15.

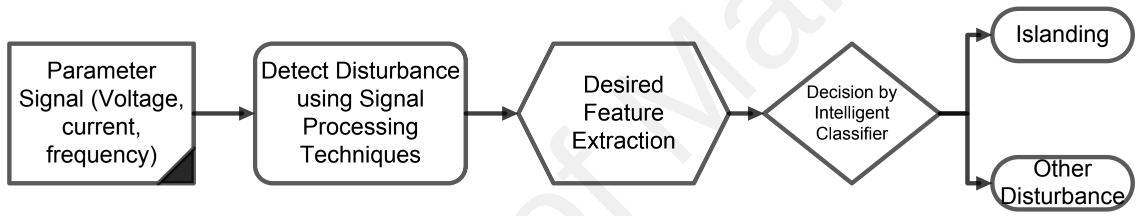

Figure 2.14: Basic block diagram of SP based technique with intelligent classifier

Guiliang (Guiliang, 2005) presented a new technique for islanding detection based on FFT for feature extraction and artificial immune system (AIS) as intelligent classifier, respectively. On the basis of the simulation results, it was verified that the proposed scheme was very efficient, and requires very advanced digital signal processor (DSP) for it to be implemented. In (Kar & Samantaray, 2014) and (Abd-Elkader et al., 2014), the researchers used an intelligent classifier, along with the DFT to check the efficiency and reliability of the system. Kar and Samantaray (Kar & Samantaray, 2014), derives 27 features through DFT pre-processor in order to train the data mining model. The data mining model consists of decision tree (DT), random forest (RF), and support vector machine (SVM). The proposed scheme is tested by taking into account the inverter and synchronous based DG in the micro-grid and the accuracy of these intelligent classifiers are compared. The accuracy of SVM and RF is very close to DT, but the implementation of DT on DSP/FPGA is quite easy compared to SVM and RF. The proposed scheme detects the islanding condition in less than 1.5 cycles. This DT model is also compared with (Far, Rodolakis, & Joos, 2012), which took into account 11 features for islanding detection. It is concluded that the proposed scheme is more comprehensive in making assessments, and seriously impact decision boundaries. The proposed scheme also provides a more generalised solution for both synchronous and inverter based DG compared to the existing intelligent anti-islanding models based only on synchronous based DG (Samantaray, El-Arroudi, et al., 2010). Abd-Elkader et al. (Abd-Elkader et al., 2014) processes the voltage and current signals with DFT to extract the 2^{nd} harmonic components. These components are fed to artificial neural network (ANN) for decision making. This proposed passive scheme for double fed induction generator (DFIG) wind turbines detect the islanding condition within 2 cycles, and has no NDZ if the load values are within the prescribed limits.

Lidula et al. (Arachchige & Rajapakse, 2011) proposed a novel pattern recognition approach for fast islanding detection. DWT is used to extract the desired features of transient voltage and current signals, and to train the decision tree (DT) classifier for islanding detection. The proposed scheme is tested on a medium voltage distribution system with multiple DGs, and it detects islanding within 24 msec. The same scheme is further tested in (Lidula & Rajapakse, 2010) for synchronous and induction type DGs. In this case, it detects islanding condition within two cycles, with more than 98% accuracy. The proposed method is again checked for VSC-based DG and induction generator. In this scenario, the islanding is detected within 3 cycles. Furthermore, it is also robust, despite the fact that the voltage and current profiles are riddled with noise signals (Lidula & Rajapakse, 2012).

In (Shayeghi & Sobhani, 2014), a novel technique is proposed based on ANFIS classifier and 'Haar' mother wavelet based DWT. The proposed technique reduces the NDZ to zero along with the islanding detection within prescribe limits. Heidari et al. (Heidari, Seifossadat, & Razaz, 2013a) uses DWT and decision tree (DT) to examine the voltage transient signal for islanding detection. It is verified that the proposed scheme detects the islanding condition within one cycle. Simplicity, speed, low cost and high accuracy are the merits associated with this technique. In (Fayyad & Osman, 2010), DWT and artificial neural network (ANN) based islanding detection technique is proposed. It is indicated that the proposed method detects the islanding condition with high accuracy. Furthermore, it is also proven that the proposed technique is superior to the commonly used under and over voltage and frequency (UFP/OFP and UVP/OVP) techniques.

Although S-transform (ST) has the potential to assess the power signals perturbances, it requires more computational time to process the signal. Thus, the conventional ST is unsuitable for authentic-time applications, unless its speed is significantly incremented. There have been some methods that reduces the computational time for the calculation of discrete ST, such as Generalized Fourier family transform (GFT) (Brown, Lauzon, & Frayne, 2010). The GFT algorithm amalgamates down sampling and signal cropping to generate a discrete Fast S-transform (DFST). Such a scheme diminishes the retrieval of unwanted information, thereby constraining the computational requisites. Dash et al. (Dash et al., 2012) proposed an incipient islanding detection method predicated on DFST and Fuzzy system. Both the negative sequence voltage and currents are quantified at the DG location, which are utilised as inputs to the DFST processing module, resulting in features like spectral energy and standard deviation. For detecting power islands, the features from DFST exhibiting consequential fluctuations are given as inputs to the Fuzzy classifier for the relegation of a non-islanding and islanding event. Upon utilising the proposed scheme on different distribution network, it is verified that the detection time is less than a cycle.

A comparative study on some of the signal processing techniques for islanding detection has been presented in (S. Mohanty et al., 2014). The proposed scheme extracts the negative sequence components of voltage signal using hyperbolic s-transform (HST), TT-transform (TTT), and mathematical morphology methods. The decision between islanding and non-islanding conditions is made by support vector machine (SVM). It is presented that HST, TTT, and mathematical morphology methods are more accurate compared to commonly used ST and WT. Furthermore, the proposed technique also works effectively in noisy and noise-free environments.

2.15 Miscellaneous Feature Extraction Techniques

Apart from these techniques, there are some other signal processing techniques playing a paramount role in feature extraction for islanding detection. In (H. S. Aziah Khamis, 2013; Khamis, Shareef, Mohamed, & Bizkevelci, 2015), the phase space technique is used to extract the desired features from the signal. In (H. S. Aziah Khamis, 2013), radial basis function (RBF) and probabilistic neural network (PNN) classifiers are utilised for decision-making in combination with phase space technique. On the basis of the results, it is verified that PNN is better and works more efficiently than RBF. In (Khamis et al., 2015), performance evaluation has been conducted between the radial basis function neural network (RBFNN) and probabilistic neural network (PNN) using phase space technique as a signal extractor. The results proved that the PNN classifier is more superior to RBFNN, and has an accuracy of 100%.

Zeineldin et al. (Zeineldin, Abdel-Galil, El-Saadany, & Salama, 2007) presented a new islanding detection technique for synchronous DGs based on total least square estimation of signal parameters via rotational invariance techniques (TLS-ESPRIT). This new technique is predicated on two incipient parameters for islanding detection; the frequency of oscillation and the damping factor of the DG frequency output. Negligible NDZ is a paramount advantage of this technique.

2.16 Comparative Analysis between Islanding Detection Techniques

It has been found that the computational intelligent classifier based techniques are the preferred over the passive, active, hybrid and signal processing based techniques for islanding detection. In detecting islanding condition, their performance surpasses those of the conventional techniques in terms of detection time and accuracy without affecting power quality. Furthermore, they can also overcome the non-detection zone and threshold setting that have been the Achilles heels of conventional techniques. These techniques also have the potential to work in multiple DER's environment with very high reliability. A performance comparison among remote, local, signal processing and computational intelligent based techniques are summarized in Table 2.4.

Table 2.4: Comparison among different islanding detection techniques

Characteristics	**Remote Techniques**	**Local Techniques**			**Signal Processing based techniques**	**Intelligent classifier based techniques**
		Passive	**Active**	**Hybrid**		
Principle	Communication between utility grid and DGR	Monitor natural effects of islanding	Inject disturbances	Combination of both passive and active	Monitor changes in system parameters.	Monitor changes in system parameters.
Detection time	Short	Short	Long	Long	Very short	Very short
Impact on power quality	No	No	High	Very small	No	No
Non detection zone	None	Large	Small	Very small	No	No
Reliability	High	Low	High	High	Very high	Very high
Cost	High	Low	Low	Low	Low but higher than intelligent techniques	Low
Effect on distribution system	None	None	Direct influence	Lower than active	None	None
Multiple DGs operation	Possible	Possible	Not possible	Possible	Possible	Possible

From Table 2.4, it can be observed that computational intelligent based techniques are more efficient and reliable compared to the existing islanding detection techniques. Although computational intelligent based techniques use similar parameters as the passive techniques, they achieve a higher precision in dealing with complex systems, due to their versatility, stability, and robustness.

2.17 Summary

In this chapter DERs, their benefits and future impact are discussed. It also discusses the operation modes of DERs. The emphasis however is islanding. Islanding imposes many technical challenges as elaborated in this chapter. Since, it is unavoidable, thus, some power supply regulators have developed various islanding standards for effective intentional islanding control.

A comprehensive review on conventional techniques of islanding detection with their advantages and weaknesses is given. This is followed by a description of well-known signal processing and computational intelligent techniques that have been incorporated into the conventional methods to improve their performance and overcome their inherent limitations. The application of intelligent classifiers, along with signal processing techniques to achieve even higher accuracy, faster detection, and better compatibility are also discussed. It is worth mentioning that the application of signal processing tools and intelligent classifiers entails no negative side effects on the power quality and system reliability. For passive islanding detection techniques, the incorporation of intelligent classifiers has helped overcome their limitations of large non detection zone and threshold setting. Efficient intelligent islanding detection techniques play an important role for a successful islanding operation of DERs. Their implementation can enhance the reliability and power quality of the system, and is thus preferable over the conventional islanding detection techniques. Hence, this research proposes a new computational intelligent islanding detection technique for distribution network connected with DERs.

CHAPTER 3: POWER SYSTEM PARAMETERS SENSITIVITY ANALYSIS

3.1 Introduction

Up till now various islanding detection techniques have been discussed. From these, passive techniques are beneficial in terms of lower power quality degradation, low-priced and extensive usage by utility companies. However, large non-detection zone and threshold setting requirement bounds the inherent advantages of these techniques.

This chapter examines the sensitivity of 16 different power system parameters that can be used in passive techniques to detect islanding and non-islanding events, followed by the performance based ranking analysis. On the basis of the ranking analysis, it is observed that the rate of change of frequency over reactive power (*df/dq*) can effectively detect minute disturbances in power supply. The choice of *df/dq* is also analyzed analytically to further validate the choice of most sensitive parameter.

3.2 Stipulation for Sensitivity Analysis

Based on the extensive literature review in Chapter 2, it can be observed that the majority of power utility companies employ passive techniques to detect islanding, mostly due to their low cost and decreased power quality problems (Laaksonen, 2013). Most passive techniques use only one of the following parameters to detect islanding, which are rate of change of frequency (Zeineldin & Kirtley, 2009), rate of change of output power (Redfern, Usta, & Fielding, 1993), change of harmonic impedance (Sumner, Palethorpe, Thomas, Zanchetta, & Di Piazza, 2002), and phase shift (Guo-Kiang, Chih-Chang, & Chen, 2003). However, it is pretty clear that techniques that depend only on a single parameter are less accurate and have a large non-detection zone (NDZ). Thus, if more parameters are utilized, the accuracy will increase while the NDZ decrease, especially in closely mismatched conditions. A literature survey on passive techniques that employ two parameters or more reveals only a few published works using a combination of selected parameters, such as the rate of change of frequency and output power (Fu-Sheng & Shyh-Jier, 2001), voltage unbalance and total harmonic distortion current (Sung-Il & Kwang-Ho, 2004), rate of change of voltage and change in power factor (Salman et al., 2001). In all of these reported works, the use of two parameters help enhances the accuracy of the passive techniques and minimizes the non-detection zone.

The introduction of computational intelligent-based approaches heralded a new era for passive islanding detection techniques. In these techniques, many parameters including indices and their corresponding rates of changes are used. Faqhruldin et al. (Faqhruldin, El-Saadany, & Zeineldin, 2014) employed 21 parameters comprising 14 indices and 7 rates of change, Alam et al. (Alam, Muttaqi, & Bouzerdoum, 2014) used 3 indices and 2 rates of change, K. El-Arroudi and G. Joos (El-Arroudi & Joos, 2007) utilized 2 indices and 2 rates of change, Kar et al. (Kar & Samantaray, 2014) employed 13 indices and 14 rates of change, and 7 indices and 4 rates of change were used by (El-Arroudi et al., 2007; Samantaray, El-Arroudi, et al., 2010). All of these parameters (indices and rate of changes) are used as inputs to different computational intelligent classifiers to distinguish islanding and non-islanding events in critical conditions. These techniques show higher accuracy and overcome the inherited issues of passive techniques such as NDZ and threshold setting. However, the use of multiple parameters in computational intelligent techniques render them quite complex, making them only effective when used with intelligent classifiers. Furthermore, it is observed that there is no proper method presented regarding the selection of parameters for classifier input. In practice, simple and economical techniques are preferable.

In view of the noteworthy benefits of the intelligent relays, it has become necessary for utility companies as well as for DER owners to understand the attributes of the passive parameters in terms of sensitivity analysis. This analysis will help the selection of parameters for classifier to discriminate the islanding events from non-islanding events. The aim of this work is to propose the islanding detection techniques hinged on performance based ranking of different passive parameters in the context of frequency, voltage, active power, reactive power, and their derivatives. Sixteen different passive parameters (Table 3.9) are studied under all possible islanding and non-islanding conditions to prioritize these parameters through simulation regarding sensitivity analysis. Based on observations, a unique passive and computational intelligent techniques utilizing the most sensitive parameters for islanding detection are proposed.

3.3 Modelling of Test System

The test system which is taken into account for sensitivity analysis and proposed islanding detection techniques belongs to current 11 kV Malaysia distribution system and is shown in Figure 3.1. It comprises of a mini hydro (MH), an induction generator (IG), a photovoltaic generation (PV), utility grid, 33 buses and 29 lumped loads. The test system is developed in PSCAD environment and the standard models of MH, IG, PV and transformers from PSCAD library are used. These models are explained in the following sub-sections briefly.

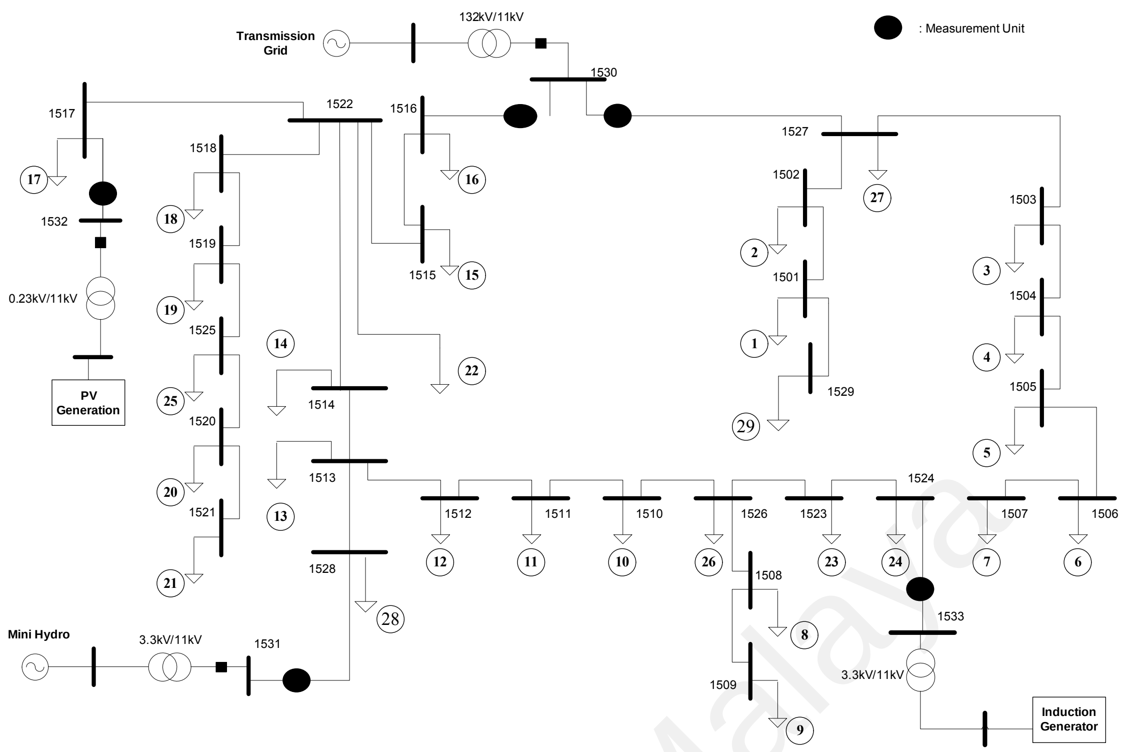

Figure 3.1: Distribution system under study

3.3.1 Mini Hydro Generator

The mini hydro type DER is modelled by using standard models of exciter, governor and hydraulic turbine provided in PSCAD/EMTDC library as follows:

3.3.1.1 Exciter Model for Synchronous Generators

The main job of an excitation system is to supply direct current to the synchronous machine field winding. Additionally, it also performs control functions essential to the satisfactory performance of power system. Control function includes the control of voltage and reactive power flow. Excitation system provides supply and automatically adjusts field current of synchronous generator to maintain the terminal voltage. Exciters are modelled as dynamic transfer functions in PSCAD/EMTDC software. The exciter model can be interfaced directly to the synchronous machine. The excitation system model chosen in this research is based on IEEE type AC1A standard model. Its block diagram is shown in Figure 3.2.

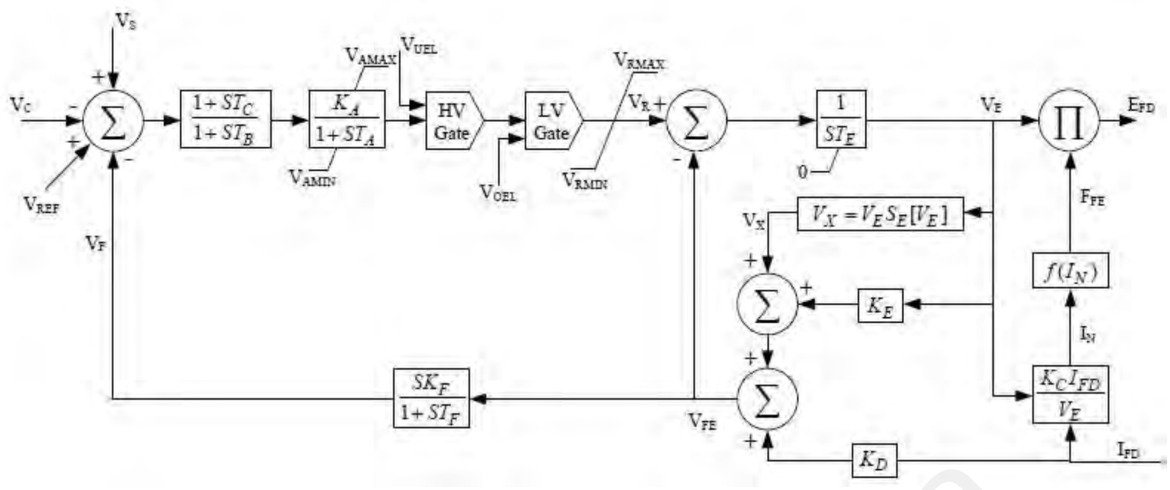

Figure 3.2: IEEE type AC1A exciter model

This model provides a field-controlled alternator excitation system with un-controlled rectifiers, and is applicable to brushless excitation systems (Kundur, 1994). The exciter does not employ self-excitation, and voltage regulator power is taken from a source that is not affected by external transients. Typical parameters used in this research are presented in Table 3.1.

Table 3.1: Values of IEEE AC1A exciter model

Parameter	**Value**	**Parameter**	**Value**	**Parameter**	**Value**
T_C	0	K_F	0.03	T_B	0
T_F	1	K_A	400	T_E	0.8
T_A	0.02	K_E	1	V_{AMAX}	14.5
K_C	0.2	V_{AMIN}	-14.5	K_D	0.38
V_{RMAX}	6.03	V_{RMIN}	-5.43	$SE_{(VE1)}$	0.1
$SE_{(VE2)}$	0.03	VE_1	4.18	VE_2	3.14

3.3.1.2 Hydraulic Turbine and Governor Model

A governor regulates the generator speed in order to keep frequency at a constant value. The governor senses speed variation and control the turbine gate for water flow. A governor and turbine determine the mechanical torque and power applied to the generator. The general block diagram consisting of hydraulic turbine and governor is shown in Figure 3.3.

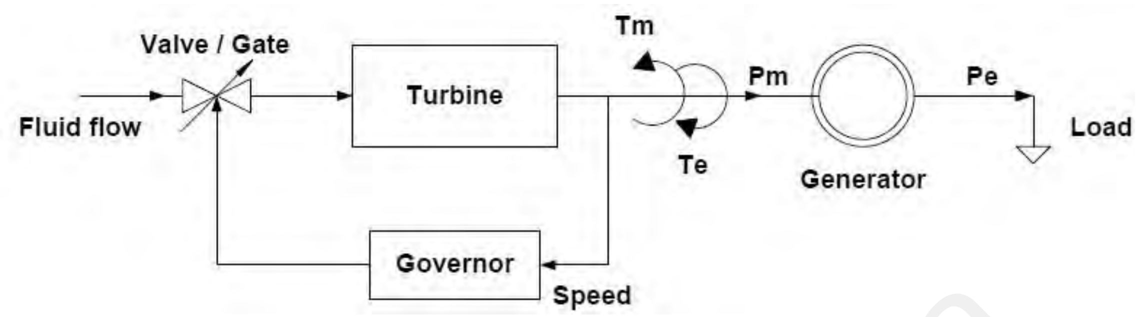

Figure 3.3: Turbine speed control with governor

In this test system, the hydraulic turbine and governor, control the system's frequency. Once the load is disconnected from the system and after demand decreases, the turbine governor must respond promptly to close the hydraulic valve and immediately divert water flow to prevent hydro turbine over speeding. It is therefore extremely important to install a fast response valve operating mechanism. Another situation is posed by rising load demand in the system. The turbine governor must respond quickly to open the hydraulic valve and avert under speeding of the hydro turbine and generator. This research work employs electro-hydraulic PID governor for speed control. Figure 3.4 shows the block diagram of electro-hydraulic PID governor.

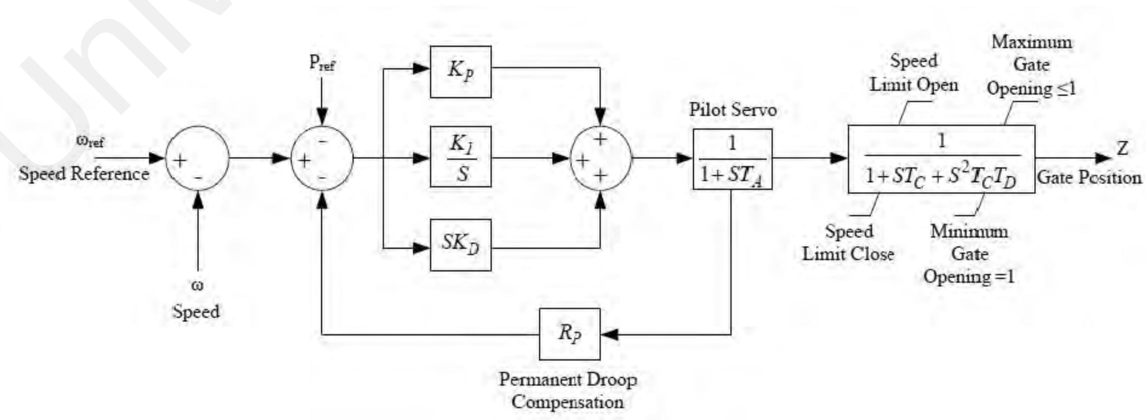

Figure 3.4: Electro-hydraulic PID governor

In Figure 3.4, T_A is the time constant of pilot valve and servomotor. T_C is a gate servo gain and T_D is the gate servomotor time constant. Permanent droop is shown by R_P. The governor model has two important parameters, maximum gate opening rate and maximum gate closing rate. These values illustrate the opening or closing of gate speed because the response in hydraulic turbine is slower than steam or gas turbine. The parameters values employed for governor are given in Table 3.2. However, the values for P, I and D are tuned by using trial and error method to provide satisfactory results.

Table 3.2: Hydraulic governor values

Parameter	**Value**	**Parameter**	**Value**
K_P	2.25	T_C	0.2
K_I	0.37	T_D	0.2
K_D	0.9	Max gate opening	0.16
T_A	0.05	Max gate closing	0.16
R_P	0.04	Dead band value	0
Max gate position	1.0	Min gate position	0

While the governor sends control signal to servomotor for controlling the turbine gate position, the servomotor controls water flow to produce power according to load demand. The transfer function for relay valve and gate servomotor is given by (Kundur, 1994):

$$\frac{G(s)}{B(s)} = \frac{K_s}{s(1+sT_p)} \tag{3.1}$$

where, K_S is servo gain and T_P is time constant of servomotor. Servomotor controls the gate of turbine through governor and hydraulic turbine converts water head potential energy into mechanical energy. The hydraulic turbine transfer function is given as below (Kishor, Saini, & Singh, 2007)

$$\frac{\Delta P_m}{\Delta G} = \frac{1 - T_w s}{1 + 0.5 T_w s} \tag{3.2}$$

Where ΔP_m represents mechanical power of turbine in per unit, ΔG represents turbine gate opening in per unit and T_w represents turbine water starting time. T_w varies with load and its values lies between 0.5 s and 4.0 s. In this research, the water column of the hydraulic turbine is considered non-elastic without surge tank. The block diagram of a hydraulic turbine is shown in Figure 3.5.

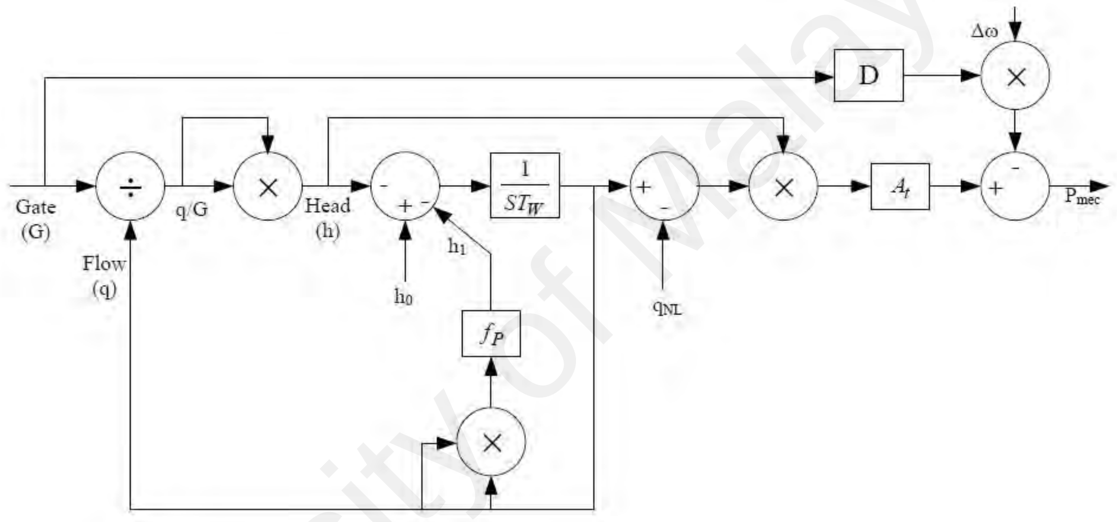

Figure 3.5: Hydraulic turbine

The parameter values of hydraulic turbine used in this research are shown in Table 3.3.

Table 3.3 Parameter values of hydraulic turbine

Parameter	**Value**	**Parameter**	**Value**
f_p	0.02	D	0.5
initial output power	0.7	Initial operating head	1.0
Rated output power	1.0		

In Table 3.3, f_p acts as a penstock head loss coefficient and D is turbine damping constant.

3.3.1.3 Synchronous Generator Model

This research employs a mini-hydro type DER, having a nominal terminal voltage of 3.3kV. It supplies a local load of 1.8 MW and 0.7 MVar and employs synchronous generators as the mean of producing electrical energy. The synchronous generator is driven by hydraulic turbine and governor control mechanism. The generator is also equipped with excitation control as it is important requirement for maintaining voltage level within permissible limits. Figure 3.6 shows the synchronous generator with PID based governor, hydraulic turbine and excitation control modelled in PSCAD.

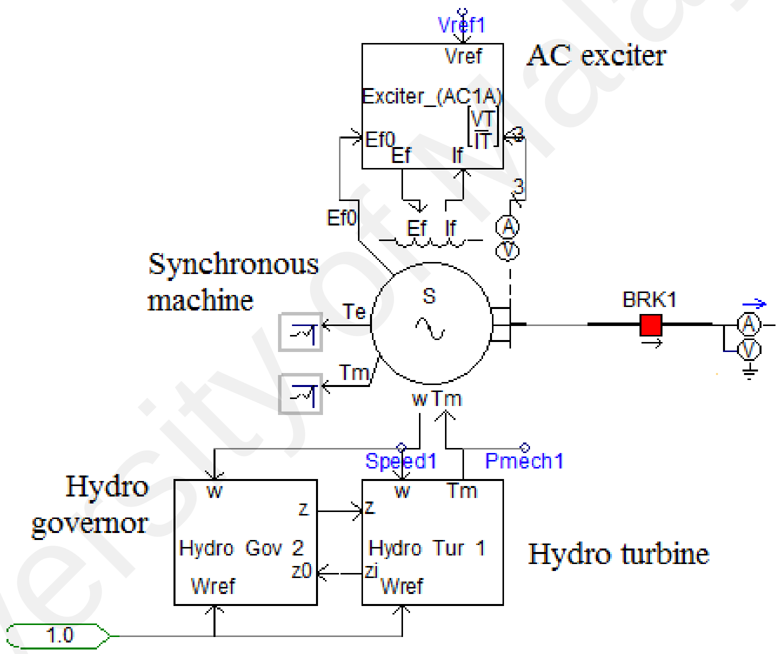

Figure 3.6: Synchronous generator

The synchronous generator parameters for this test system are given in Table 3.4.

Table 3.4: Synchronous generator parameters

Parameter	Value
Rated RMS line-to-line voltage	3.3 kV
Rated RMS line current	350 A
Inertia constant (*H*)	2.5 s
Iron loss resistance	300 p.u
Base angular frequency	314.159 rad/s
Armature resistance [*Ra*]	0.01 p.u
Potier reactance [*Xp*]	0.104 p.u
Unsaturated reactance [*Xd*]	0.838 p.u
Unsaturated transient reactance [*Xd'*]	0.239 p.u
Unsaturated transient time [*Tdo'*]	8.0 s
Unsaturated sub transient reactance [*Xd''*]	0.12 p.u
Unsaturated sub transient time [*Tdo''*]	0.05 s
Unsaturated reactance [*Xq*]	0.534 p.u
Unsaturated sub transient reactance [*Xq''*]	0.12 p.u
Unsaturated sub transient time [*Tqo''*]	0.1 p.u
Air gap factor	1.0

3.3.2 Modelling of PV Generation

The brief description of the PV system is as follows:

3.3.2.1 PV Array

The parameters which were used to define the PV module in this research are shown in Table 3.5.

Table 3.5: Parameters of the PV module

PV array parameters	No. of modules connected in series/array	20
	No. of module strings connected in parallel/array	20
	No. of cells connected in series/module	108
	No. of cells strings in parallel/module	4
	Reference irradiation (W/m^2)	1000
	Reference cell temperature (^0C)	25
PV cell parameters	Effective area/cell (m2)	0.01
	Series resistance/cell (Ω)	0.02
	Shunt resistance/cell (Ω)	1000
	Diode ideality factor	1.5
	Band gap energy (eV)	1.103
	Saturation circuit current at reference conditions/cell (A)	$1x10^{-9}$
	Short circuit current at reference conditions/cell (A)	2.5
	Temperature coefficient of photo current (A/K)	0.001

The model follows the Standard Test Conditions (STC) where a module is consistently checked in a laboratory with intensity of irradiance of 1000 W/m^2, AM1.5 solar spectrum reference and module temperature of 25±2 ^{0}C (61215-2:2005, 2005).

3.3.2.2 Maximum Power Point Tracking

The output current (*Ipv*) and voltage (*Vpv*) from the PV array is inserted into a first order low pass filter bearing magnitude, G = 1 and a time constant, T = 0.01 seconds which cleans the high frequency components. The cleaned voltage (*Vpv_F*) and current (*Ipv_F*) signals are injected into the incremental conductance tracking algorithm based MPPT control block. This algorithm is centred at the slope of PV array power curve whose value is 0 at the Maximum Power Point (MPP). It is positive if it lies on the left of MPP or negative if it lies on right. MPP can be traced by comparing the instantaneous conductance (I/V) with the incremental conductance ($\Delta I/\Delta V$) (Esram & Chapman, 2007):

$$\frac{\Delta I}{\Delta V} = \frac{-I}{V}, \qquad \text{at MPP}$$

$$\frac{\Delta I}{\Delta V} > \frac{-I}{V}, \qquad \text{left of MPP} \tag{3.3}$$

$$\frac{\Delta I}{\Delta V} < \frac{-I}{V}, \qquad \text{right of MPP}$$

According to this condition, the reference voltage (*Vmppt*) produced from MPPT enforces the PV module to work. The basic incremental conductance tracking algorithm is shown in Figure 3.7.

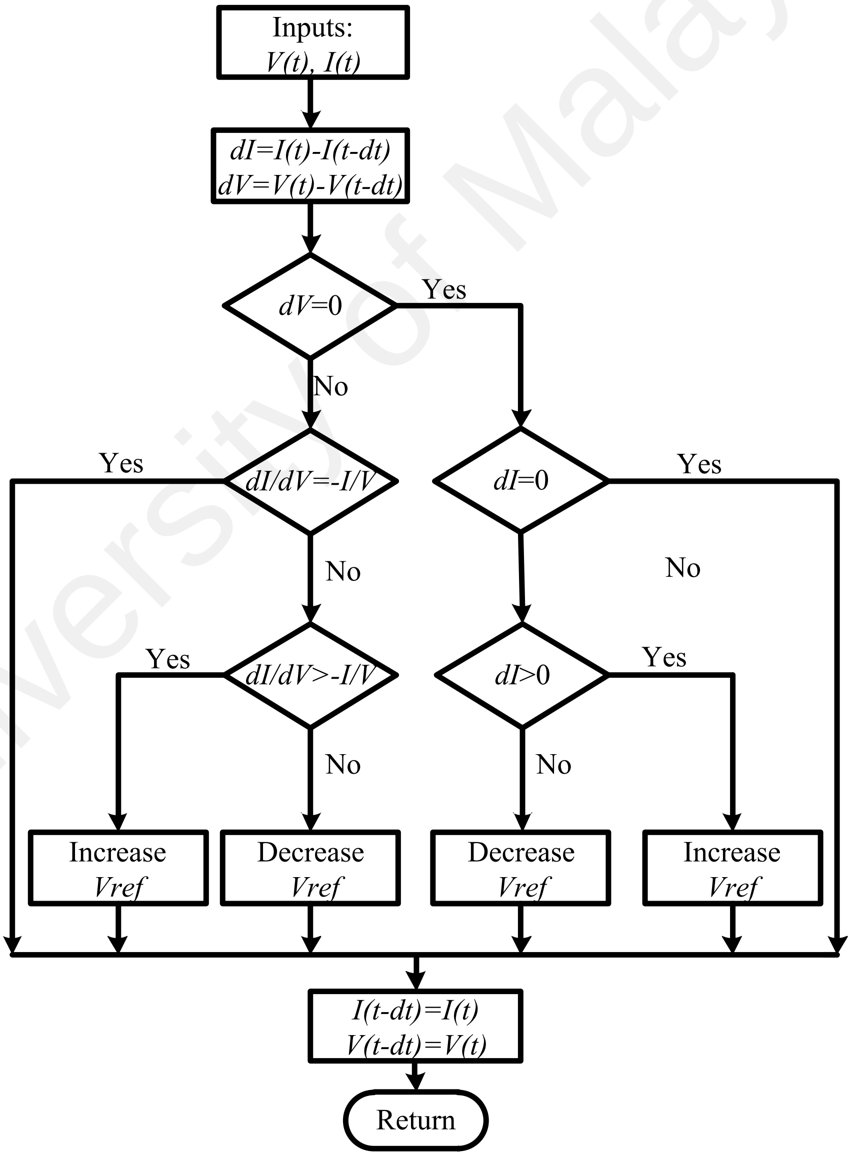

Figure 3.7: Incremental conductance tracking algorithm

3.3.3 Induction Generator

An induction generator (0.05MW), used in this research has a nominal terminal voltage of 3.3kV. The associated parameters are shown in Table 3.6.

Table 3.6: Induction generator parameters

Parameter	**Value**
Base angular frequency	314.16 rad/sec
Stator resistance	0.02 p.u
First cage resistance	0.12 p.u
Second cage resistance	0.012 p.u
Stator unsaturated leakage reactance	0.0792 p.u
Unsaturated magnetizing reactance	3.86 p.u
Rotor unsaturated mutual reactance	0.122 p.u
Second cage unsaturated reactance	0.105 p.u
Polar moment of inertia	5.0 sec
Mechanical damping	0.008 p.u

3.3.4 Transformer

Each generating unit is connected with a step-up transformer. The step-up transformers convert the generated voltage to 11 kV voltage, as the distribution voltage level is 11 kV. The transformer parameters employed in this research are also based on real values of transformers employed by TNB, Malaysia. Table 3.7 shows the parameters of each of the transformers connected to the mini hydro, PV generation, induction generator and the grid.

Table 3.7: Transformers parameter

Parameter	**Mini hydro**	**PV**	**Induction Generator**	**Grid**
Type	Step-up (3.3kV/11kV)	Step-up (0.23kV/11kV)	Step-up (3.3kV/11kV)	Step-down (132kV/11kV)
3-phase transformer MVA	2MVA	1MVA	0.6 MVA	2MVA
Primary winding type	Delta	Star	Delta	Delta
Secondary winding type	Star	Star	Star	Star
Positive sequence leakage reactance	0.08 p.u	0.1 p.u	0.045 p.u	0.08 p.u
Air core resistance	0.2 p.u	0.2 p.u	0.2 p.u	0.2 p.u
Inrush decay time constant	1s	0.5s	1.0 s	1s
Knee voltage	1.25 p.u	1.25 p.u	1.25 p.u	1.25 p.u
Magnetizing current	0.001%	0.1%	1%	0.001%

3.4 Modelling of System in IEEE 1547 Test Frame

The IEEE 1547-2003 protocol provides a standard test frame to verify the performance of the islanding detection techniques. Hence, the 33-bus system (Figure 3.1) is modeled on the aforementioned test frame, as shown in Figure 3.8.

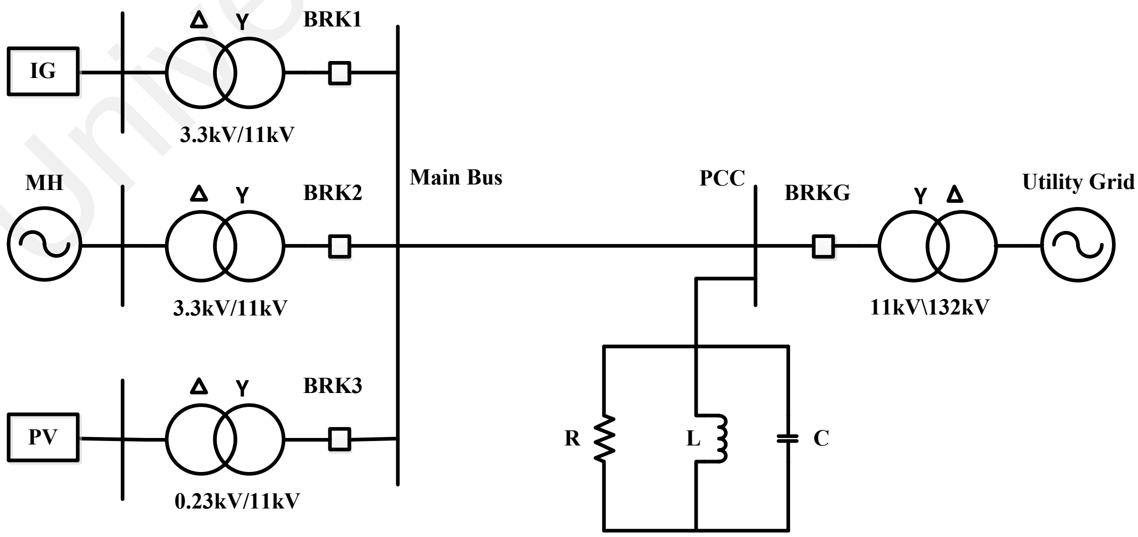

Figure 3.8: IEEE 1547 standard test system

The performance of the islanding detection scheme depends entirely on the nature of the load. Hence, the IEEE 1547 standard recommends selecting a parallel RLC load to validate the performance of an islanding detection technique, as it is more rigorous as opposed to other types of load. The IEEE 1547 test frame indices for the DERs and loads are presented in Table 3.8.

Table 3.8: IEEE test frame indices

Indices	Value	Indices	Value
Mini hydro rating	2 MVA	Voltage (L-L)	11 kV
Induction generator rating	0.05 MW	Resistance	42.46 Ω
Photovoltaic generation	1.00 MW	Capacitance	29.11 μF
Frequency	50 Hz	Inductance	0.348 H

3.5 Simulation Analysis for Sensitive Parameter Selection

The performance analysis of multiple passive parameters, such as rate of change of power (*dp/dt*), rate of change of reactive power (*dq/dt*), rate of change of frequency (*df/dt*), rate of change of voltage (*dv/dt*), and all other possible combinations were evaluated via simulations. Table 3.9 list details of these parameters.

Table 3.9: Different passive parameters used for sensitivity analysis

No.	Passive parameters
1	Rate of change of active power (*dp/dt*)
2	Rate of change of frequency (*df/dt*)
3	Rate of change of reactive power (*dq/dt*)
4	Rate of change of voltage (*dv/dt*)
5	Rate of change of reactive power over active power (*dq/dp*)
6	Rate of change of reactive power over voltage (*dq/dv*)
7	Rate of change of frequency over reactive power (*df/dq*)
8	Rate of change of voltage over active power (*dv/dp*)
9	Rate of change of active power over reactive power (*dp/dq*)
10	Rate of change of voltage over reactive power (*dv/dq*)
11	Rate of change of reactive power over frequency (*dq/df*)
12	Rate of change of active power over voltage (*dp/dv*)
13	Rate of change of active power over frequency (*dp/df*)
14	Rate of change of voltage over frequency (*dv/df*)
15	Rate of change of frequency over active power (*df/dp*)
16	Rate of change of frequency over voltage (*df/dv*)

In total, 16 parameters were selected and tested on the standard IEEE 1547 test frame for various islanding and non-islanding events, such as single phase faults, three phase fault, and load and capacitor switching cases at different power mismatches between generation and load demands, as shown in Table 3.10.

Table 3.10: Test cases

Testing scenarios	Grid supply		DER's supply	
	P_{GRID} (MW)	Q_{GRID} (MVar)	P_{DER} (MW)	Q_{DER} (MVar)
Islanding	0.05	0.05	2.85	1.106
	0.10	0.10	2.85	1.106
	0.15	0.15	2.85	1.106
	0.20	0.20	2.85	1.106
Load switching	0.05	0.05	2.85	1.106
	0.10	0.10	2.85	1.106
	0.15	0.15	2.85	1.106
	0.20	0.20	2.85	1.106
Capacitor switching	0.05	0.05	2.85	1.056
	0.10	0.10	2.85	1.006
	0.15	0.15	2.85	0.956
	0.20	0.20	2.85	0.906
Faults	0.05	0.05	2.85	1.106
	0.10	0.10	2.85	1.106
	0.15	0.15	2.85	1.106
	0.20	0.20	2.85	1.106

The magnitudes of these parameters were observed after ignoring the initial transients. The results of these parameters are illustrated as follows:

3.5.1 Islanding Events

The behavior of 16 parameters are analyzed on the IEEE standard test frame as depicted in Figure 3.8 under islanding scenario at a power mismatch of 0.05, 0.10, 0.15 and 0.20 MW and MVar respectively. The response of these parameters during islanding conditions are shown in Figure 3.9.

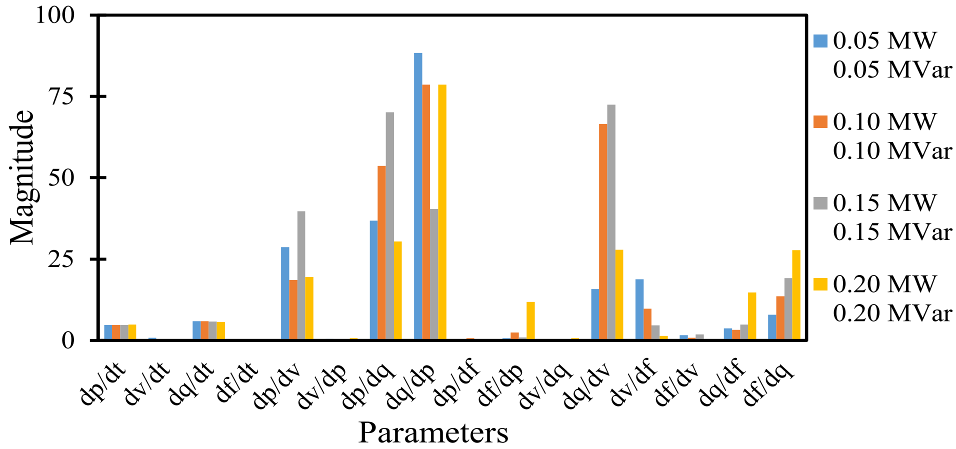

Figure 3.9: Performance analysis of parameters at islanding events

3.5.2 Load Switching Events

The performance of the 16 parameters are also evaluated under non-islanding scenario such as load switching conditions. The response of these parameters during load increment and decrement events are shown in Figures 3.10 and 3.11 respectively.

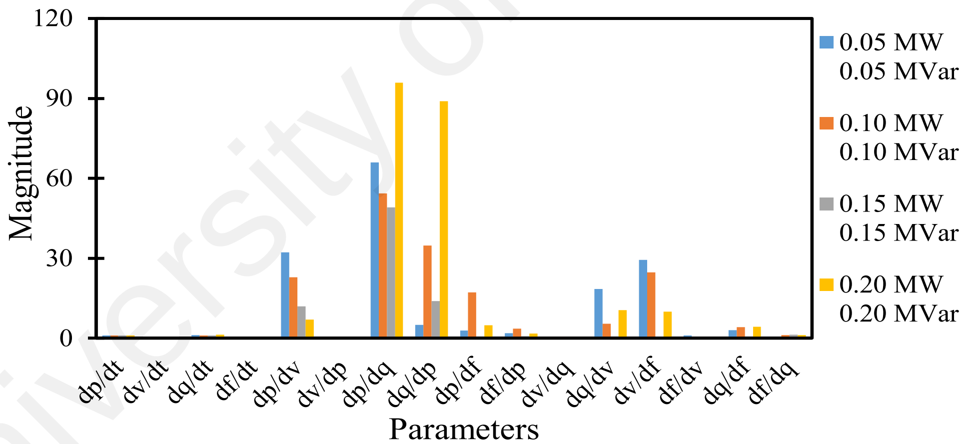

Figure 3.10: Performance analysis of parameters at load increment events

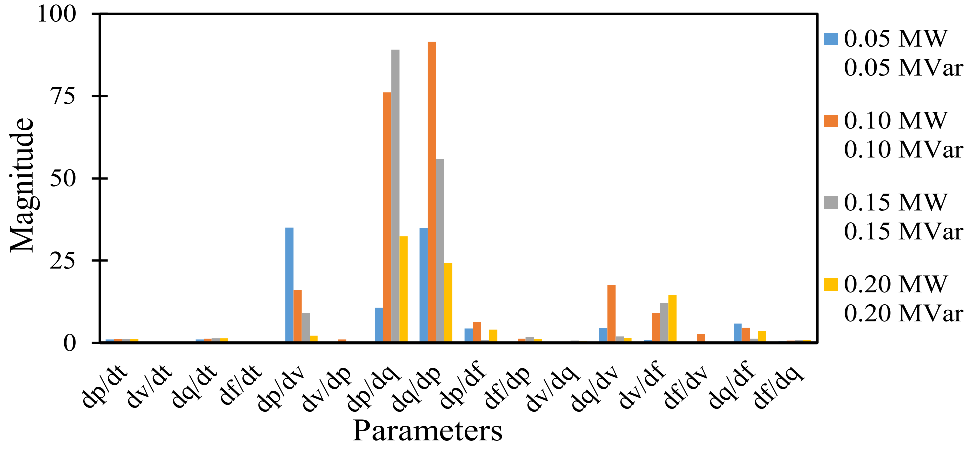

Figure 3.11: Performance analysis of parameters at load decrement events

3.5.3 Single and Three Phase Fault Events

Then the performance of the 16 parameters are weighed under various fault scenarios at different power mismatch conditions. The response of these parameters during single and three phase fault events are shown in Figures 3.12 and 3.13 respectively.

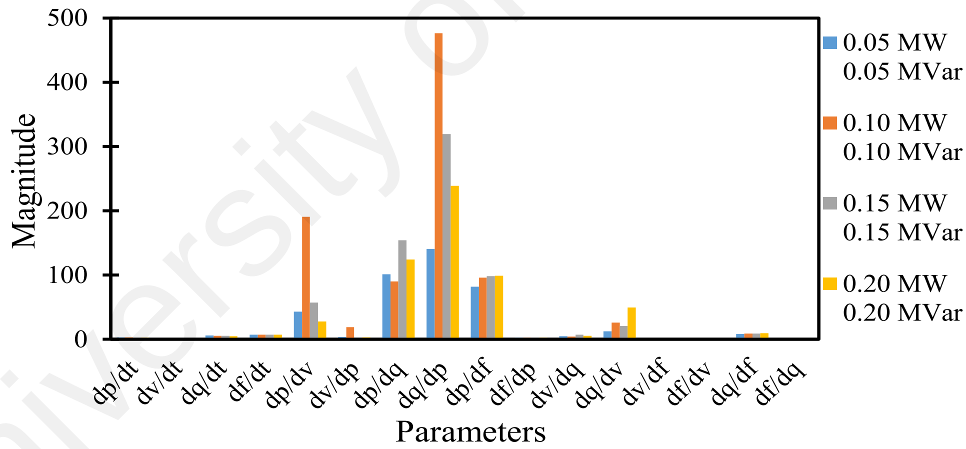

Figure 3.12: Performance analysis of parameters at single phase fault events

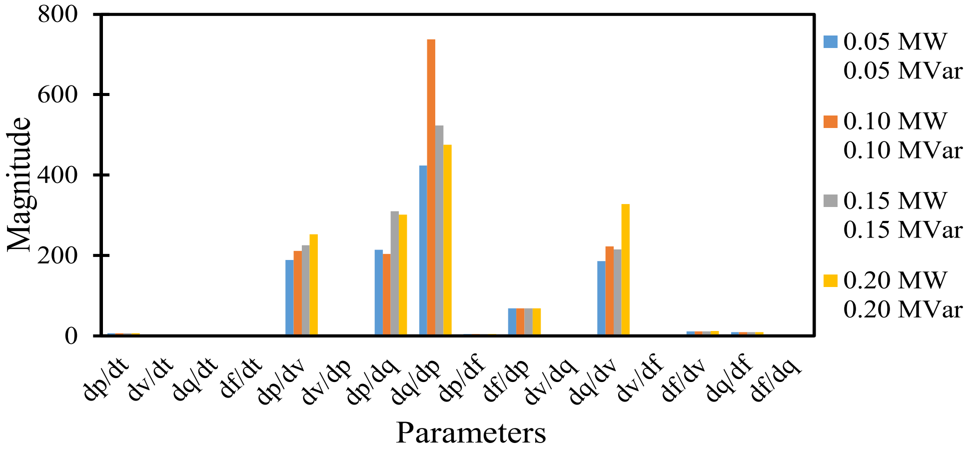

Figure 3.13: Performance analysis of parameters at three phase fault events

3.5.4 Capacitor Switching Events

The response of the 16 parameters are also assessed under capacitor switching scenarios at different power mismatch conditions. The response of these parameters during capacitor connection and disconnection are shown in Figures 3.14 and 3.15 respectively.

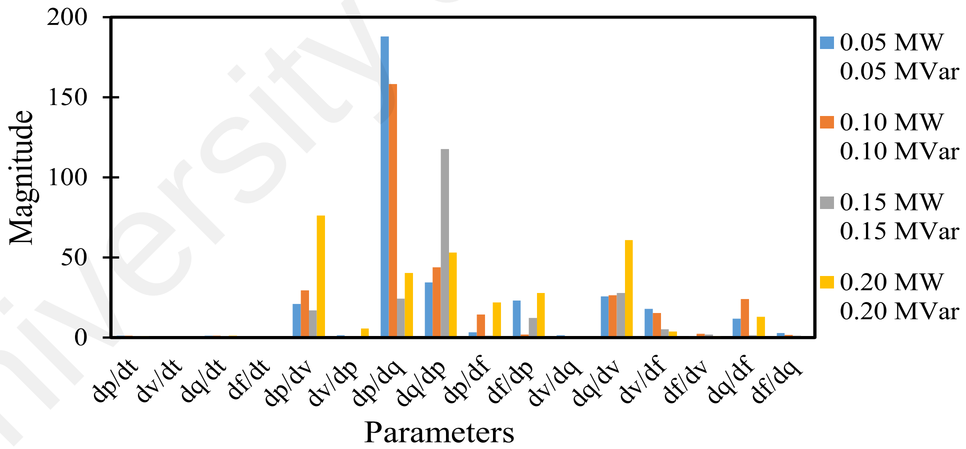

Figure 3.14: Performance analysis of parameters at capacitor connection events

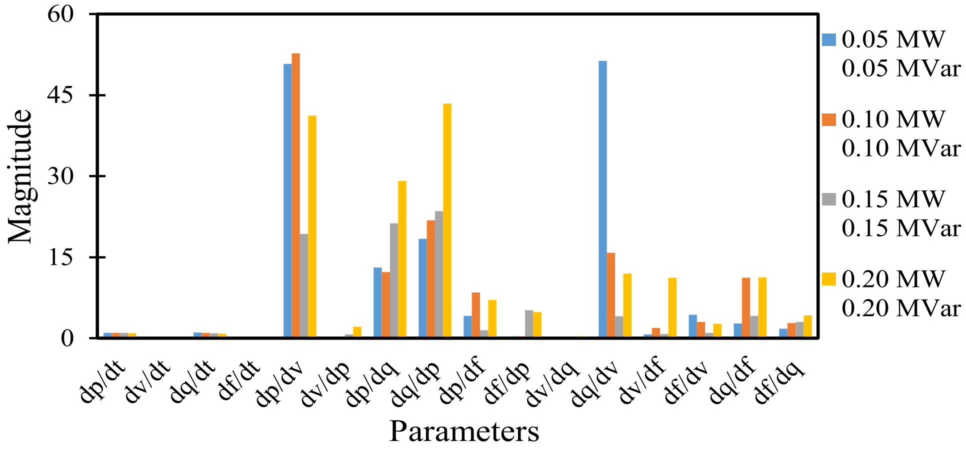

Figure 3.15: Performance analysis of parameters at capacitor disconnection events

It is quite clear from Figures 3.9 - 3.15 that at different power mismatches, each passive parameter shows a different ability to sense the deviation in the system. Further, it is also observed that some of the parameters are more affected by islanding scenarios as compared to non-islanding scenarios. However, some parameters show more deviations during non-islanding events than islanding events but majority of these parameters shows a mixed behaviour during islanding and non-islanding scenarios. Hence, it is best to line-up each of the passive parameter on the basis of its ability to sense different power system events.

3.6 Performance based Ranking Analysis of Passive Parameters

From the sensitivity analysis, it has been found that each passive parameter has its own ability to sense the deviations in the power system. However, it is necessary to arrange the passive parameters according to their sensitivity.

3.6.1 Generalized Ranking Analysis Algorithm

The steps taken in the generalized ranking are summarized as below:

i. Consider the magnitude of parameter at islanding event (x_i) as threshold value for a certain power mismatch (PM_j), where, i is the parameter (i.e *dp/dt*, *dv/dt*, … *df/dq*),

x is the islanding magnitude, PM is the power mismatch and j = 0.05, 0.10, 0.15, 0.20 (MW & MVar).

ii. Compare the non-islanding magnitudes of that parameter (y_i) with that of islanding event for the same power mismatch (PM_j), where y is the non-islanding magnitude.

iii. If the non-islanding magnitude (y_i) is less than the islanding/threshold magnitude (x_i), assign the value 1 (successfully detected as non-islanding case) otherwise zero.

iv. The performance average $(P.A)$ of selected parameter is calculated for the respective power mismatch.

$$(P.A)_i \| (PM)_j = \frac{\sum_{k_{\min}=1}^{k_{\max}=6} y_{i,k}}{k_{\max}} \tag{3.4}$$

v. Repeat the above procedure (step i to iv) for the selected parameter for different power mismatches.

vi. Calculate the percentage of average of these performances at different power mismatches to determine the overall performance $(O.P)$ of particular parameter.

$$(O.P)_i = \left[\frac{\sum_{j=0.05,0.10,0.15,0.20} (P.A)_i \| (PM)_j}{4} \right] \times 100\% \tag{3.5}$$

vii. Repeat step i to vi for all parameters.

The average performances of 16 parameters at power mismatches of 0.05, 0.10, 0.15 and 0.20 MW & MVar are illustrated as follows.

3.6.2 Average Performance at 0.05 MW and 0.05 MVar

The average performance of the 16 power system parameters is assessed according to the generalized algorithm discussed earlier. The illustration at 0.05 MW and 0.05 MVar power mismatch condition is as follows.

First, the magnitude of each parameter of an islanding case for a certain power mismatch is recorded as threshold. Then it is compared to the magnitudes of all non-islanding cases with the same power mismatch. If the value is less than that of the islanding threshold, assign a value of 1 (successfully detected as non-islanding case), otherwise it will be zero. For instance, the islanding value of *dv/df* is 18.83 kV/Hz at a power mismatch of 0.05 MW and 0.05 MVar as shown in Figure 3.9. It is considered as the threshold value and all non-islanding values of *dv/df* (Figures 3.10-3.15) at 0.05 MW and 0.05 MVar power mismatches are compared with it**.** It is observed that all non-islanding values are less than this except for the load increment scenario (29.40 kV/Hz) as evident in Figure 3.10. Thus, the non-islanding events whose values are less than threshold value are assigned as 1 and the load increment value is assigned zero. In the end, the performance average is calculated for *dv/df* using equation (3.4). The procedure is repeated for all other parameters for the respective power mismatches. The average performance of the 16 parameters at 0.05 MW and 0.05 MVar is shown in Figure 3.16.

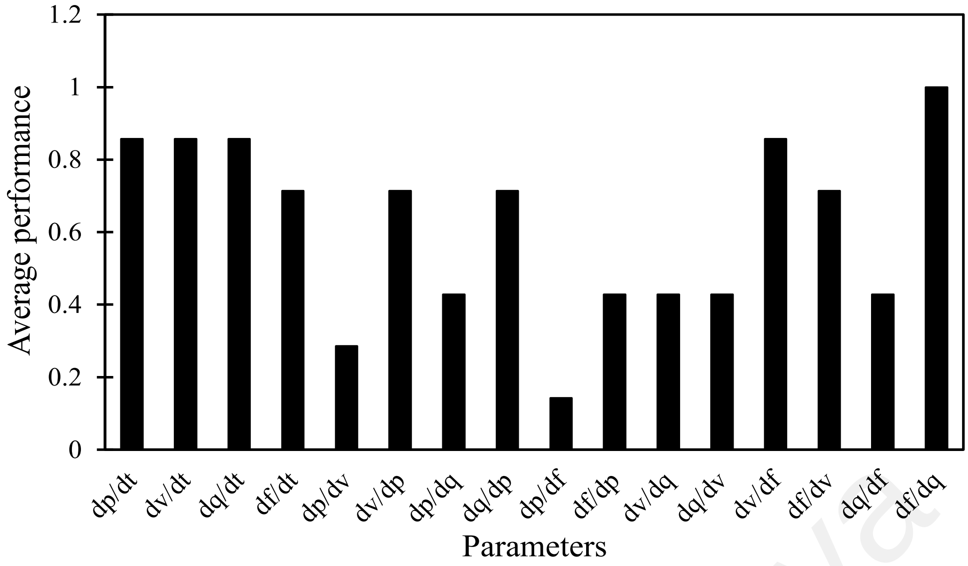

Figure 3.16: Average performance at 0.05 MW and 0.05 MVar

3.6.3 Average Performance at 0.10 MW and 0.10 MVar

The average performance of the 16 parameters at 0.10 MW and 0.10 MVar power mismatch condition is assessed in similar fashion as the case for 0.05 MW and 0.05 MVar. The result is shown in Figure 3.17.

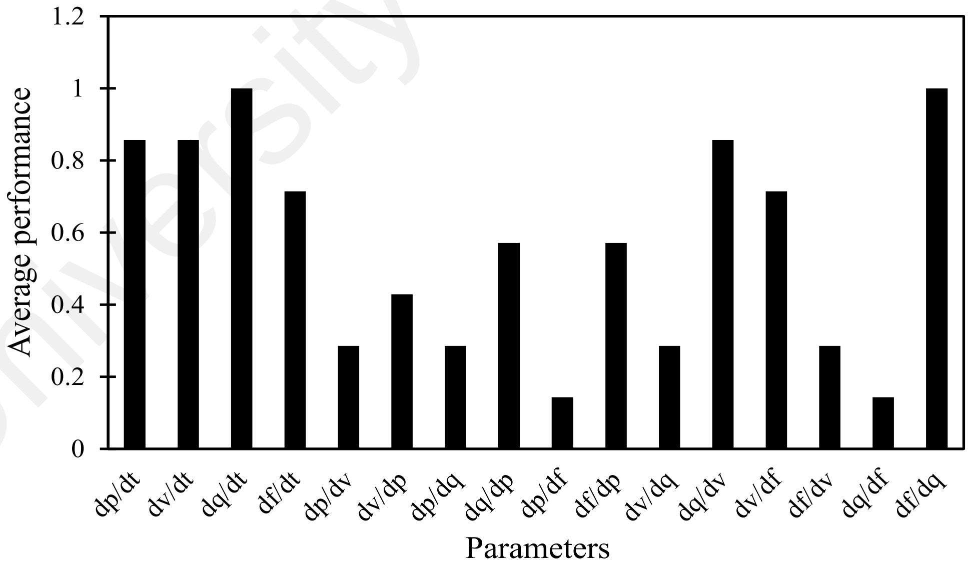

Figure 3.17: Average performance at 0.10 MW and 0.10 MVar

3.6.4 Average Performance at 0.15 MW and 0.15 MVar

The average performances of the 16 parameters for 0.15 MW and 0.15 MVar power mismatch condition is shown in Figure 3.18.

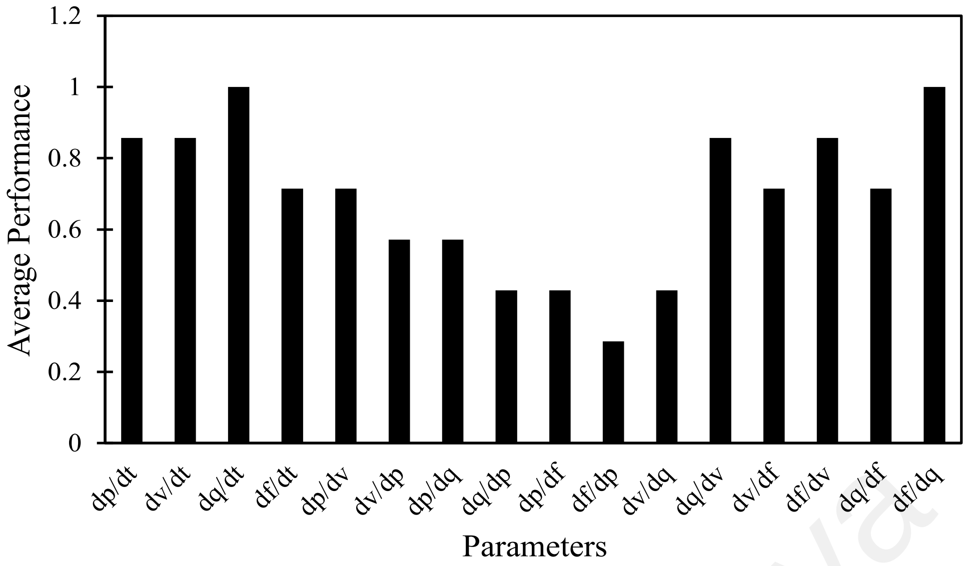

Figure 3.18: Average performance at 0.15 MW and 0.15 MVar

3.6.5 Average Performance at 0.20 MW and 0.20 MVar

The average performance of 16 parameters at 0.20 MW and 0.20 MVar power mismatch condition by following the aforementioned algorithm is shown in Figure 3.19.

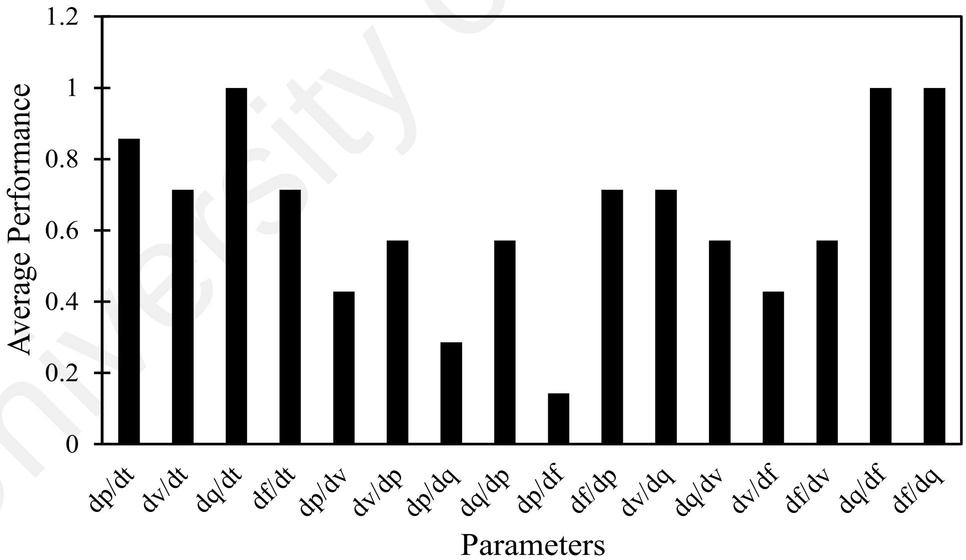

Figure 3.19: Average performance at 0.20 MW and 0.20 MVar

3.6.6 Overall Performance

Figures 3.16-3.19 shows the average performance of all parameters at respective power mismatches. The general performance of these parameters is obtained by calculating the percentage of average of these performances (at different power mismatches) by using equation (3.5), as shown in Figure 3.20.

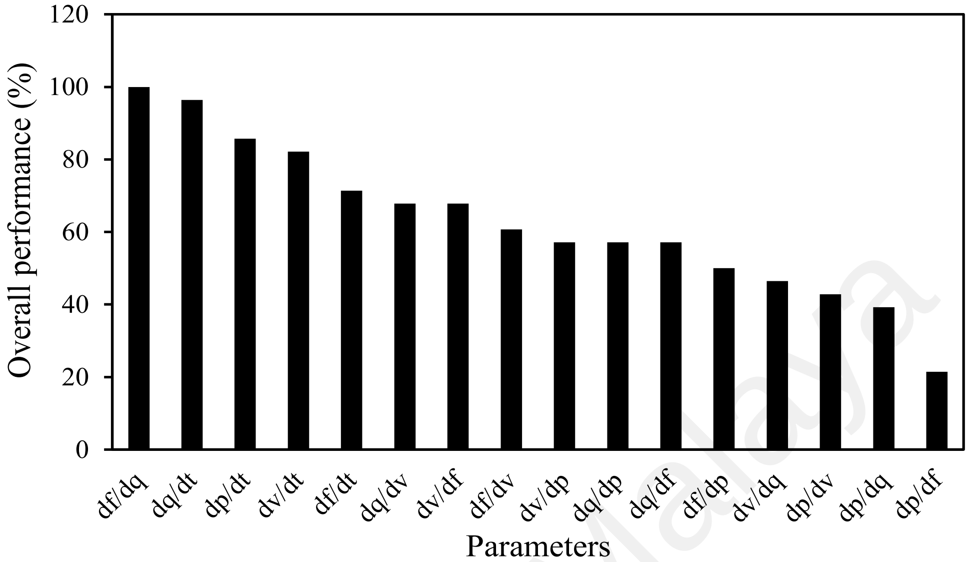

Figure 3.20: Overall performance of passive parameters

From Figure 3.20, the overall performance of *df/dq* is the highest. It is followed by the *dq/dt* and *dp/dt*. Therefore, it can be inferred that the rate of change of frequency over reactive power (*df/dq*) has highest potential to detect the small disturbances in the power system.

3.7 Analytical Analysis of most Sensitive Parameter

From the ranking analysis, it is found that *df/dq* is capable of sensing even minute variations. However, it is also necessary to analyse the relation between the variations in frequency with respect to change in reactive power. The analysis is detailed as follows:

A power mismatch ($\Delta P, \Delta Q$) always occurs between the output of the DER's and the associated load in real time conditions. The mismatched load is represented by $R + \Delta R, L + \Delta L$ and $C + \Delta C$. During normal conditions, the power mismatch is compensated by the utility supply ($P_{Utility}, Q_{Utility}$). However, when the utility supply is cut off from the distribution network, this mismatched load is solely dependent on DER's supply

(P_{DER}, Q_{DER}), which ultimately changes the voltage and the frequency. Figure 3.21 illustrates the system's behavior after being disconnected from the grid. If there is a large power mismatch, then the voltages and frequencies might exceed their respective nominal values corresponding to the associated voltage and frequency relays tripping DER's supply (Zhihong et al., 2004).

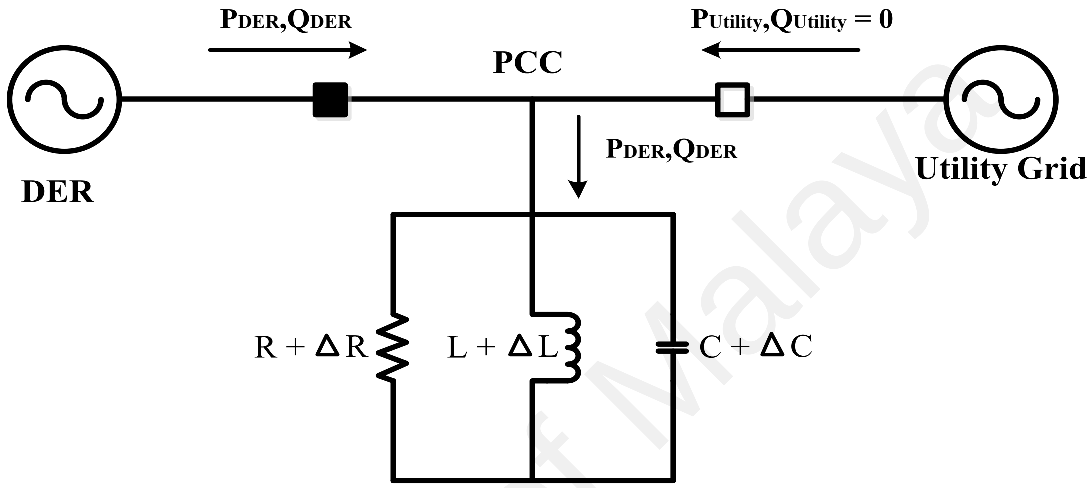

Figure 3.21: System behavior after grid disconnection

In normal conditions, the power consumed by the *RLC* load (P_L, Q_L) is represented by equations (3.6) and (3.7) in the following form (Jun et al., 2013; Ye et al., 2013):

$$P_L = P_{DER} + P_{Utility} = \frac{3V_{PCC}^2}{R} \tag{3.6}$$

$$Q_L = Q_{DER} + Q_{Utility} = 3V_{PCC}^2\left(\frac{1}{2\pi fL} - 2\pi fC\right) \tag{3.7}$$

$$Q_L = P_L R\left(\frac{1}{2\pi fL} - 2\pi fC\right) \tag{3.8}$$

Where V_{PCC} and f are the voltage and frequency, respectively, at the point of common coupling (PCC), while *RLC* represents the resistance, inductance, and capacitance of the load. From equation (3.6), it is clear that the variation in the voltage due to islanding conditions depend on the value of the active power mismatch ($\Delta P = P_L - P_{DER}$). If DER supplies constant active power, the relation between the change in voltage (ΔV) and active power mismatch is expressed in the following form (Zeineldin et al., 2006).

$$\Delta P = P_{DER}\left(\frac{1}{\left(1+{\Delta V}/{V_{PCC}}\right)^2} - 1\right) \tag{3.9}$$

Similarly, it can also be inferred from equation (3.8) that the variation in frequency (Δf) due to islanding condition is dependent on both active and reactive power mismatches. If the DER operates at a unity power factor, the relation between $\Delta Q$and $\Delta f$is described by (Zeineldin et al., 2006).

$$\Delta Q = \frac{3V_{PCC}^2}{2\pi fL}\left(1 - \frac{f^2}{(f+\Delta f)^2}\right) \tag{3.10}$$

However, the case differs in real-time environments. When the utility supply is cut off from the distribution system, variations will be induced in the voltage at the PCC due to an active power mismatch. This also affects the consumption of the load's reactive power, inducing a reactive power mismatch between the DER's and the load, which ultimately deviates the frequency (Roscoe, Burt, & Bright, 2014; Xiaolong & Yongli, 2014). The power consumed by the *RLC* load during islanding condition is illustrated below:

$$P_L = P_{DER} = \frac{3\left(V_{PCC}(1+\Delta V)\right)^2}{R+\Delta R} \tag{3.11}$$

$$Q_L = Q_{DER} = 3\left(V_{PCC}\left(1+\Delta V\right)\right)^2 \times$$

$$\left\lfloor \frac{1}{2\pi\left(f+\Delta f\right)\left(L+\Delta L\right)} - 2\pi\left(f+\Delta f\right)\left(C+\Delta C\right) \right\rfloor \tag{3.12}$$

Since, the utility supply compensates for the active and reactive power mismatch, the following equations can be obtained by analyzing equations (3.6) - (3.8), (3.11), and (3.12).

$$R\left(P_{DER}+\Delta P\right)\left(\frac{1}{2\pi fL} - 2\pi fC\right) = \left(R+\Delta R\right)P_{DER} \times$$

$$\left(\frac{1}{2\pi\left(f+\Delta f\right)\left(L+\Delta L\right)} - 2\pi\left(f+\Delta f\right)\left(C+\Delta C\right)\right) \tag{3.13}$$

$$3V_{PCC}^2\left(\frac{1}{2\pi\left(f+\Delta f\right)\left(L+\Delta L\right)} - 2\pi\left(f+\Delta f\right)\left(C+\Delta C\right)\right) + \Delta Q =$$

$$3V_{PCC}^2\left(\frac{1}{2\pi fL} - 2\pi fC\right) \tag{3.14}$$

By analyzing equations (3.13) and (3.14), the relation between $\Delta P, \Delta Q$and $\Delta f$is expressed as:

$$\Delta P = \frac{P_{DG}}{f}\left[1+\left(\frac{f}{\Delta f}\right)\left(\frac{\Delta C}{C}\right)\right]\Delta f \tag{3.15}$$

$$\Delta Q = -\frac{Q_{DG}}{f}\left[1+\left(\frac{f}{\Delta f}\right)\left(\frac{\Delta C}{C}\right)\right]\Delta f \tag{3.16}$$

It is clear from equations (3.15) and (3.16), the active and reactive power mismatch causes the frequency to deviate from the nominal value during an islanding condition.

This deviation will be counterbalanced by an active power mismatch. Therefore, both the active and reactive power mismatches influence frequency deviations. Furthermore, if the variations in active and reactive power mismatch are similar, the frequency fluctuations become more considerable due to the opposite signs of ΔP and ΔQ. However, the variations in frequency with respect to reactive power mismatch are most impactful compared to the variation in frequency vis-à-vis active power mismatch. Eventually, the change in frequency with respect to reactive power (*df/dq*) reveals the minute variations expeditiously.

3.8 Summary

Passive techniques based on single parameter are less accurate and have large NDZ as compared to those techniques which use two or more parameters for discrimination. Furthermore, the efficiency of intelligent techniques is solely reliant on usage of multiple parameters. The selection of multiple parameters is always a point of interest for both utility companies as well as for DER owners. Hence, the study undertaken involves a comprehensive sensitivity analysis of 16 different power system parameters used for islanding detection. The most sensitive parameter (*df/dq*) is selected by performance based ranking analysis. The choice of *df/dq* is further analyzed analytically and it is shown that active and reactive power mismatch has an opposing effect on the variation of frequency (*df*) in real time environment.

CHAPTER 4: PROPOSED METHODOLOGIES FOR ISLANDING DETECTION TECHNIQUES

4.1 Introduction

Commonly, remote, passive and active islanding detection techniques have been proposed by various researchers. Each of these techniques has certain merits and demerits. Hence, an efficient technique is required, which should possess a smaller non-detection zone, higher efficiency, and minimal influence on power quality. To address this problem, the ranking analysis of 16 different power system parameters has been performed on the basis of sensitivity. In this regard, this chapter presents a new passive islanding detection technique for successful islanding detection by employing the most sensitive parameter. However, the non-detection zone and threshold setting issues of passive technique are resolved by proposing a new intelligent islanding detection technique. The uniqueness of proposed intelligent technique is that it uses the minimum features for discrimination between islanding and non-islanding events. Furthermore, the performance of ANN classifier is improved by using the optimization approaches (EP and PSO).

4.2 Proposed Passive Islanding Detection Technique

After prioritize the 16 different power system parameters on the basis of sensitivity analysis in chapter 3, it is determined that the rate of change of frequency over reactive power (*df/dq)* is the most sensitive indicator. A new passive islanding detection technique that employs this parameter is subsequently proposed. The generalized methodology of the proposed passive technique is illustrated as follows.

The proposed passive technique measures the absolute *df/dq* at every half cycle. The proposed technique is initiated when:

$$\left(df / dq\right)_{meas} > \left(df / dq\right)_{\min} \tag{4.1}$$

where $(df/dq)_{min}$ is the minimum set point that avoids the unnecessary activation of the proposed technique. If and only if (4.1) is satisfied, the process of determining the maximum magnitude of df/dq ($(df/dq)_{meas}$) is activated. In this process, the initial transients are neglected after the event starts to ensure that the data reached a certain degree of certainty. After this, $(df/dq)_{meas}$ is determined within a certain period of time, while islanding is detected when:

$$\left(df / dq\right)_{meas} > \left(df / dq\right)_{\max} \tag{4.2}$$

where $(df/dq)_{max}$ is the threshold value to distinguish islanding from all other non-islanding events. Values for $(df/dq)_{min}$ and $(df/dq)_{max}$ are determined from the analysis presented in section 3.5. In non-islanding cases, most of the values fall below that of unity. Hence, we set $(df/dq)_{min}$ to unity to avoid excessive activation, while $(df/dq)_{max}$ is set in such a way that will allow it to discriminate between the remaining non-islanding and islanding events. However, both of these values are specific to certain systems, and can be set accordingly. The flowchart of the proposed technique is shown in Figure 4.1.

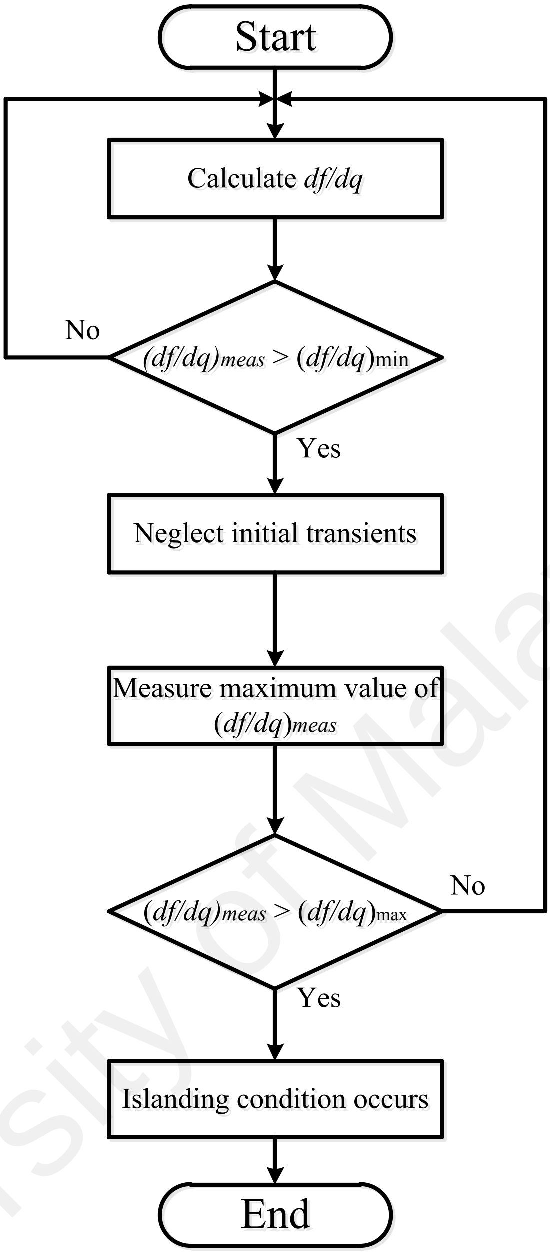

Figure 4.1: Flow chart of proposed islanding detection technique

4.3 Proposed Intelligent Islanding Detection Technique

The proposed passive islanding detection technique greatly reduces the non-detection zone. However, it does not perform well if the power mismatch is less than 0.05 MW and 0.05 MVar. Hence, non-detection zone is still present in the proposed passive technique. Furthermore, the setting of threshold value requires special consideration. These drawbacks can be overcome by using a computational intelligent classifier. The introduction of intelligent classifiers is heralded as a new era for passive islanding detection techniques. They render improvements in cost, accuracy, computational time, and reliability. Intelligent classifiers that are commonly used for decision making are fuzzy logic, decision tree, support vector machine, adaptive neuro fuzzy inference system and artificial neural network (Laghari et al., 2014). The intelligent classifiers used in islanding detection techniques employ many features as inputs to identify islanding from non-islanding events. For instance, in (Faqhruldin et al., 2014), (Alam et al., 2014), (Kar & Samantaray, 2014), (El-Arroudi et al., 2007; Samantaray, El-Arroudi, et al., 2010) and (Abd-Elkader et al., 2014; Ghazi & Lotfi, 2010) a total of 21, 5, 27, 11 and 6 features are used respectively.

Artificial neural network (ANN) is broadly used classifiers for islanding detection. It can learn from the given data directly with little computation complexity. It is also adaptive, able to handle various nonlinear relationships and can generalize solutions for new data set (Hammerstrom, 1993). In several researches ANN and its modified forms are implemented for islanding detection. ANN based islanding detection techniques have been proposed for multiple inverter based DG (Fayyad & Osman, 2010) and hybrid inverter based DG (ElNozahy et al., 2011). The data to train ANN are extracted from the 6th and 7th level of discrete wavelet transform (DWT) respectively. The maximum accuracy obtained by simulation are 97.77% (Fayyad & Osman, 2010) and 99.1% (ElNozahy et al., 2011). Another ANN based hybrid islanding detection technique suitable for synchronous based DER is proposed in (Ghazi & Lotfi, 2010). It utilizes 6 features and the accuracy obtained is 88.9%. Allam et al. (Abd-Elkader et al., 2014) used ANN to discriminate islanding conditions from other non-islanding events in a system supported by wind power. The inputs to the ANN are discrete Fourier Transform (DFT) coefficients of the analyzed signals. Different types of ANN such as self-organizing map (SOM) neural network (Moeini et al., 2010; Moeini et al., 2011), extension neural network (ENN) (Chao et al., 2011; Meng Hui et al., 2015), probabilistic neural network (PNN) (Lidula & Rajapakse, 2009), and modular probabilistic neural network (MPNN) (Soumya R. Mohanty et al., 2013) are implemented in islanding detection issues.

It is observed that a high detection accuracy is obtainable by ANN based islanding detection techniques using many features. However, when more parameters are used, the algorithms become more complex, computationally heavier and require more data storage. It also increases the time to process the reference data which is ultimately used to discriminate between islanding and non-islanding events. It is advantageous to reduce the number of features used as inputs to the classifier while maintaining or improving its accuracy. To obtain the best performance of the ANN classifier, its indices such as learning rate, momentum and number of neurons in hidden layers must be chosen properly (Illias, Chai, Abu Bakar, & Mokhlis, 2015). Since finding the optimal values of these parameters by trial and error is tedious and time consuming, an optimization technique can be used to reach the optimal combination.

Many optimization techniques are employed to regulate the ANN parameters. They are broadly classified as evolutionary algorithms and swarm intelligence. Evolutionary algorithms (EA) are algorithms based on evolutionary process and they include evolution strategies, evolutionary programming, gene expression programming and genetic programming. Ant colony optimization, intelligent water drops and particle swarm optimization falls under the category of swarm intelligence. In this research, the evolutionary programming (EP) and particle swarm optimization (PSO) are selected in order to comparatively investigate their performance. EP represents a particular class of evolutionary algorithm inspired by evolutionary biology. It uses a simple and direct method of representing system parameters. It is also robust and able to reach global solutions. PSO is a swarm based optimization technique inspired by the social behavior of bird flocking and fish schooling. Research in (del Valle, Venayagamoorthy, Mohagheghi, Hernandez, & Harley, 2008) has shown that it is more advantageous than other evolutionary optimization techniques such as EA. The main advantages of PSO are listed as follows.

1) Its implementation is easy which requires very few parameters to fine-tune.

2) Every particle remembers its own previous best value which makes it more effective in terms of memory capability as compared to EA.

3) It is more proficient in preserving the diversity of the swarm, since all the particles use the data associated to the most effective particle in order to advance themselves. This is different from EP in which the worse solutions are discarded and only the good ones are saved.

Hence, in this work, the possibility of using various optimization techniques to minimize the number of input features to an ANN classifier for detecting islanding condition is explored. Furthermore, a comparative investigation using EP and PSO is carried out to find the best possible values of ANN indices (learning rate, momentum and number of neurons for hidden layer). A brief introduction of EP and PSO is given below.

4.3.1 Evolutionary Programming (EP)

EP is a stochastic optimization technique based on the evolutionary biological process. In order to obtain the global minima, the EP contains different evolutionary process such as initialization, fitness computation, mutation, combination, tournament selection and transcription of next generation (Abdullah, Musirin, & Othman, 2010; Yousefi, Hooshyar, Ahmad, & Darus, 2015). The fitness function is used to determine the strength of the candidate solution. The individuals which survive are recognized as the fittest individuals which will continue to the next generation. The individuals are then mutated in each generation to produce new population based on the following Gaussian mutation expression:

$$x_{i+m,j} = x_{i,j} + N\left[0, \beta\left(x_{j\max} - x_{j\min}\right)\left(\frac{f_i}{f_{\max}}\right)\right] \tag{4.3}$$

where, *xi+m,j* represents the mutated individual, *xi,j* represents the current individual, *xjmax* and *xjmin* represents the maximum and minimum value of the individuals in the particular population and *fi* and *fmax* represents the current fitness value and maximum fitness value respectively. The new population is assessed and then combined with the original population before the selection of the fittest individual. This process is then reiterated.

4.3.2 Particle Swarm Optimization (PSO)

PSO is a swarm optimization approach which is based upon nature inspired interacting agents (del Valle et al., 2008; L. Lin, Qi, Jun-yong, & Chuan, 2008). Initially, the system parameters such as dimension of particles, population size and inertia factor are defined. In order to update the particle, the velocity of each particle is evaluated based on the following expression:

$$v_i^{k+1} = w.v_i^k + c_1 r_1^k (p_{besti}{}^k - x_i^k) + c_2 r_2^k (g_{besti}{}^k - x_i^k) \tag{4.4}$$

where i = 1,2,…..size of swarm, w is the inertia weight which is usually varied linearly from 0.9 to 0.4, r_1 and r_2 are random numbers in the range of [0,1] , c_1 and c_2 are acceleration factors and k represents the iteration number. The *pbest* represents the best objective function for the current iteration and *gbest* denotes the global optima. The position of the new particle is then updated based on (4.5):

$$x_i^{k+1} = x_i^k + v_i^{k+1} \tag{4.5}$$

where v_i represents the velocity, x_i represents the current particle and x_i^{k+1} represents the updated particle. The process then iterates until the maximum iteration is reached.

4.3.3 Data Generation

A large number of islanding and non-islanding events were simulated on the test frame (Figure 3.1), in order to provide the intelligent classifier with substantial information to discriminate between these events. For islanding events, different power mismatches between DER's and power consumed by the local load were simulated. The range between the active and reactive power mismatch is further categorized into small power mismatch (0% to 30%) and large power mismatch (30% to 100%). Islanding detection at small power mismatch or perfectly matched conditions are given special consideration because it is very difficult to detect islanding at these conditions (Sareen, Bhalja, & Maheshwari, 2016; Zeineldin & Kirtley, 2009). The non-islanding events include load switching, capacitor bank switching, motor switching, DER tripping, single phase to ground fault, double phase to ground fault, three phase to ground fault and phase to phase fault at each bus. Table 4.1 comprehends the cases used in this work.

Table 4.1: Simulated cases with corresponding islanding status

Scenarios	Case Description	Island Status
Islanding	Small power mismatch at each bus (Up to 30% of P- and Q-mismatch with a step of 5%).	1
	Large power mismatch at each bus (30-100% of P- and Q-mismatch with a step of 10%).	
Non-islanding	Load switching at each bus from 0.05 MW& 0.05 MVar to 1.00 MW & 1.00 MVar with a step of 5%.	0
	Capacitor switching at each bus bearing capacity of 0.10, 0.30 and 0.50 MVar.	
	Motor switching at each bus	
	Following fault cases at each bus: 1) Single phase to ground fault 2) Double phase to ground fault 3) Three phase to ground fault 4) Phase to phase fault	
	DER's tripping	

4.3.4 Selected Features

Intelligent islanding detection techniques which have been discussed earlier uses many parameters as inputs to the classifier. Since, our focus is to obtain a higher accuracy by using less input features, only features which are exceptionally sensitive to islanding and non-islanding events are utilized. In section 3.6, 16 different power system parameters were ordered on the basis of sensitivity analysis under islanding and non-islanding events. Three parameters, namely *df/dq*, *dp/dt* and *dq/dt* show high discriminating traits that are useful for islanding detection. Hence, in this proposed technique, the same features are selected for further investigation:

a) Variation in power (*dp/dt*)

b) Variation in reactive power (*dq/dt*)

c) Rate of change of frequency over reactive power (*df/dq*).

4.4 Training and Testing Data Formation

The test system in Figure 3.1 is used to validate the performance of the proposed intelligent islanding detection technique. The absolute values of *df/dq*, *dp/dt* and *dq/dt* are measured on the island side and the data are sampled every half cycle to form the data bank. In this simulation, all islanding and non-islanding events are initiated when the system is stable, t = 1.0 s. The maximum value of *df/dq*, *dp/dt* and *dq/dt* are determined for 5 cycles in order to form the data bank for the classifier.

A total of 1461 different islanding and non-islanding events are simulated. Out of those 390 islanding events are created by taking into account different combination of active and reactive power mismatches. The remaining are 1071 non-islanding events that include load, capacitor and motor switching of different values. Furthermore, generator tripping and different types of faults such as single phase to ground, double phase to ground, three phase to ground and phase to phase faults are also considered. After forming the data bank, different percentages (50%, 60% and 70%) of the total data are used for training and the corresponding remaining (50%, 40% and 30%) for testing purposes. The selection of the testing data from the islanding and non-islanding events is done both systematically and inter-systematically.

4.4.1 Systematic Selection

The data bank consists of different islanding and non-islanding events simulated at 30 buses. The events/cases simulated at each bus are illustrated in Table 4.1. The islanding and non-islanding cases simulated at each bus are approximately 13 and 36 respectively. The data (islanding and non-islanding) collected from bus 1 to 10 are placed into group B1. Similarly, data from bus 11 to 20 and 21 to 30 are placed in group B2 and B3 respectively.

4.4.1.1 50% Training and 50% Testing

Here, 50% of the total data (730) is used for training and the remaining 50% for testing purposes. The islanding and non-islanding data are classified into 3 groups, B1, B2 and B3. Here, B1, B2 and B3 groups represent the respective data from buses 1 to 10, 11 to 20 and 21 to 30 respectively. The islanding and non-islanding events for each group of buses are further categorized into 2 sets. From each group of buses, half of the events are selected for testing and remaining are used for training as indicated in Figure 4.2.

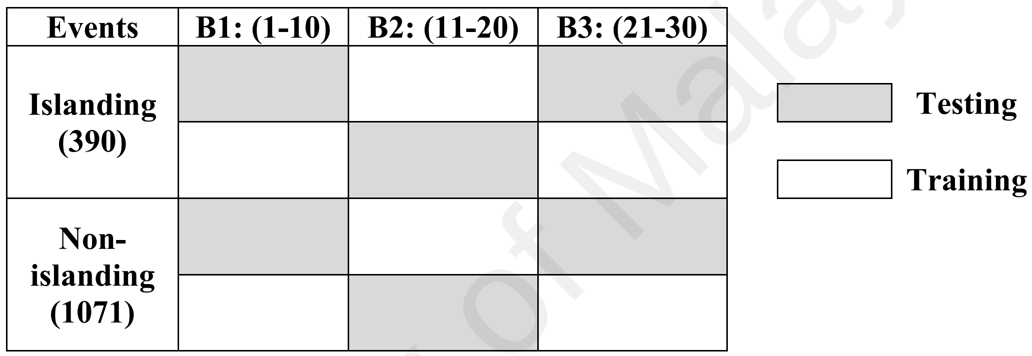

Figure 4.2: 50% training and 50% testing

4.4.1.2 60% Training and 40% Testing

Here, 60% of the total data (877) is used for training and the remaining 40% (584) for testing purposes. Similar to 50% training and 50% testing data formation, the islanding and non-islanding data are classified again into 3 groups, B1, B2 and B3. Here again, B1, B2 and B3 groups represent the respective data from buses 1 to 10, 11 to 20 and 21 to 30 respectively. The islanding and non-islanding events for each group of buses are further categorized into 5 sets. From each group of buses, approximately two-fifth of the events are selected for testing and remaining are used for training as indicated in Figure 4.3.

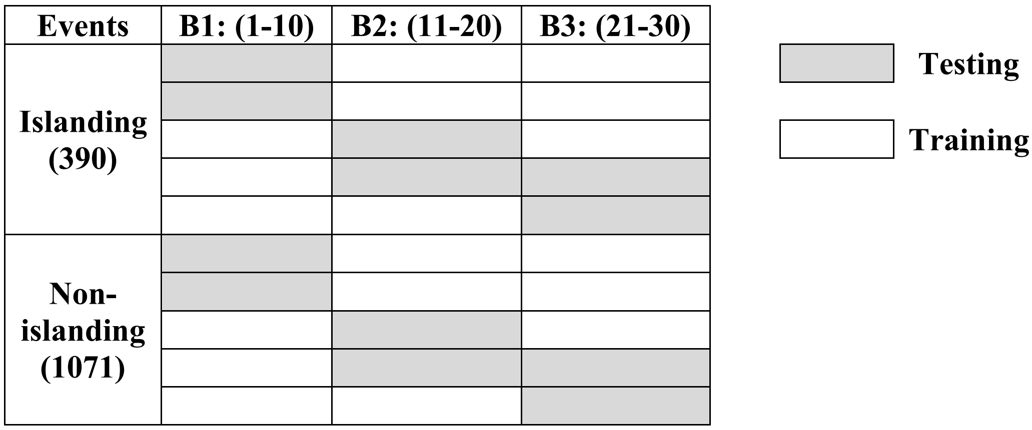

Figure 4.3: 60% training and 40% testing

4.4.1.3 70% Training and 30% Testing

Here, 70% of the total data (1027) is used for training and the remaining 30% (434) for testing purposes. Just like the previous data formations, the islanding and non-islanding data are classified again into 3 groups, B1, B2 and B3. However, the islanding and non-islanding events for each group of buses are categorized into 3 sets. From each group of buses, approximately one-third of the events are selected for testing and remaining are used for training as shown in Figure 4.4.

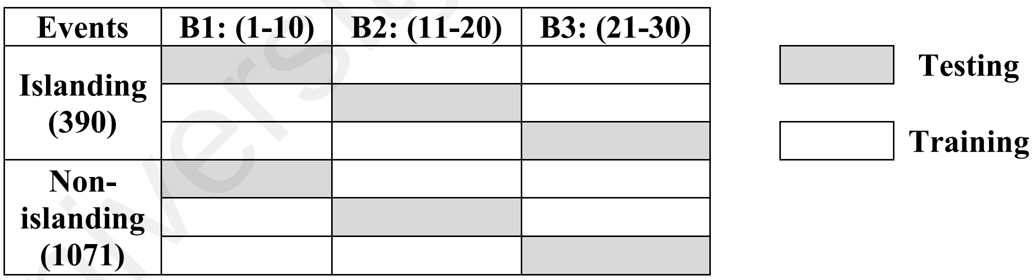

Figure 4.4: 70% training and 30% testing

4.4.2 Inter-systematic Selection

4.4.2.1 50% Training and 50% Testing

Here, the groups and corresponding sets formation is the same as that in systematic selection (50% training and 50% testing). However, the events which are selected for training and testing are opposite to that of corresponding systematic selection as shown in Figure 4.5.

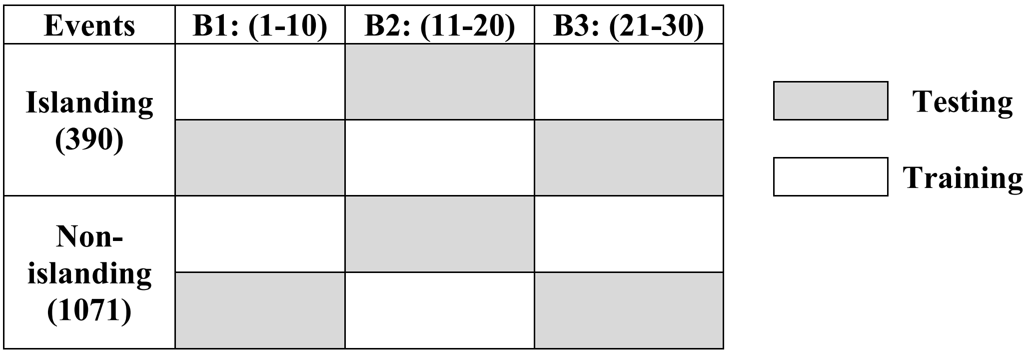

Figure 4.5: 50% training and 50% testing

4.4.2.2 60% Training and 40% Testing

Here again, the groups and corresponding sets formation is the same as that in systematic selection (60% training and 40% testing). However, the events which are selected for training and testing differs from the corresponding systematic selection as shown in Figure 4.6.

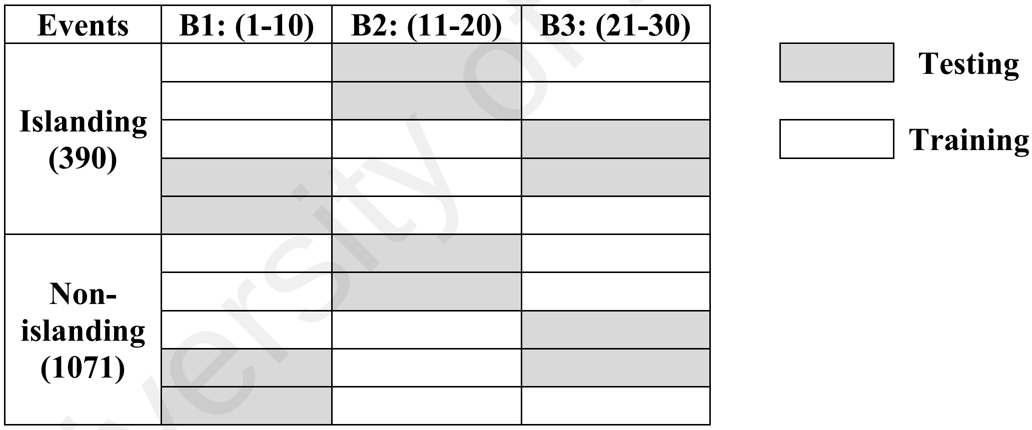

Figure 4.6: 60% training and 40% testing

4.4.2.3 70% Training and 30% Testing

Similar to the systematic selection (70% training and 30% testing), the groups and corresponding sets formation are the same. However, the events which are selected for training and testing varies from the corresponding systematic selection as shown in Figure 4.7.

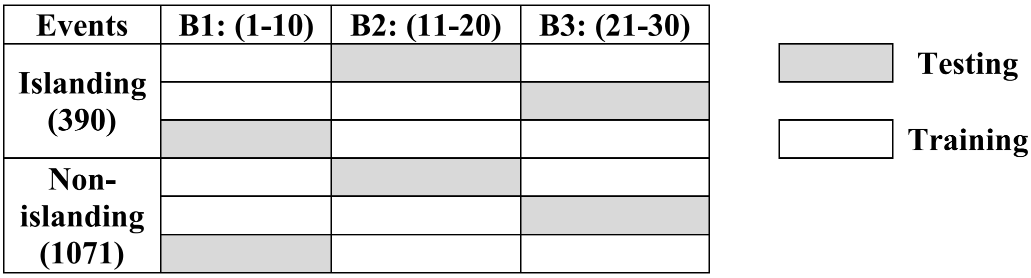

Figure 4.7: 70% training and 30% testing

4.5 Proposed Algorithm

The proposed detection technique has two main stages:

1. The optimal selection of ANN parameters using optimization techniques (EP & PSO) by employing minimum number of input features.
2. Training of optimal ANN classifier and discrimination of events. The detailed description of this is as follows:
    i. In total 1461 cases were simulated in PSCAD, which includes all possible combinations of islanding and non-islanding scenarios.
    ii. The variations in real and reactive power (*dp/dt*, *dq/dt*) and rate of change of frequency over reactive power (*df/dq*) are measured at the target DER.
    iii. Minimum number of features are used as inputs to the ANN classifier. In this regards, two set of inputs are used, wherein, each set has two input features (*df/dq* & *dp/dt*, *df/dq* & *dq/dt*).
    iv. Since, ANN alone is heuristic in nature, the optimal values of ANN parameters (learning rate, momentum and number of neurons) for the two sets of inputs are obtained by using optimization techniques (EP & PSO).
    v. By employing the optimal values of indices obtained in step iv, a comparison between stand-alone ANN, ANN-EP and ANN-PSO is made based on the regression value (R) in order to find the best set of input features.

vi. ANN classifier is trained to discriminate islanding and non-islanding events using the best set of input features and optimal parameters.

vii. The detection time and accuracy of the ANN classifier is calculated using the testing data.

viii. In order to obtain the most robust islanding detection technique, the process was carried out 5 times for average accuracy calculation.

In this proposed algorithm, the offline process takes into account the selection of input set, optimal values of parameters for ANN and training of classifier. Once these processes are done, the classifier is ready to discriminate islanding and non-islanding events both on- and off-line. Since testing can be done online, this technique is applicable for real time execution.

4.6 ANN Analysis for Feature Selection

The variations in power (*dp/dt*), reactive power (*dq/dt*) and rate of change of frequency over reactive power (*df/dq*) were used as input features and 1461 different islanding and non-islanding scenarios were analyzed in this work. To perform the ANN analysis, the input features are grouped into 2 sets. Set 1 and 2 includes *dp/dt* & *df/dq* and *dq/dt* & *df/dq* respectively. Furthermore, different percentages (50%, 60% and 70%) of the total data for these 2 sets are selected systematically and inter-systematically for training purpose as illustrated in section 4.4.

4.6.1 Using Stand-alone ANN

In this scenario, the simulations were accomplished by employing different number of hidden layers, number of neurons, learning rate (LR) and momentum constant (MC) in ANN. The procedure for finding the optimum ANN model is illustrated as follows:

4.6.1.1 Varying the Number of Neurons in Hidden Layers:

Before finding the best parameters of LR and MC, their typical values (0.05 and 0.95 respectively) were utilized to observe the value of R. Lavenberg-Marquart (TRAINLM) and Gradient Descent with momentum weight and bias function (LEARNGDM) were considered as the training and learning function. The number of neurons in hidden layers were increased from 2 to 30 with an increment of 2 by keeping other parameters constant. The transfer function of hidden layer was logsig-logsig while pure-linear (PURELIN) was used for output layer. The objective function used in this study is based on the maximization of the regression value. The ANN model bearing maximum value of R for the 2 sets of inputs, by using the typical values of LR and MC for different percentages of training data using systematic and inter-systematic selection, is shown in Table 4.2 as default values.

Table 4.2: ANN analysis using default values

ANN Indices	Training data percentages using											
	Systematic selection						Inter-systematic selection					
	50%		60%		70%		50%		60%		70%	
	Set 1	Set 2	Set 1	Set 2	Set 1	Set 2	Set 1	Set 2	Set 1	Set 2	Set 1	Set 2
Neurons in 1st hidden layer	2	2	2	2	2	2	2	2	2	2	2	2
Neurons in 2nd hidden layer	10	10	10	10	10	10	10	10	10	10	10	10
Learning Rate (LR)	0.05	0.05	0.05	0.05	0.05	0.05	0.05	0.05	0.05	0.05	0.05	0.05
Momentum Constant (MC)	0.95	0.95	0.95	0.95	0.95	0.95	0.95	0.95	0.95	0.95	0.95	0.95
Regression (R)	0.9211	0.9423	0.9546	0.9534	0.9215	0.9211	0.9273	0.9280	0.9418	0.9419	0.9501	0.9496

Based upon the investigation, the number of neurons selected for hidden layers are 2 and 10 respectively, because for lower values it gives lower value of regression and for higher values it does not produce any further improvement.

4.6.1.2 Varying the Value of LR and MC:

The value of LR and MC parameters are varied separately. This is carried out by keeping one of them constant while varying the other. The indices are varied from 0 to

0.9 with an increment of 0.01. In this investigation, the MC is initially held constant while the value of LR is increased from 0 to 0.9 with a step of 0.01 and vice versa. The optimum results are illustrated in Table 4.3 as tuned values.

Table 4.3: ANN analysis using tuned values

ANN Indices	Training data percentages using											
	Systematic selection						Inter-systematic selection					
	50%		60%		70%		50%		60%		70%	
	Set 1	Set 2	Set 1	Set 2	Set 1	Set 2	Set 1	Set 2	Set 1	Set 2	Set 1	Set 2
Neurons in 1st hidden layer	2	2	2	2	2	2	2	2	2	2	2	2
Neurons in 2nd hidden layer	10	10	10	10	10	10	10	10	10	10	10	10
Learning Rate (LR)	0.08	0.63	0.32	0.80	0.01	0.04	0.44	0.62	0.55	0.88	0.50	0.59
Momentum Constant (MC)	0.22	0.49	0.77	0.45	0.90	0.65	0.83	0.49	0.78	0.67	0.49	0.86
Regression (R)	0.9216	0.9427	0.9549	0.9547	0.9304	0.9356	0.9287	0.9299	0.9424	0.9420	0.9507	0.9525

4.6.2 Using ANN-EP

EP is integrated with ANN in order to find the optimal values of LR, MC and number of neurons in the hidden layers. The simulation process was carried out for 10 times to validate the robustness of the proposed technique. Next, the ANN is trained with the optimal values acquired from EP. The ANN-EP results for both sets of input upon using systematic and inter-systematic selection are shown in Table 4.4.

Table 4.4: ANN-EP analysis

ANN Indices	Training data percentages using											
	Systematic selection						Inter-systematic selection					
	50%		60%		70%		50%		60%		70%	
	Set 1	Set 2	Set 1	Set 2	Set 1	Set 2	Set 1	Set 2	Set 1	Set 2	Set 1	Set 2
Neurons in 1st hidden layer	2	2	2	2	2	2	2	2	2	2	2	2
Neurons in 2nd hidden layer	15	29	3	24	4	29	5	12	29	12	5	25
Learning Rate (LR)	0.3596	0.0596	0.4192	0.4046	0.1075	0.01	0.0675	0.9696	0.0496	0.6406	0.1438	0.0270
Momentum Constant (MC)	0.2432	0.2815	0.2245	0.3441	0.5915	0.6693	0.1099	0.2639	0.7490	0.5710	0.3359	0.6645
Regression (R)	0.9246	0.9431	0.9571	0.9561	0.9388	0.9697	0.9344	0.9395	0.9448	0.9586	0.9524	0.9735

4.6.3 Using ANN-PSO

In order to find the optimal values of LR and MC, the ANN is further integrated with PSO. The procedure of ANN-EP is used for finding the optimal values in ANN-PSO. The optimal values of LR, MC and number of neurons in hidden layers and the value of R from this method are illustrated in Table 4.5 as ANN-PSO.

Table 4.5: ANN-PSO analysis

ANN Indices	Training data percentages using											
	Systematic selection						Inter-systematic selection					
	50%		60%		70%		50%		60%		70%	
	Set 1	Set 2	Set 1	Set 2	Set 1	Set 2	Set 1	Set 2	Set 1	Set 2	Set 1	Set 2
Neurons in 1st hidden layer	2	2	2	2	2	2	2	2	2	2	2	2
Neurons in 2nd hidden layer	6	5	5	28	5	5	9	10	12	4	4	8
Learning Rate (LR)	0.2230	0.9062	0.2345	0.0092	0.9372	0.5572	0.1980	0.3842	0.9790	0.9748	0.1993	0.7918
Momentum Constant (MC)	0.3737	0.5001	0.0249	0.4824	0.0814	0.6464	0.4508	0.3958	0.2999	0.5117	0.5192	0.4629
Regression (R)	0.9279	0.9434	0.9572	0.9800	0.9706	0.9996	0.9386	0.9422	0.9468	0.9796	0.9526	0.9965

4.7 Summary

This chapter presents the methodologies of the proposed passive and intelligent islanding detection techniques. The proposed passive technique is based on the rate of change of frequency over reactive power (*df/dq*) to detect islanding under various conditions. It uses two threshold values for measurement of the rate of change of frequency over reactive power (*df/dq*). The first threshold value is used to avoid unnecessary activation of the technique and second is used to make discrimination between islanding and non-islanding events.

This chapter also proposes an intelligent islanding detection technique based on Artificial Neural Network (ANN) that employs minimal features from the power system. The accuracy of the trained ANN is improved by optimizing the learning rate, momentum and number of neurons in the hidden layers using Evolutionary Programming (EP) and Particle Swarm Optimization (PSO) at different percentages of training data using systematic and inter-systematic selection. The performance comparison between stand-alone ANN, ANN-EP and ANN-PSO in the form of regression value is performed to obtain the best feature combination for an efficient islanding detection.

CHAPTER 5: VALIDATION OF PROPOSED ISLANDING DETECTION TECHNIQUES

5.1 Introduction

This chapter deals with the validation of the proposed passive and intelligent islanding detection technique on a real Malaysian distribution system. Various islanding and non-islanding case studies are performed to demonstrate the performance of the proposed islanding detection techniques. Furthermore, error analysis is carried out to further support the choice of intelligent technique.

5.2 Simulation Results of Proposed Passive Technique

The test system in Figure 3.8 recommended by the IEEE 1547 standard is used to validate the performance of the proposed passive islanding detection technique. Details of the proposed technique are already explained in section 4.2. In this simulation, all islanding and non-islanding events are initiated at 0.05 sec once the system is stabilized. The threshold values used to discriminate islanding from non-islanding events are 1 Hz/MVar for $(df/dq)_{min}$, and 7.5 Hz/MVar for $(df/dq)_{max}$. The initial transients are neglected for 7 cycles. This value is determined from the simulations, where it is sufficient to neglect the initial transients. The maximum value of $(df/dq)_{meas}$ is determined for 3 cycles. Hence, islanding can be detected within 10 cycles (200 ms for 50 Hz system). The behavior of f_{meas} and $(df/dt)_{meas}$ are also observed for different scenarios. Moreover, the response of $(df/dt)_{meas}$ is compared with $(df/dq)_{meas}$ to further validate the significance of the proposed technique. In this simulation, power mismatch between the grid and DER's is set between 0.05 MW and 0.05 MVar. This value is the smallest value that can still significantly distinguish islanding and non-islanding events. The values of R, L and C for different amounts of mismatched loads are detailed in Table 5.1.

Table 5.1: Values of R, L and C

Load amount		R (Ω)	L (H)	C (μF)
Real power (MW)	Reactive power (MVar)			
0.05	0.05	2420	7.71	1.32
0.1	0.1	1210	3.85	2.63
0.15	0.15	806.6	2.57	3.95
0.2	0.2	605	1.92	5.26
1.0	1.0	121	0.38	2.63
0.05	0.01	2420	38.5	0.26
0.01	0.05	12100	7.71	1.32

5.2.1 Islanding at Large Power Mismatch

In this scenario, the islanding case is simulated when the power mismatch between the DER's and the load is 1.0 MW and 1.0 MVar. The DER's supplies a load of 2.85 MW and 1.106 MVar, whereas the utility energizes the remaining loads, resulting in a total load of 3.85 MW and 2.106 MVar. The f_{meas}, $(df/dq)_{meas}$ and $(df/dt)_{meas}$ responses for this case are shown in Figures 5.1 and 5.2.

It is noticed from Figures 5.1 and 5.2 that when islanding occurs at 0.05 sec, the proposed technique measures the *df/dq*. It is initiated when $(df/dq)_{meas}$ exceeds $(df/dq)_{min}$ and after ignoring the initial transients, it picks up its maximum value from the 3 cycles. Figure 5.2 shows that $(df/dq)_{meas}$ for this case is 85.90 Hz/MVar, which is greater than $(df/dq)_{max}$, and more significant than $(df/dt)_{meas}$. Hence, the proposed technique correctly detects this event as islanding, and sends the signal to the breaker to trip the DER's.

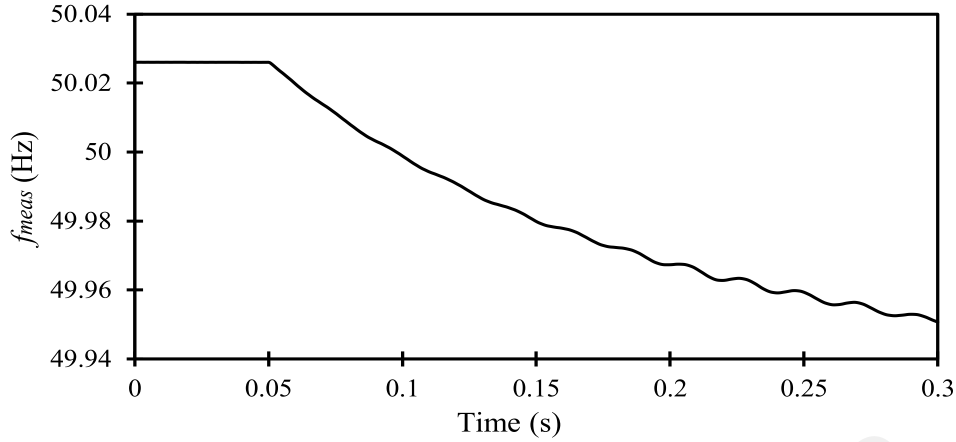

Figure 5.1: Frequency response for islanding scenario at large power mismatch

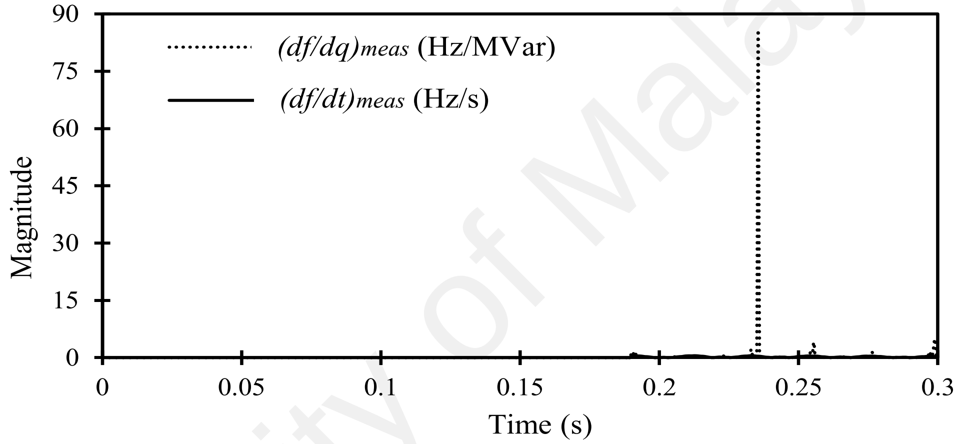

Figure 5.2: *df/dq* and *df/dt* responses for islanding scenario at large power mismatch

5.2.2 Islanding at Small Power Mismatch

In this case, the islanding scenario is simulated at a power mismatch of 0.05 MW and 0.05 MVar between the DER's and the load. Here, the DER's supplies a load of 2.85 MW and 1.106 MVar, while the utility energizes the remaining load. The f_{meas}, $(df/dq)_{meas}$ and $(df/dt)_{meas}$ responses for this case are shown in Figures 5.3 and 5.4.

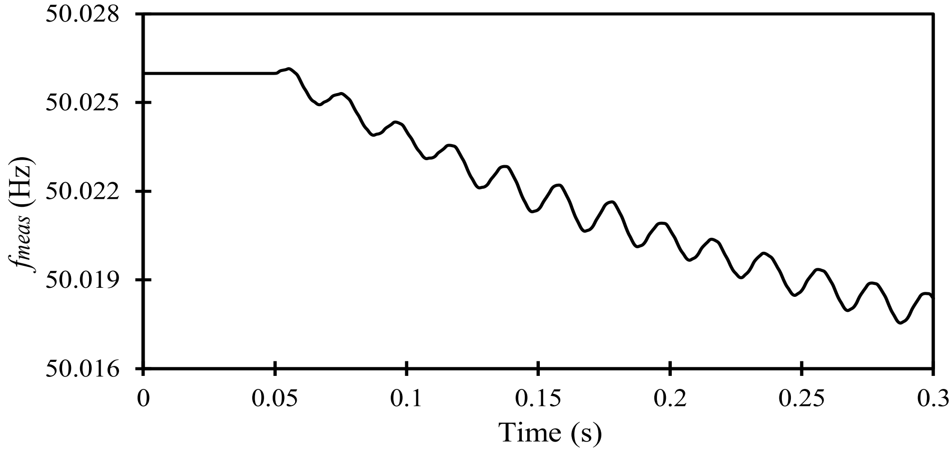

Figure 5.3: Frequency response for islanding scenario at small power mismatch

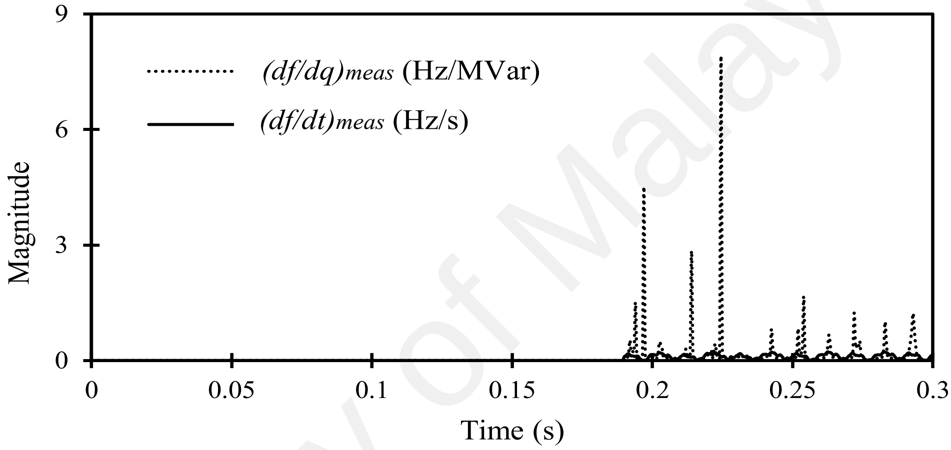

Figure 5.4: *df/dq* and *df/dt* responses for islanding scenario at small power mismatch

Figure 5.4 shows that the $(df/dq)_{meas}$ for this case is 7.92 Hz/MVar, which is greater than df/dq_{max} (7.5 Hz/MVar), and a lot more prominent than $(df/dt)_{meas}$. Hence, the proposed technique correctly detects this event as islanding, and sends the signal to trip the breakers of DER's.

5.2.3 Load Increment and Decrement Scenarios

For this analysis, load increment and decrement of 0.05 MW & 0.05 MVar, 0.10 MW & 0.10 MVar, 0.15 MW & 0.15 MVar and 0.2 MW & 0.2 MVar are applied. The values of R and L for these simulated cases are given in Table 5.1. The behavior of $(df/dq)_{meas}$ for these simulated cases are tabulated in Table 5.2.

Table 5.2: $(df/dq)_{meas}$ response for load switching

Load	$(df/dq)_{meas}$ response for load	
	Increment	**Decrement**
0.05 MW & 0.05 MVar	0.42 Hz/MVar	0.51 Hz/MVar
0.10 MW & 0.10 MVar	1.16 Hz/MVar	0.69 Hz/MVar
0.15 MW & 0.15 MVar	1.21 Hz/MVar	0.86 Hz/MVar
0.20 MW & 0.20 MVar	1.27 Hz/MVar	0.91 Hz/MVar

The responses of f_{meas}, $(df/dq)_{meas}$ and $(df/dt)_{meas}$ for load increment and decrement cases at 0.20 MW & 0.20 MVar are shown in Figures 5.5-5.8, respectively.

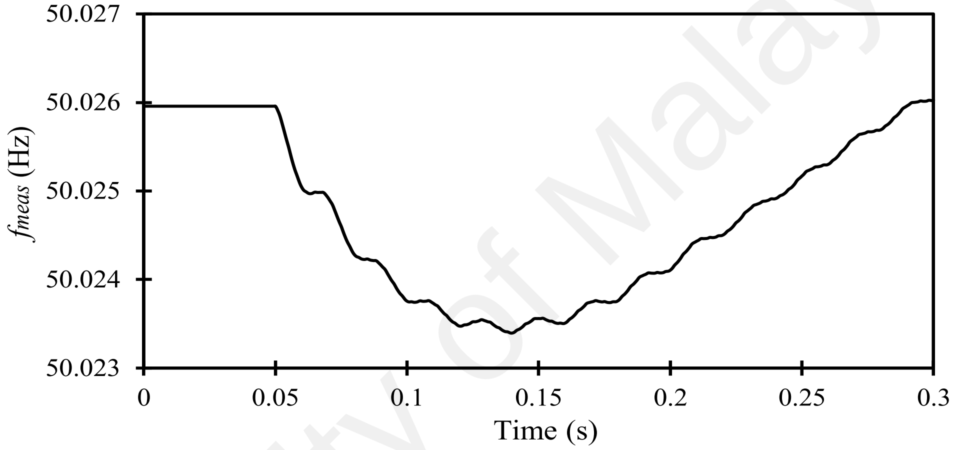

Figure 5.5: Frequency response for load increment scenario

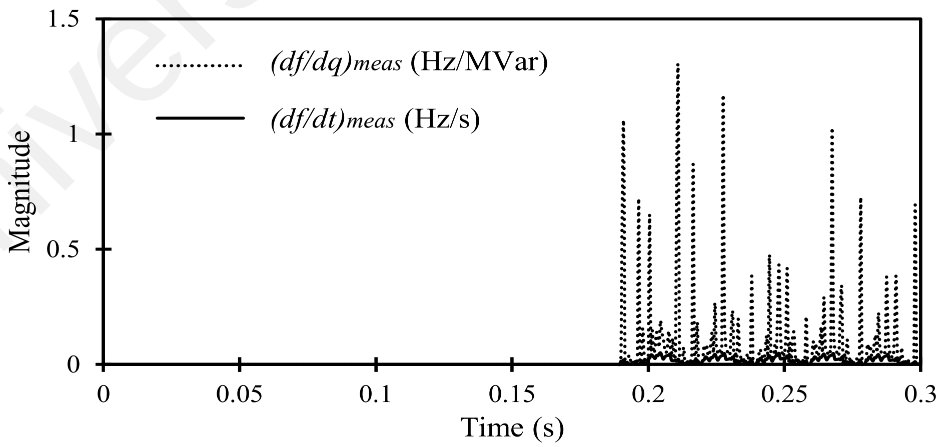

Figure 5.6: Behavior of *df/dq* and *df/dt* for load increment scenario

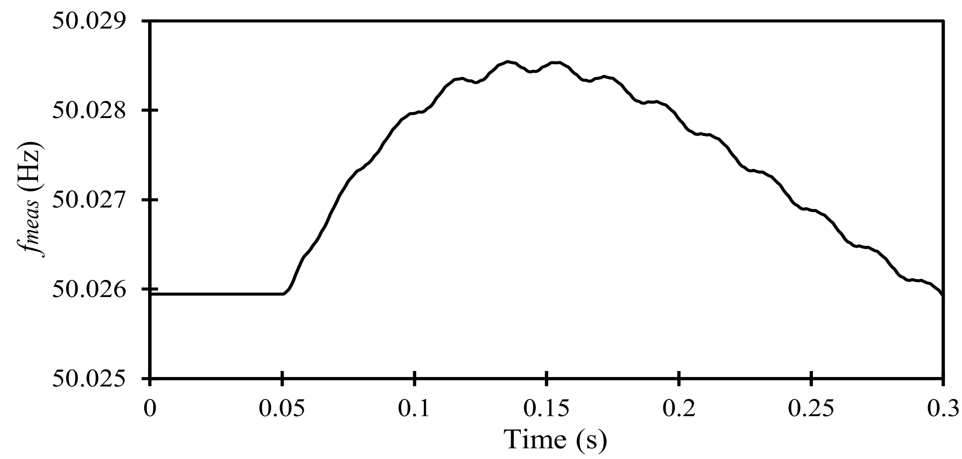

Figure 5.7: Frequency response for load decrement scenario

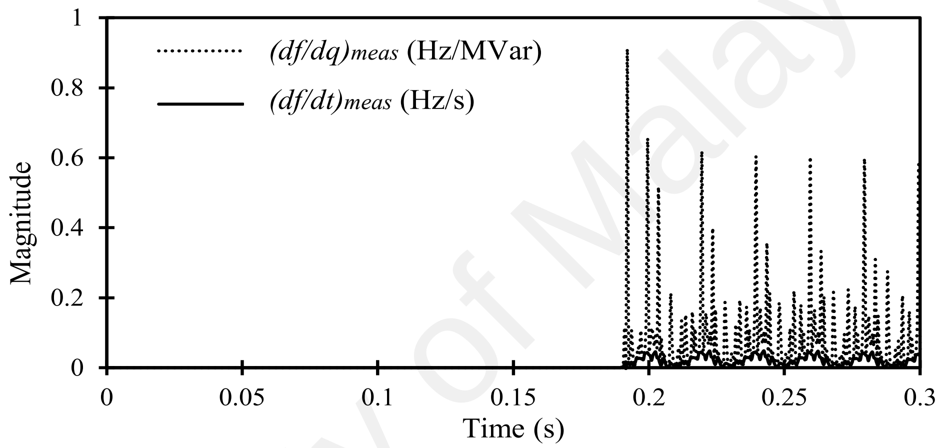

Figure 5.8: Behavior of *df/dq* and *df/dt* for load decrement scenario

Figures 5.6 and 5.8 show that the $(df/dq)_{meas}$ for these cases are 1.27 Hz/MVar, and 0.91 Hz/MVar respectively, which are smaller than the threshold value ($(df/dq)_{max}$) of 7.5 Hz/MVar . Hence, the proposed technique detects this event as non-islanding scenario, which allows the distribution system to continue operating normally.

5.2.4 Capacitor Switching Scenarios

In order to validate the effectiveness of the proposed islanding detection technique for leading power factor conditions, connection and disconnection of capacitor banks bearing capacities of 0.05, 0.10, 0.15 and 0.20 MVar are simulated. The values of capacitor for these are given in Table 5.1. The values of $(df/dq)_{meas}$ for these cases are illustrated in Table 5.3.

Table 5.3: $(df/dq)_{meas}$ response for capacitor switching

Capacitor bank (MVar)	$(df/dq)_{meas}$ response for	
	Capacitor connection	Capacitor disconnection
0.05	2.68 Hz/MVar	1.79 Hz/MVar
0.10	1.65 Hz/MVar	2.83 Hz/MVar
0.15	0.95 Hz/MVar	3.01 Hz/MVar
0.20	0.21 Hz/MVar	4.60 Hz/MVar

The responses of f_{meas}, $(df/dq)_{meas}$ and $(df/dt)_{meas}$ for capacitor connection and disconnection having capacity of 0.20 MVar are shown in Figures 5.9-5.12, respectively.

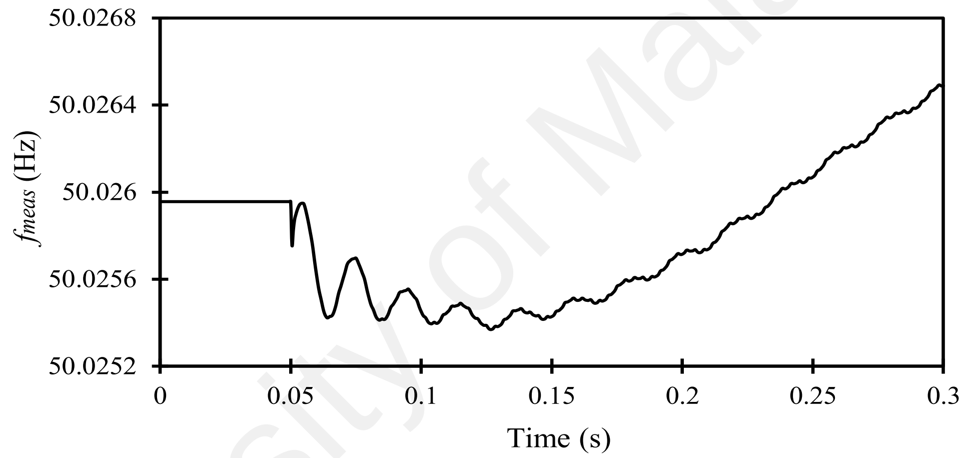

Figure 5.9: Frequency response for capacitor connection scenario

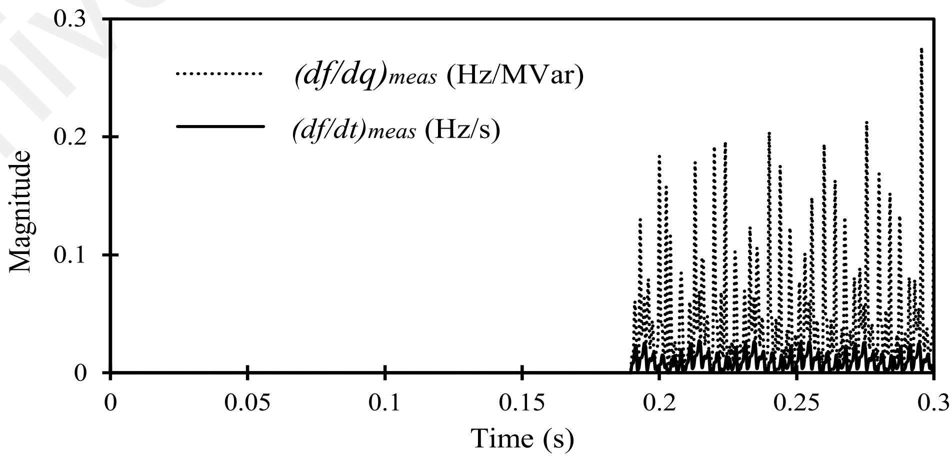

Figure 5.10: Behavior of *df/dq* and *df/dt* for capacitor connection scenario

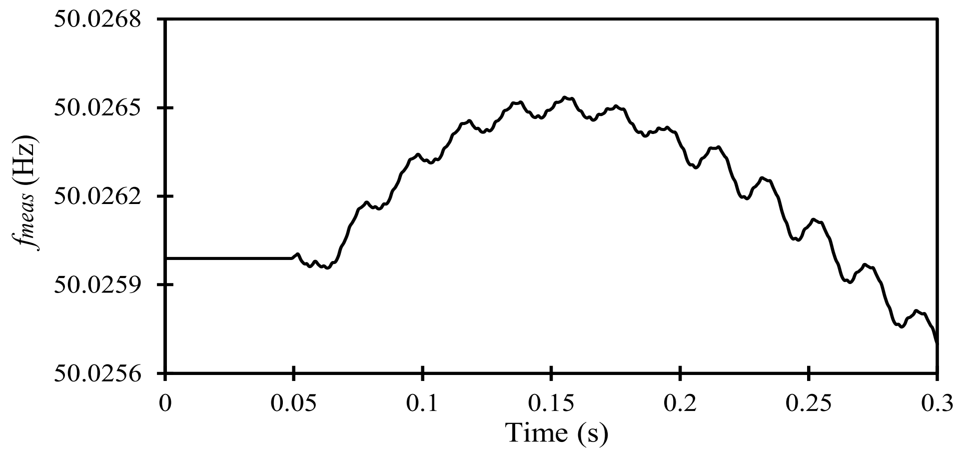

Figure 5.11: Frequency response for capacitor disconnection scenario

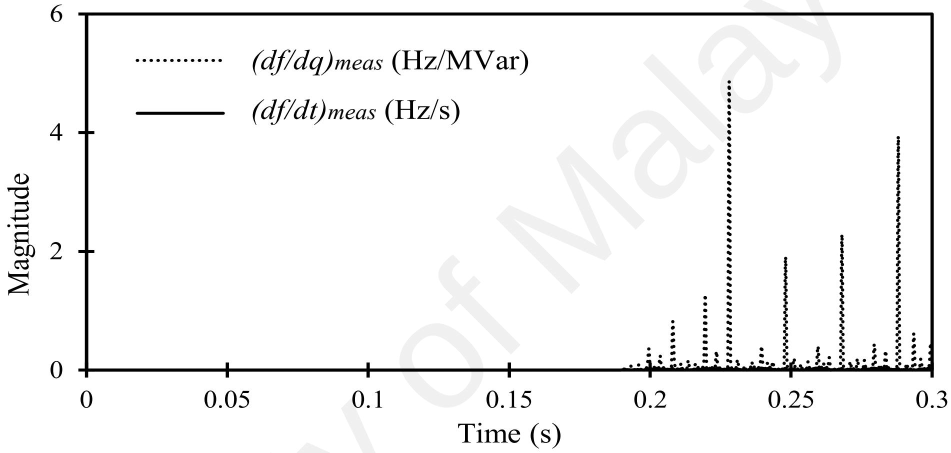

Figure 5.12: Behavior of *df/dq* and *df/dt* for capacitor disconnection scenario

The values of $(df/dq)_{meas}$ for these cases are 0.21 Hz/MVar (Figure 5.10) and 4.6 Hz/MVar (Figure 5.12) respectively, which are smaller than the threshold value ($(df/dq)_{max}$) of 7.5 Hz/MVar . Hence, it is substantiated that the proposed technique can correctly recognize these events as non-islanding conditions.

5.2.5 Single and Three Phase Scenarios

In this case, the performance of the proposed technique is tested for single and three-phase fault conditions at a power mismatch of 0.05 MW and 0.05 MVar between load and DERs. The responses of f_{meas}, $(df/dq)_{meas}$ and $(df/dt)_{meas}$ for single-and three-phase faults are shown in Figures 5.13-5.16, respectively.

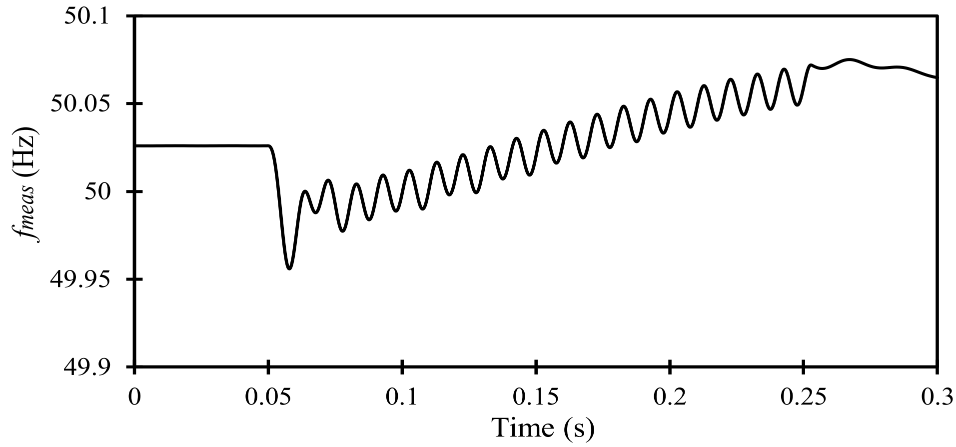

Figure 5.13: Frequency response for single phase fault scenario

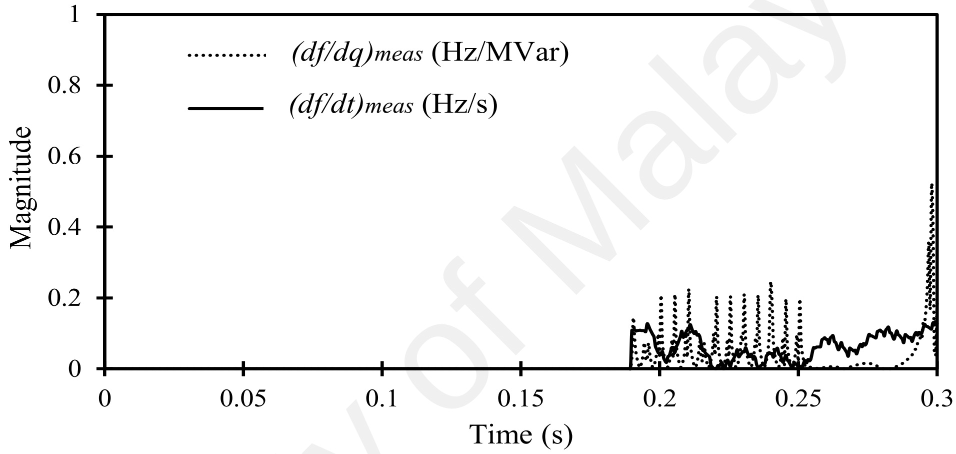

Figure 5.14: Behavior of *df/dq* and *df/dt* for single phase fault scenario

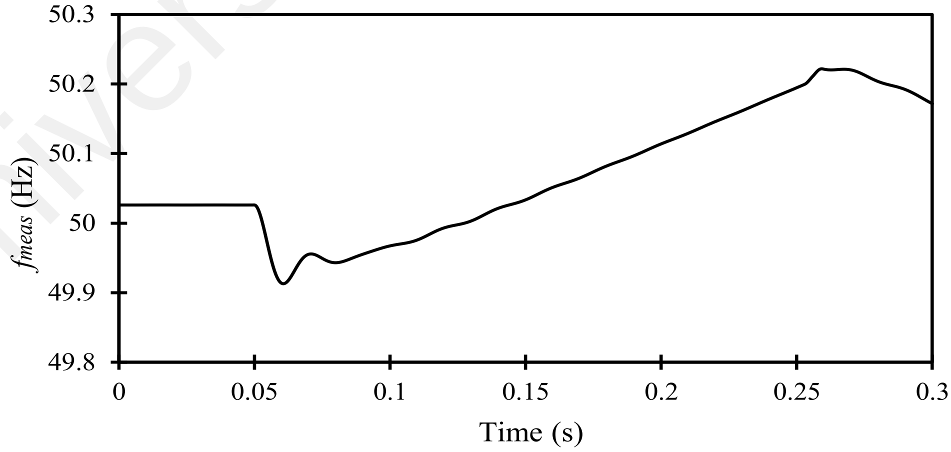

Figure 5.15: Frequency response for three phase fault scenario

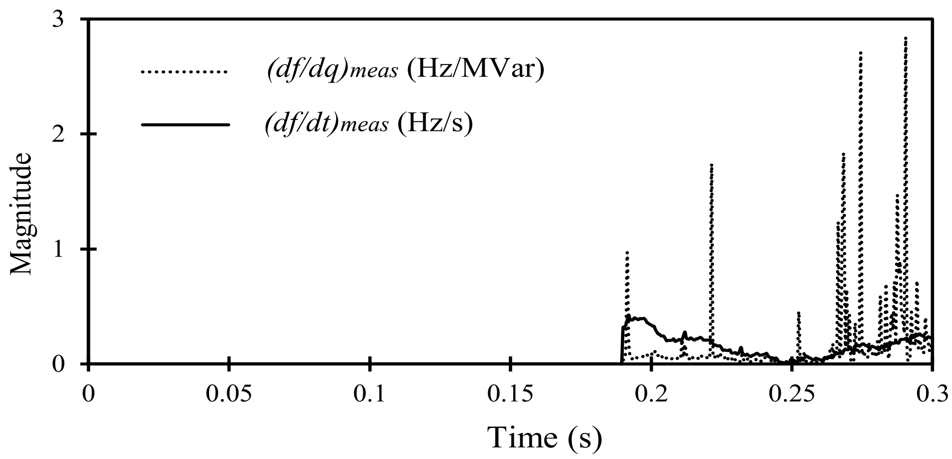

Figure 5.16: Behavior of *df/dq* and *df/dt* for three phase fault scenario

The $(df/dq)_{meas}$ for both single-and three-phase faults for the specified interval are 0.24 Hz/MVar (Figure 5.14) and 1.74 Hz/MVar (Figure 5.16) respectively. It is observed that both values are lower than the threshold value (7.5 Hz/MVar). This confirms that the proposed technique is able to distinguish islanding and fault conditions.

5.2.6 Induction Motor Starting Scenario

In this case, the performance of the proposed technique is tested for the starting effect of induction motor. Since, induction motor has very low power factor during starting which may result in malfunctioning in the performance of islanding detection technique. The power factor of induction motors varies with load, typically from around 0.85 or 0.90 at full load to as low as 0.35 at no-load due to stator and rotor leakage and magnetizing reactance's. For this purpose, the starting effect of a 400 kW induction motor is simulated when the active and reactive power of the total load is 2.85 MW and 1.106 MVar respectively. The f_{meas}, $(df/dq)_{meas}$ and $(df/dt)_{meas}$ responses for this case is shown in Figures 5.17 and 5.18.

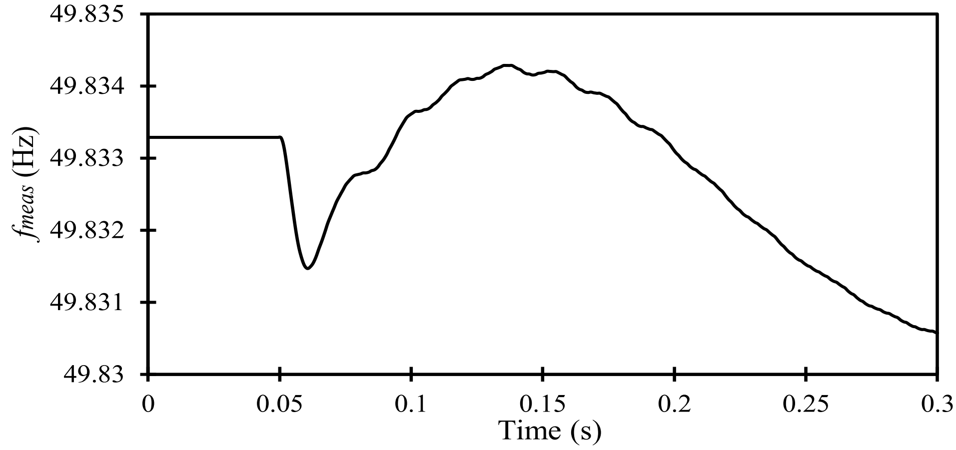

Figure 5.17: Frequency response for induction motor starting scenario

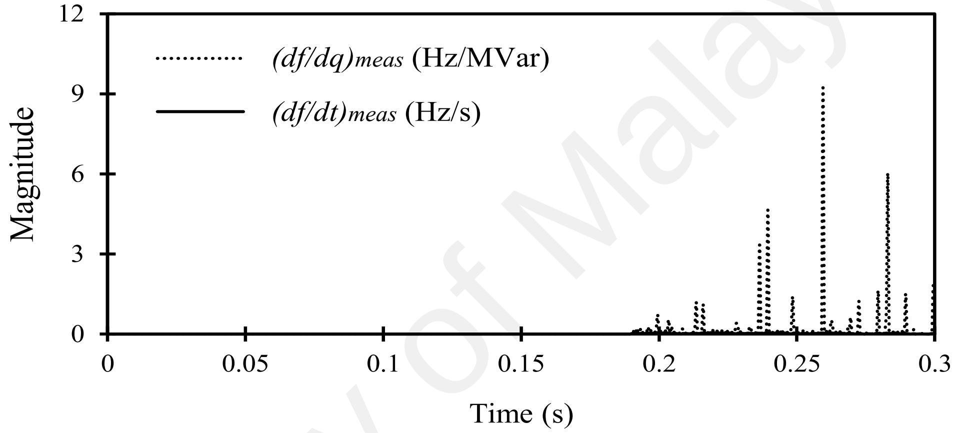

Figure 5.18: Behavior of *df/dq* and *df/dt* for induction motor starting scenario

The $(df/dq)_{meas}$ for this case is 4.64 Hz/MVar, which is less than the threshold. Hence, it is seen that the proposed technique can distinguish the starting effect of the induction motor and islanding events.

5.2.7 Impact under Different Active and Reactive Power Conditions

The proposed technique is also tested on different active and reactive power conditions. 4 cases (0.05 MW & 0.01 MVar, 0.01 MW & 0.05 MVar, 0.50 MW & 0.30 MVar and 0.30 MW & 0.50 MVar) are examined and the values of R, L and C for the cases are provided in Table 5.1. The responses of $(df/dq)_{meas}$ for islanding and non-islanding scenarios under unbalanced power conditions are presented in Table 5.4.

Table 5.4: ($df/dq)_{meas}$ for different active and reactive power conditions

Testing scenarios	Case I 0.05 MW, 0.01 MVar	Case II 0.01 MW, 0.05 MVar	Case III 0.50 MW, 0.30 MVar	Case IV 0.30 MW, 0.50 MVar
Islanding	83.15	14.93	36.05	44.86
Load decrement	0.27	0.64	4.7	0.85
Load increment	3.22	1.11	6.9	3.80
Single phase fault	1.01	5.3	1.66	1.65
Three phase fault	1.13	0.80	1.15	0.17
Induction motor starting	3.58	4.00	7.35	7.8
Capacitor connection	0.89	2.85	10.3	3.41
Capacitor disconnection	1.59	1.79	2.80	7.10

It can be observed that the proposed technique successfully distinguishes islanding from non-islanding events under different active and reactive power conditions.

5.2.8 Generator Inertia and Exciter Type

The performance of the proposed technique is tested for multiple generator inertia and exciter for a mini-hydro generator. The power mismatch in all of these cases is again 0.05 MW and 0.05 MVar. Islanding and non-islanding events are tested for the generator inertia, with values of 1.5 and 2.5 using IEEE type AC1A and AC2A exciters. The simulation results of these are shown in following sub-sections.

5.2.8.1 Results using Exciter Type AC1A

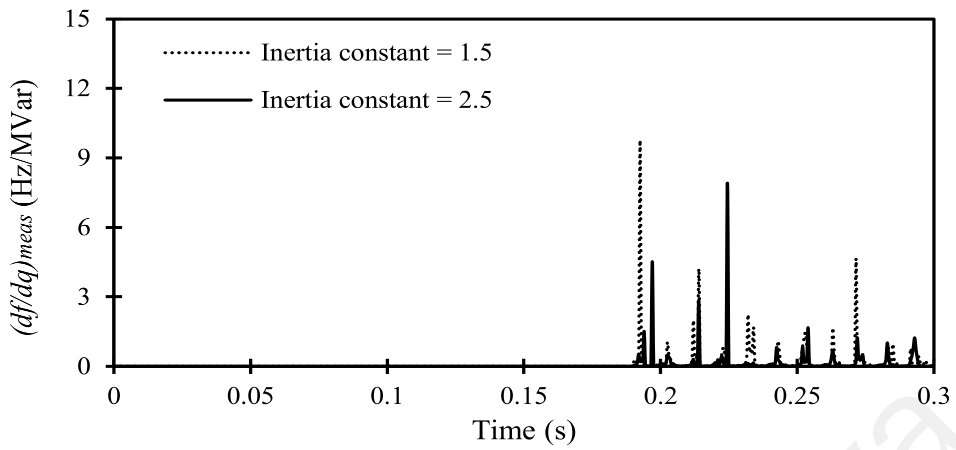

Figure 5.19: Islanding scenario

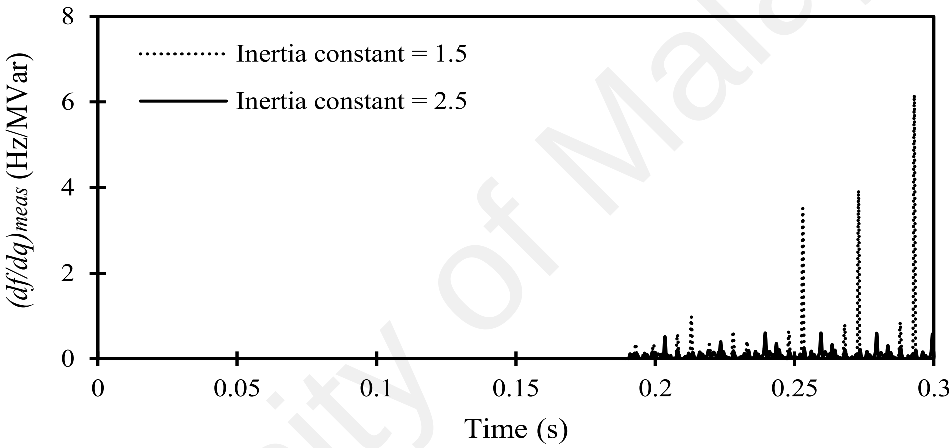

Figure 5.20: Load decrement scenario

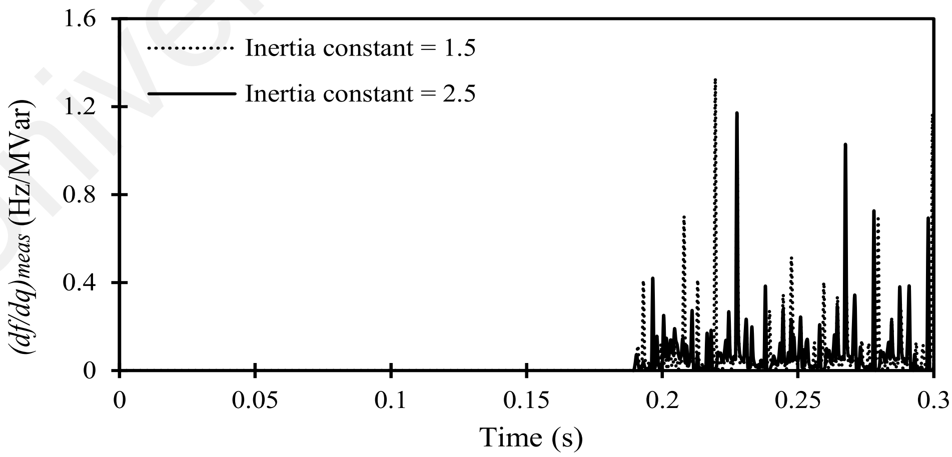

Figure 5.21: Load increment scenario

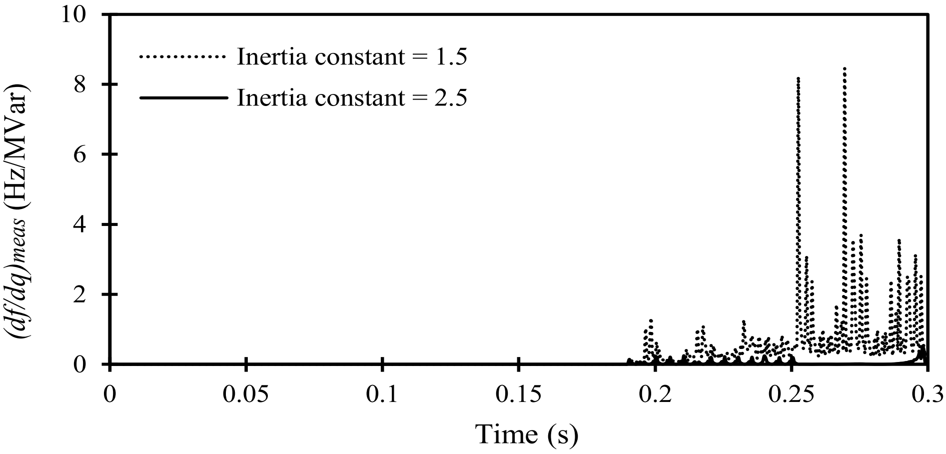

Figure 5.22: Single phase fault scenario

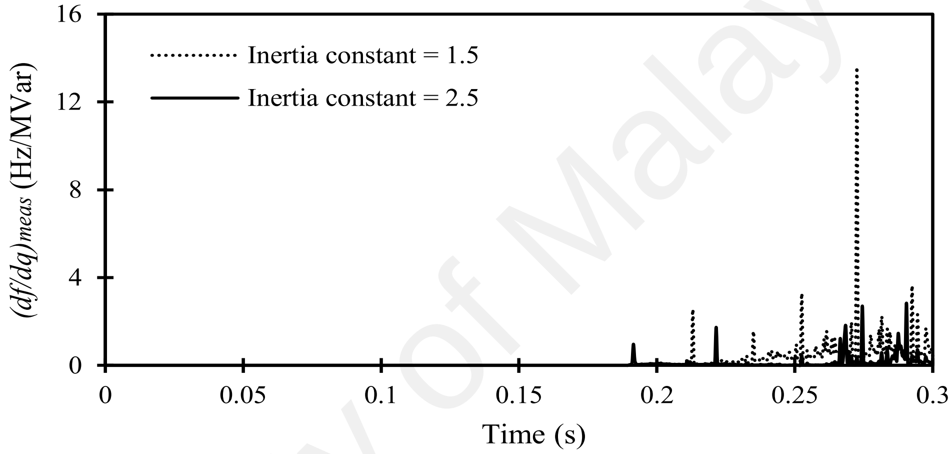

Figure 5.23: Three phase scenario

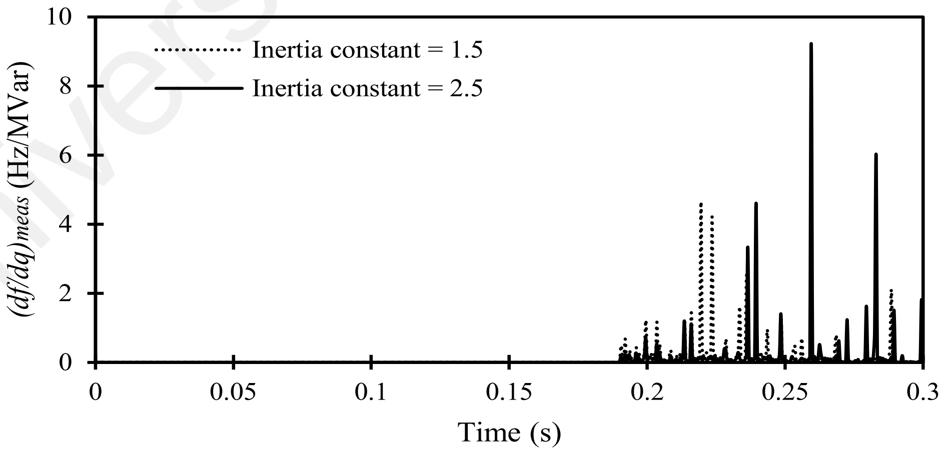

Figure 5.24: Induction motor starting scenario

5.2.8.2 Results using Exciter Type AC2A

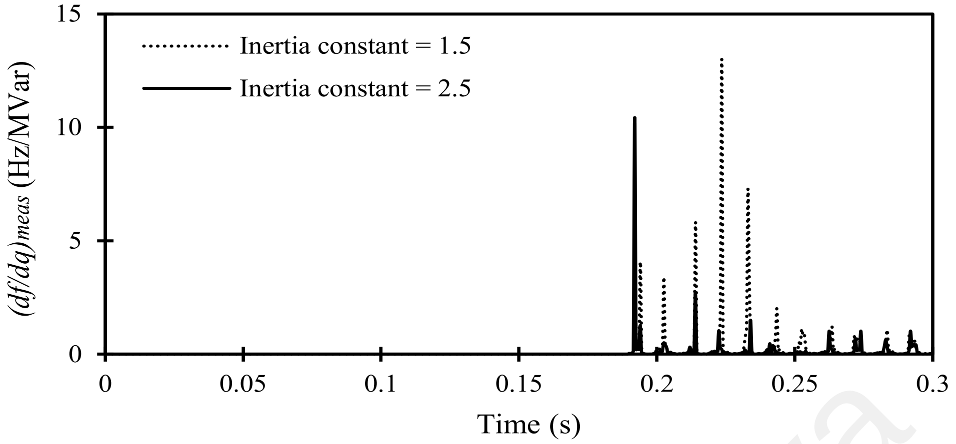

Figure 5.25: Islanding scenario

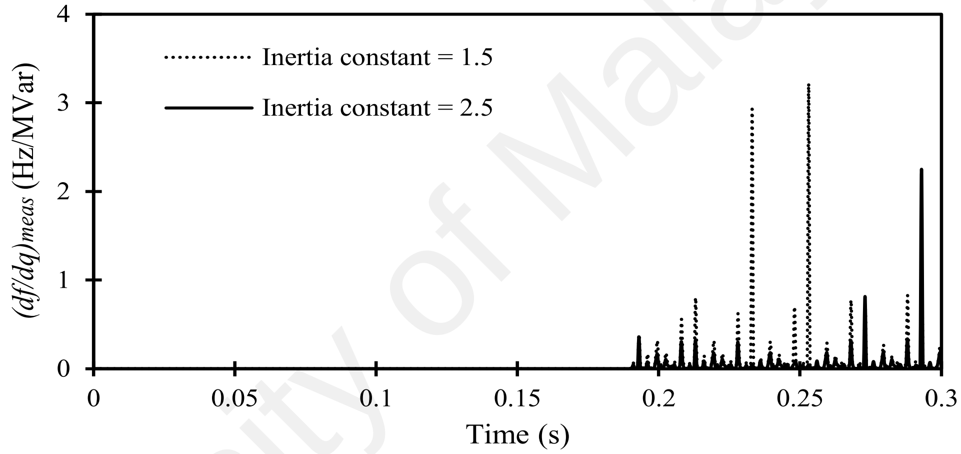

Figure 5.26: Load decrement scenario

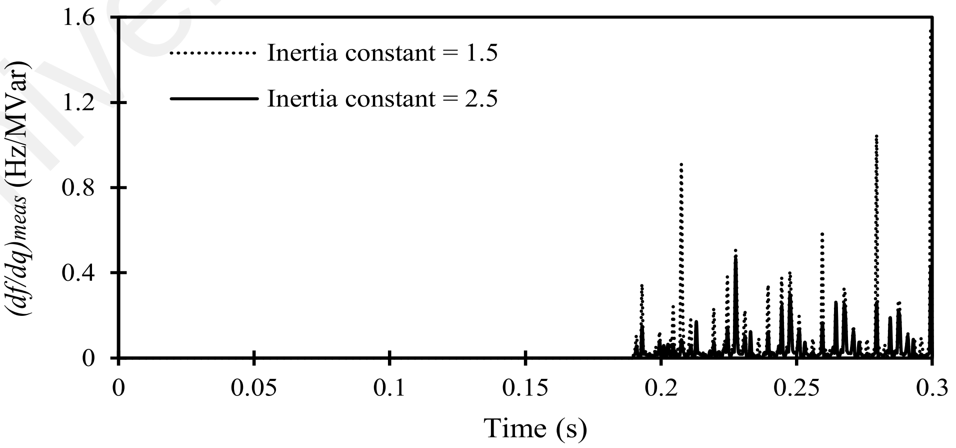

Figure 5.27: Load increment scenario

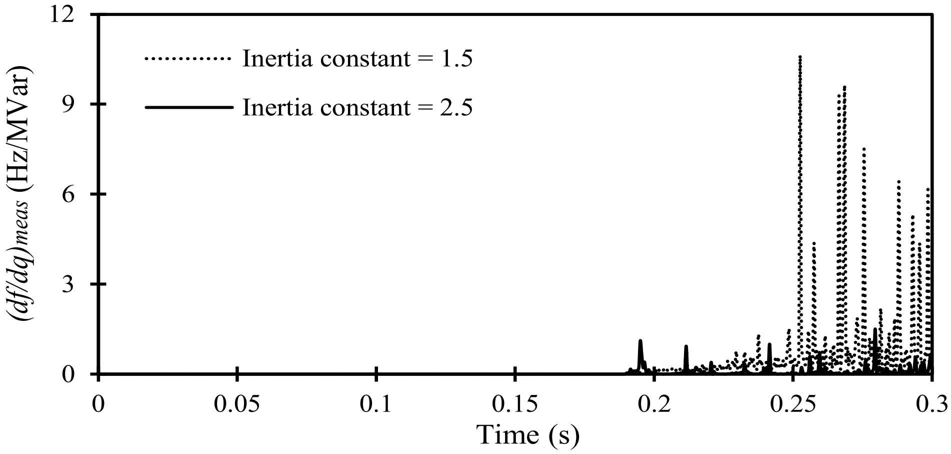

Figure 5.28: Single phase fault scenario

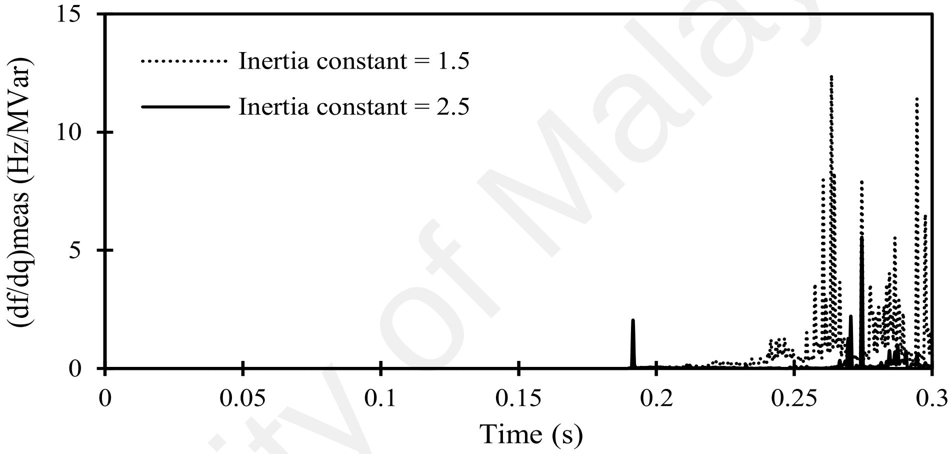

Figure 5.29: Three phase scenario

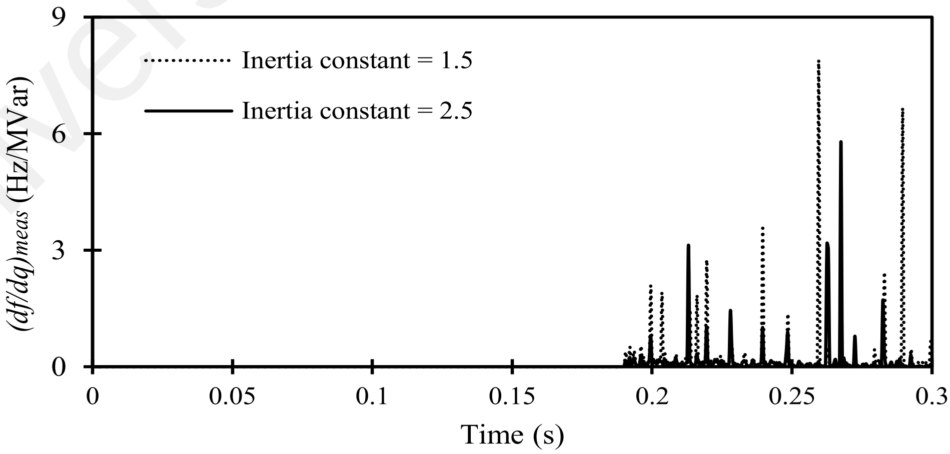

Figure 5.30: Induction motor starting scenario

The responses of $(df/dq)_{meas}$ for varying generator inertia using different exciters are summarized in Table 5.5.

Table 5.5: $(df/dq)_{meas}$ for varying generator inertia using different exciters

Testing scenarios / **Generator inertia**	**Exciter**			
	AC1A		**AC2A**	
	1.5	**2.5**	**1.5**	**2.5**
Islanding	9.77	7.92	13.56	10.4
Load decrement	0.98	0.51	2.93	0.36
Load increment	1.32	0.42	0.90	0.46
Single phase fault	1.33	0.24	1.10	1.10
Three phase fault	2.55	1.74	1.29	2.05
Induction motor starting	4.64	4.60	3.50	3.13

From Table 5.5, it is quite clear that the value of $(df/dq)_{meas}$ varies with changes in the generator inertia and the exciter type of Mini-Hydro generator. However, this parameter is still able to distinguish islanding and non-islanding conditions.

5.2.9 Quality Factor

The performance of the proposed technique is also tested for different quality factors (Q_f) when the power mismatch between the DER's and the load is 0.05 MW and 0.05 MVar, respectively. Islanding and non-islanding scenarios are tested at a Q_f of 1.8 and 2.5. The values of R, L and C for different Q_f are:

Q_f= 1.8: R = 42.46 Ω, L = 0.0750 H and C = 135 µF

Q_f= 2.5: R = 42.46 Ω, L = 0.0541 H and C = 187.53 µF

The responses of $(df/dq)_{meas}$ under both conditions are given in Table 5.6.

Table 5.6: $(df/dq)_{meas}$ for different quality factors

Testing scenarios	Quality factor	
	1.8	**2.5**
Islanding	10.5	12.5
Load decrement	1.24	1.64
Load increment	2.57	2.96
Single phase fault	2.66	2.76
Three phase fault	3.50	3.71
Induction motor starting	2.65	4.90

It is quite clear that for different quality factors, the proposed parameter varies. However, it still has the capability of distinguishing islanding and non-islanding events.

5.3 NDZ of Conventional and Proposed Passive Technique

NDZ is the key feature that reflects the efficacy of the islanding detection technique. It is defined as a region where the islanding detection technique stops working. For active power, the NDZ is determined by (Zeineldin et al., 2006):

$$\Delta P = -3V \times \Delta V \times I \times \cos\varphi \tag{5.1}$$

where, ΔP is the active power imbalance, V is the rated voltage, I is the rated current, $cos\varphi$ is the power factor, and ΔV is the voltage deviation.

The maximum and minimum voltage limits used in the distribution network of Malaysia are 1.1 p.u and 0.9 p.u, respectively. On the basis of these voltage levels, the deviation in voltage (ΔV) is -0.1 and 0.1, respectively. The NDZ region for active power imbalance of the distribution system being studied is 0.285 MW and -0.285 MW, respectively. For reactive power, the NDZ is determined by (Zeineldin et al., 2006):

$$\Delta Q = \frac{3V^2}{\omega_n L}\left(1 - \frac{f_n^2}{\left(f_n \pm \Delta f\right)^2}\right) \tag{5.2}$$

where, V is the rated voltage, f_n is the nominal frequency and Δf is the frequency deviation and $\omega_n = 2 \times \pi \times f$.

The allowable frequency range of Malaysian distribution network varies from 49.5 Hz to 50.5 Hz, which results in frequency deviation (Δf) between -0.5 Hz to 0.5 Hz. Hence, the NDZ, with respect to reactive power imbalance of the under study distribution system is 0.303183 MVar and -0.312417 MVar, respectively. On the basis of the simulation results, it is also observed that the proposed technique works efficiently when the power imbalance is 0.05 MW and 0.05 MVar. Thus, the proposed technique increases the accuracy and also reduces the NDZ compared to OVP/UVP and OFP/UFP based conventional techniques, as shown in Figure 5.31.

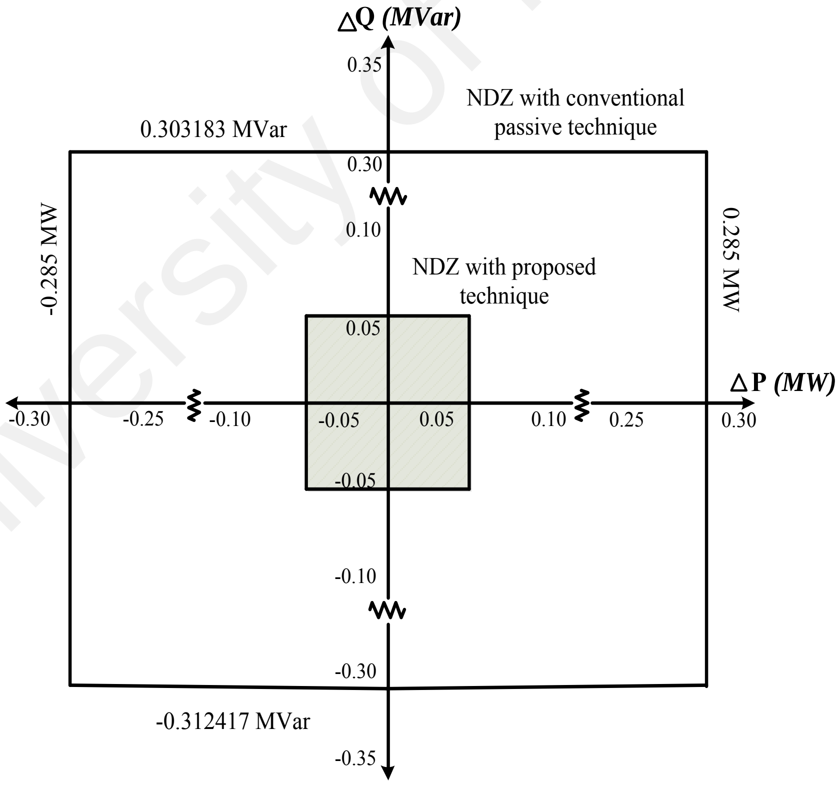

Figure 5.31: NDZ plot

5.4 Simulation Results of Proposed Intelligent Technique

In section 4.6, the ANN analysis for features selection is presented. The input features are grouped into 2 sets (*df/dq*, *dp/dt* and *df/dq*, *dq/dt*). Different percentages

(50%, 60% and 70%) of the total data for these 2 sets are selected systematically and inter-systematically for training purpose. Based on ANN analysis, it is observed that whether training data is selected systematically or inter-systematically, the regression value obtained for different cases are very close to each other for both set 1 and 2, as illustrated in Table 4.2-4.5. Upon keen investigation, it has been found that the regression value for the 2nd set of input features (*df/dq*, *dq/dt*) shows a higher value compared to 1st set of input features (*df/dq*, *dp/dt*). Furthermore, it is also observed that the regression value for the both sets of input features has higher value if the ANN indices are selected optimally. Thus, regression value obtained by ANN by using EP and PSO exhibits higher performance/regression value compared to default and tuned approach. However, in order to finally select the trained file for testing, it is important to ascertain which optimization technique (EP or PSO) is able to reach the global minimum quickly. The convergence curve of EP and PSO for 70% of training set using systematic and inter-systematic selection is shown in Figures 5.32-5.35.

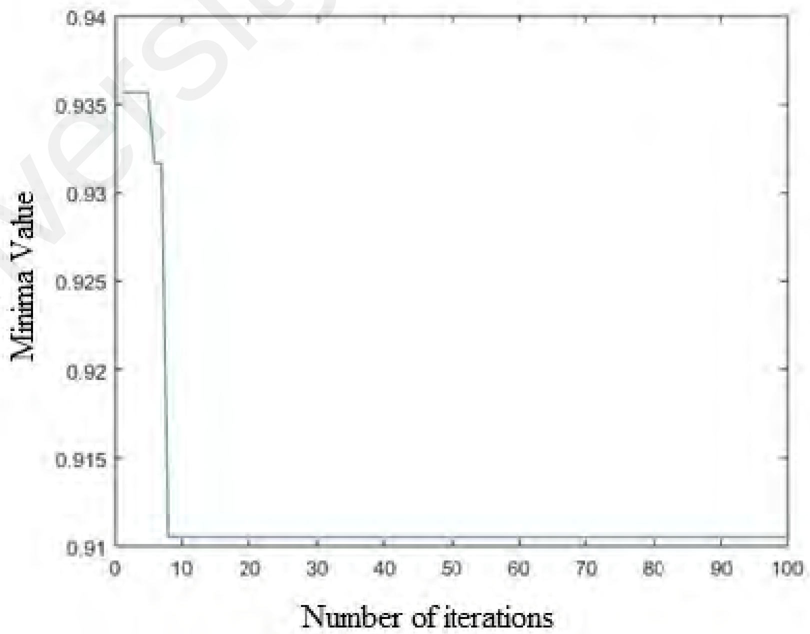

Figure 5.32: ANN-EP convergence curve for 70% training data using inter-systematic selection

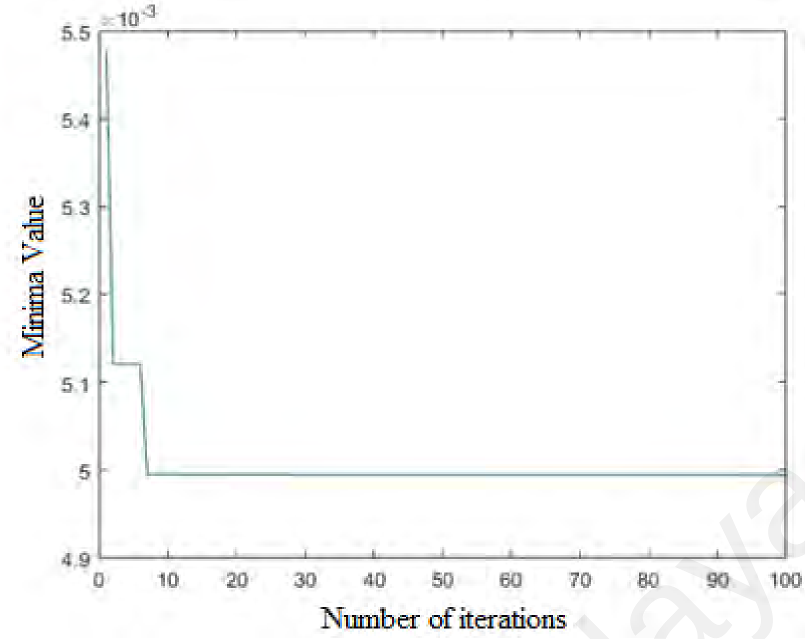

Figure 5.33: ANN-PSO convergence curve for 70% training data using inter-systematic selection

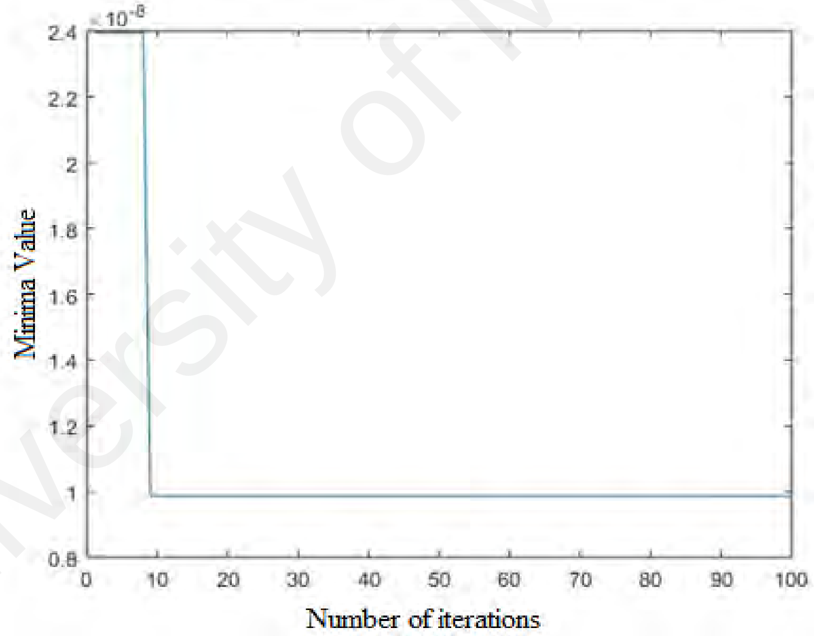

Figure 5.34: ANN-EP convergence curve for 70% training data using systematic selection

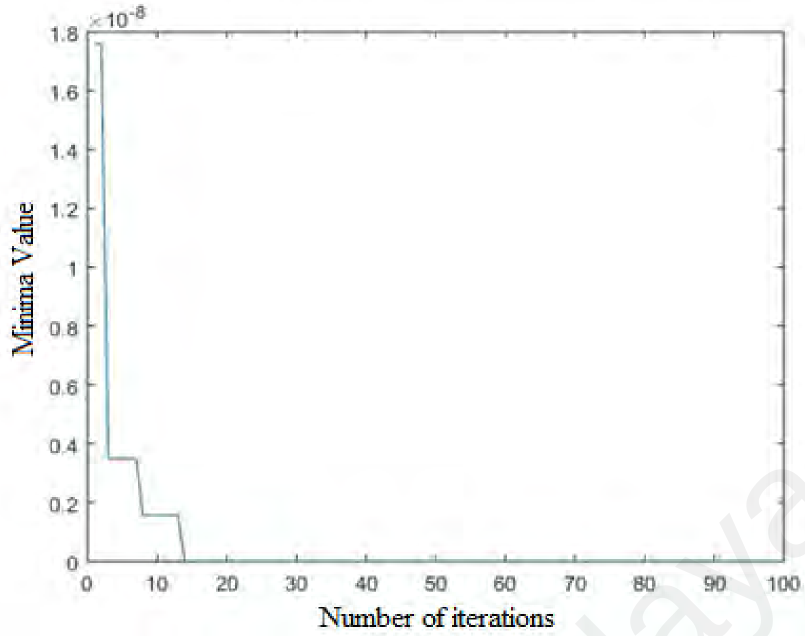

Figure 5.35: ANN-PSO convergence curve for 70% training data using systematic selection

It is quite clear from the convergence curve that EP is able to reach global minimum whether the data is selected systematically or inter-systematically. However, the case is quite different in PSO. Using inter-systematic selection, the algorithm converges or reaches the global minimum faster compared to systematic selection of training data. However, the regression value using systematic selection is comparably higher than the inter-systematic selection. Therefore, ANN-PSO gives the highest regression value for set 2 (*df/dq*, *dq/dt*) for 70% of training data using systematic selection as presented in Table 4.5. Hence, we perform the on- and off-line testing using this set of input. The trained ANN file obtained by systematic selection of 70% of training data is used for testing purpose.

5.4.1 Off-line Testing

Upon successful training of the ANN using the optimal values obtained from EP and PSO, the performance is validated for 434 various islanding and non-islanding events in MATLAB environment. Here, 114 events fall under the category of islanding events and the remaining fall under the category of non-islanding events. Figure 5.36 illustrates the testing response of the proposed technique for the 2nd set of input features (*df/dq*, *dq/dt*) using ANN-PSO for 70% of systematic selection. All the events (as tabulated in Table 4.1) are detected accurately by ANN-PSO for the 2nd set of input (*df/dq*, *dq/dt*) for 70% of systematic selection. Therefore, the proposed islanding detection technique exhibits higher accuracy even under closely mismatched conditions as compared to others (Abd-Elkader et al., 2014; Ghazi & Lotfi, 2010). The results shown here further validate the choice of input data set. Hence the 2nd set of input based on ANN-PSO for 70% of training data selected by systematic way is used to carry out the on-line testing.

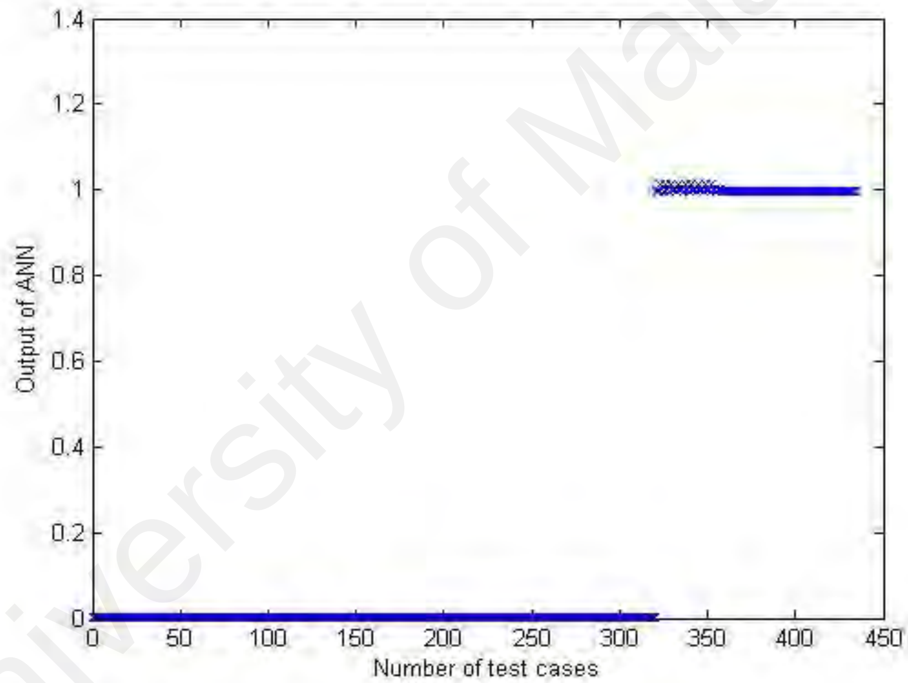

Figure 5.36: Off-line testing using 2nd set of ANN-PSO

5.4.2 On-line Testing

The proposed islanding detection technique is also evaluated online to validate its performance. Here, the developed network model in PSCAD is interfaced with the trained ANN in MATLAB. The on-line testing scenario is presented in Figure 5.37. The load is energized by both utility grid and DER's. The signals (*df/dq, dq/dt*) are measured at the point of common coupling (PCC) and are sent to the MATLAB environment. The

ANN block will decide the output signal on the basis of ANN-PSO trained file. The output signal trips the DER's breaker (BRK 1, 2 and 3) upon sensing that the utility supply is disconnected.

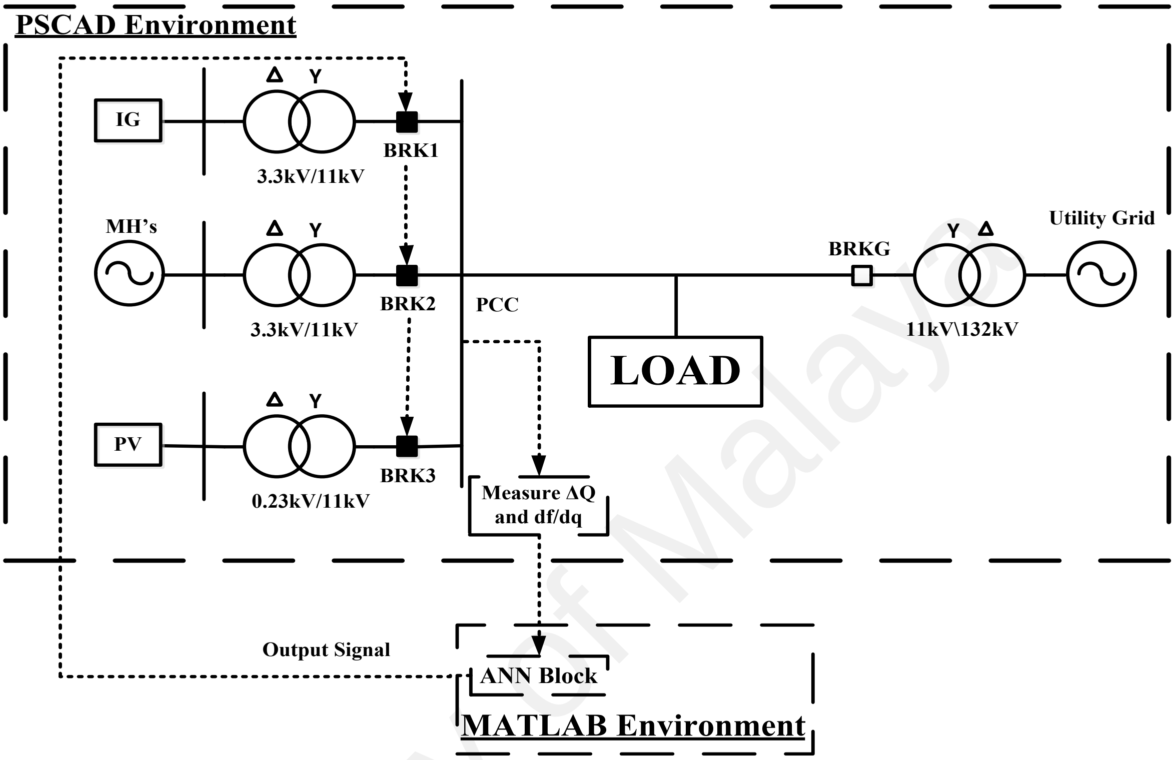

Figure 5.37: On-line testing scenario

For on-line testing, 2 islanding and 10 non-islanding events are evaluated at different buses which are tabulated in Table 5.5. All events are initialized at t = 1 sec, once the system is stabilized.

Table 5.7: Evaluated cases for on-line testing

Scenarios	Testing events	Testing Bus Number
Islanding	At small power mismatch (0.003 MW and 0.002 MVAr)	14
	At large power mismatch (1.03 MW and 0.98 MVAr)	28
Non-islanding	Load increment of 0.96 MW and 1.10 MVAr	22
	Load decrement of 0.21 MW and 0.18 MVAr	18
	Capacitor connection of 0.50 MVAr	20
	Capacitor disconnection of 0.30 MVAr	12
	Induction motor starting at zero power mismatch	6
	Single phase to ground fault at power mismatch of 1.13 MW and 0.98 MVAr	18
	Double phase to ground fault at power mismatch of 0.007 MW and 0.004 MVAr	2
	Three phase to ground fault at power mismatch of 0.003 MW and 0.002 MVAr	13
	Phase to phase fault at power mismatch of 1.07 MW and 0.995 MVAr	29
	Induction generator tripping at power mismatch of 0.003 MW and 0.002 MVAr	21

5.4.2.1 Evaluation Under Islanding Scenarios

To investigate the islanding scenarios, the performance of the proposed technique is evaluated for different active and reactive power mismatches. Therefore, small and large power mismatch conditions, as tabulated in Table 5.5, are evaluated here as an example.

In these conditions, the utility supply is disconnected at t=1 sec. Upon disconnection of utility supply, Figures 5.38 and 5.39 shows the behavior of rate of change of frequency over reactive power (*df/dq*) and rate of change of reactive power (*dq/dt*) respectively at a small power mismatch of 0.003 MW and 0.002 MVar.

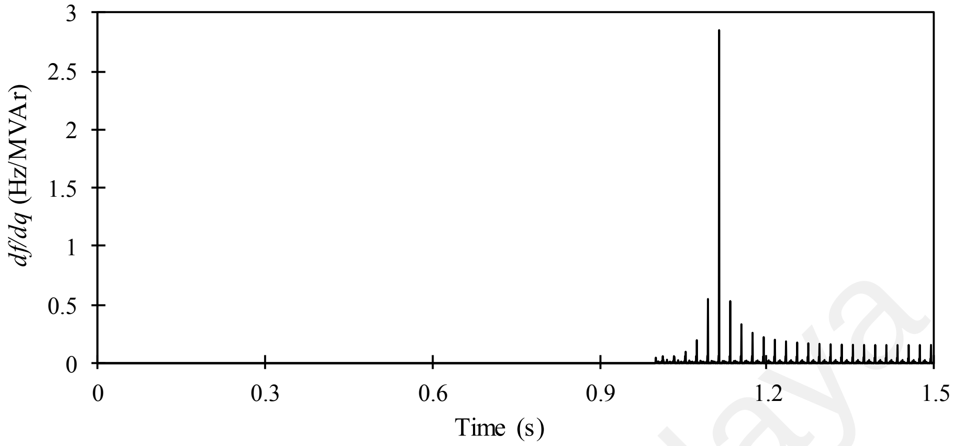

Figure 5.38: *df/dq* response at closely mismatched condition

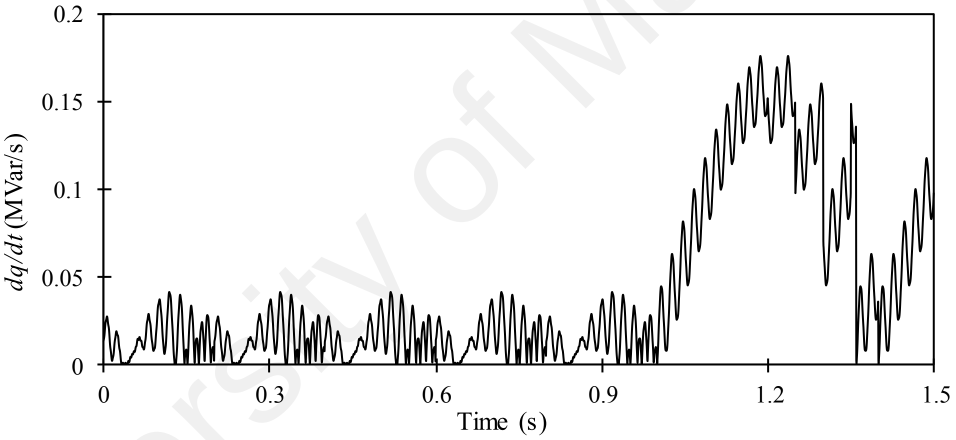

Figure 5.39: *dq/dt* response at closely mismatched condition

Similarly, the behavior of rate of change of frequency over reactive power (*df/dq*) and rate of change of reactive power (*dq/dt*) at a large power mismatch of 1.03 MW and 0.98 MVar is shown in Figures 5.40 and 5.41.

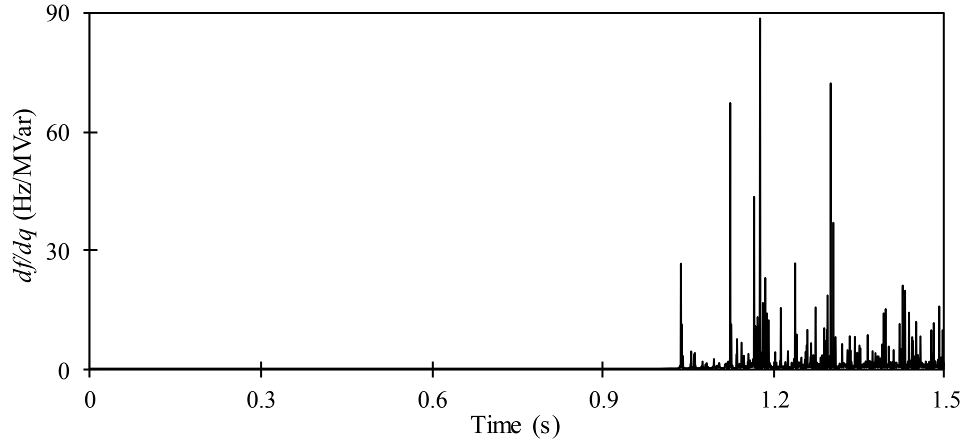

Figure 5.40: *df/dq* response at large power mismatched condition

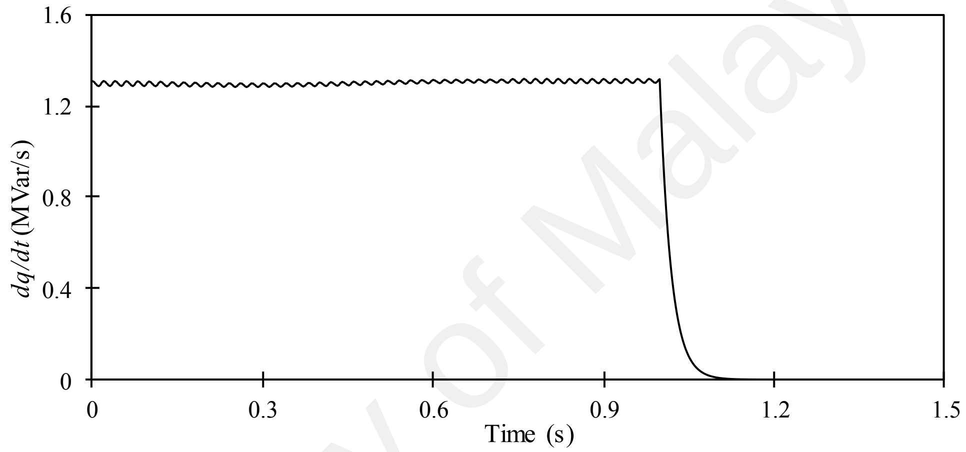

Figure 5.41: *dq/dt* response at large power mismatched condition

The corresponding ANN-PSO output is shown in Figure 5.42. On the basis of simulation results, it is quite clear that the islanding conditions are detected accurately.

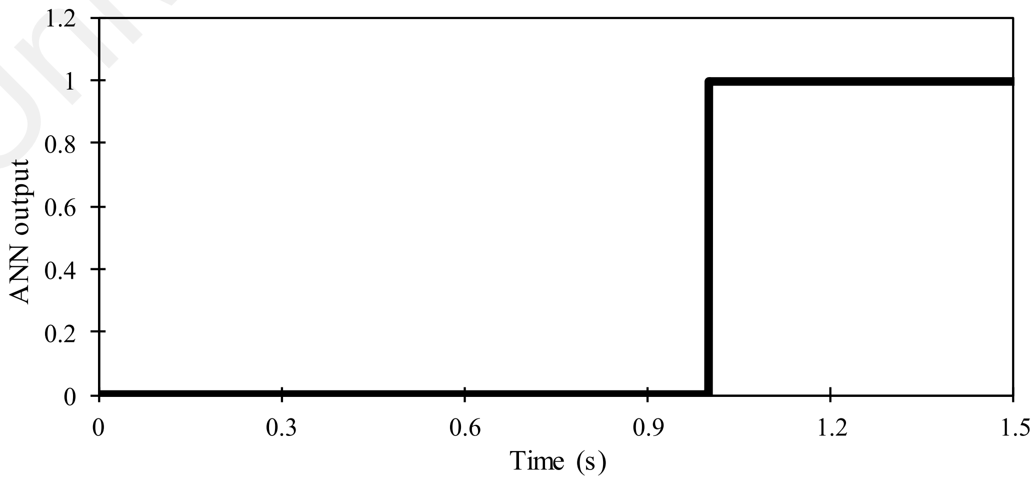

Figure 5.42: ANN-PSO output at islanding condition

5.4.2.2 Evaluation under Non-islanding Scenarios

The performance of the proposed technique is also evaluated online for non-islanding scenarios which includes the switching of load and capacitor, different types of faults such as single, double and three phase to ground faults, phase to phase faults, induction motor starting and induction generator tripping are also tested at different buses, as tabulated in Table 5.5. Similar to the islanding scenarios, all the non-islanding scenarios are also switched at t = 1 sec.

The behavior of rate of change of frequency over reactive power (*df/dq*) and rate of change of reactive power (*dq/dt*) are shown in Appendix. The corresponding ANN-PSO output for non-islanding events are shown in Figure 5.43. Similar to the islanding events, the non-islanding conditions are also detected precisely.

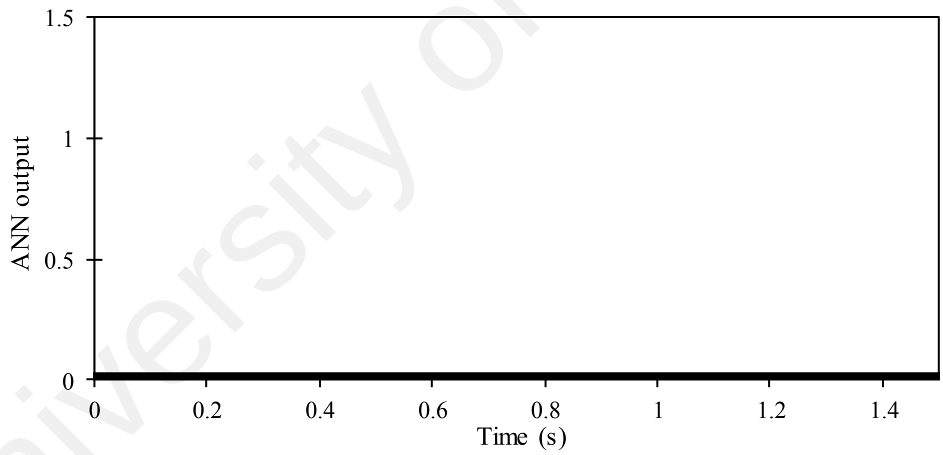

Figure 5.43: ANN-PSO output at non-islanding conditions

5.5 Error Analysis

From the simulation results of proposed ANN-PSO based intelligent technique, it is found that this technique has the ability to work proficiently in closely mismatched conditions which has always been the Achilles heels in the passive technique. In order to significate the performance of proposed intelligent technique and to check the compatibility of the ANN-PSO based trained file, different percentages of error have been introduced in testing data (434 cases i.e 30% of total data). This errored testing data is verified by using the selected ANN-PSO based trained file. The analysis on percent error increment and decrement is discussed in the following sub-sections.

5.5.1 Gradual Percentage Increment in *df/dq* and *dq/dt*

In this condition, different percentages of error (8%, 13%, 19%, 24%, 30%, 33%, 37%, 42% and 46%) in terms of increment has been introduced in both *df/dq* and *dq/dt* features. The ANN-PSO trained file is used to validate the performance under this condition. Normally, all islanding cases fall at 1 and non-islanding cases fall at 0 as shown in Figure 5.32. However, upon error introduction, the values do not exactly fall on 0 and 1, that is, some of the islanding events moves towards non-islanding and vice versa. Hence, discrimination between islanding and non-islanding values is made by setting the threshold values (0.5 and 0.7). The results for error analysis at percent increment are illustrated in Table 5.8. It is quite clear from Table 5.8 that false detection cases increase as the percentage of error increases.

Table 5.8: Error analysis at percent increment

Percent Increment in df/dq & dq/dt	Cases not detected accurately			
	0.5 threshold		0.7 threshold	
	Islanding	Non-Islanding	Islanding	Non-Islanding
8	3	9	3	9
13	6	14	5	11
19	8	16	5	13
24	10	17	8	16
30	13	23	11	21
33	16	36	13	29
37	19	46	15	36
42	23	51	16	42
46	29	66	22	54

5.5.2 Gradual Percentage Decrement in *df/dq* and *dq/dt*

Here, gradual percentage decrement has been introduced in both *df/dq* and *dq/dt* features similar to percentage increment in section 5.5.1. The ANN-PSO trained file is used again to authenticate the performance under this condition. The results for error analysis at percentage decrement are clarified in Table 5.9. It is quite clear from Table 5.9 that percentage of false detection increases as the percentage of error increases.

Table 5.9: Accuracy analysis at percent decrement

Percent Decrement in df/dq & dq/dt	Cases not detected accurately			
	0.5 threshold		0.7 threshold	
	Islanding	Non-Islanding	Islanding	Non-Islanding
8	3	9	3	9
13	3	12	3	8
19	9	11	10	11
24	11	18	11	17
30	12	22	12	19
33	12	28	12	23
37	15	36	15	31
42	17	56	15	48
46	19	107	19	111

5.6 Summary

In this chapter, the simulation results of the proposed passive and ANN-PSO based intelligent techniques has been presented. The simulation results confirm the ability of the proposed passive technique to distinguish islanding and non-islanding events. The proposed passive technique discerns islanding up to a very small power mismatch of 0.05 MW and 0.05 MVar, resulting in highly enhanced accuracy, low cost, and zero impact on power quality, making it appropriate for real-world execution. The detection time of the proposed passive technique is 200 ms (10 cycles), which is a small fraction of the allowable time of 2 seconds set by the IEEE 1547 standard.

Furthermore, the simulation results of an ANN-PSO based intelligent islanding detection technique using minimum number of input features are also presented. Based on the ANN analysis, it can be seen that the ANN-PSO gives the highest regression using two inputs namely *df/dq* and *dq/dt*. Then, this intelligent technique was subjected to on and offline tests involving various islanding and non-islanding events. The simulation results vindicate that the proposed intelligent technique has the ability to differentiate islanding from non-islanding events such as load increment, load decrement, capacitor switching, generator tripping, starting effect of the induction motor and different types of faults accurately. The detection time of the proposed technique is 120 ms (6 cycles) which is a small fraction of the allowable time of 2 seconds set by the IEEE 1547 standard.

Upon error introduction, it is observed that false detection cases increase as the percentage of error increases. Furthermore, it has been found that the intelligent technique works proficiently up to 8% of error introduction in both the input parameters.

CHAPTER 6: CONCLUSION AND FUTURE WORK

This thesis addresses an important technical issue of islanding detection in a distribution network connected with DERs. The main objective of the work undertaken is to develop an efficient passive and intelligent islanding detection technique by employing sensitivity/performance based ranking analysis of different power system parameters.

6.1 Conclusion

Increasing price of electricity, deregulation of electric supply and availability of a wide variety of renewable energy sources have brought about a new era of distributed generation. Although distributed generation offers many benefits, it faces many obstacles due to economic and technical reasons. A technical issue called unintentional islanding is the most prominent among them. The successful islanding operation of distribution network requires two main technical issues to be resolved. First, it requires an efficient islanding detection technique to detect the grid disconnection. Secondly, it requires suitable load shedding scheme to optimally shed the load. The main focus of this research is to detect the utility supply disconnection by using the efficient islanding detection techniques. To address islanding detection issue, this research has successfully proposed a new passive and intelligent islanding detection techniques based on the most sensitive parameters.

At the onset of a non-islanding event, it is observed that the transient intensity of power system parameters is high, and then gradually decreases. On the other hand, for an islanding event, the intensity of the transients remains the same, or slightly increases. Hence, if the initial transient period is neglected and the measurements of the power indices are taken after this duration, islanding can be distinguished from non-islanding events quite easily. However, this requires the use of discriminative parameters with sufficient sensitivity. The study undertaken involves a comprehensive analysis of 16 different parameters used for islanding detection and the selection of the most sensitive parameters are made on the basis of ranking analysis. By using sensitivity based raking analysis, it has been found that *df/dq* is the most sensitive one followed by *dq/dt* and *dp/dt*. To evaluate the choice of *df/dq* as the selected parameter, a new passive technique that employs *df/dq* was developed and tested on various islanding and non-islanding events. From the simulation results, it can be observed that the proposed technique has the ability to differentiate islanding from non-islanding events, such as load increment, load decrement, capacitor switching, different types of faults, and the starting effect of the induction motor. The proposed technique can detect islanding event up to a very small power mismatch of 0.05 MW and 0.05 MVar for the studied system. The detection time of the proposed technique is 200 ms (10 cycles), which is a small fraction of the allowable time of 2 seconds set by the IEEE 1547 standard. Thus, the accuracy of the proposed technique is highly enhanced, making it suitable for real time implementation.

In this work, an ANN based islanding detection technique using minimum number of input features is also proposed. In the foray of intelligent islanding detection techniques based on ANN, it is observed that the accuracy is proportional to the number of inputs used. The more the inputs the higher the accuracy. However, the use of many features increases the cost and complexity of the system for practical application. This is because, as the number of inputs increase, more sensors and storage space are required. This will ultimately, increase the processing time of data training. In this regard, it is best to use a minimum number of features while maintaining the accuracy. The values of the ANN parameters are fine-tuned using EP and PSO algorithms to yield an optimal performance. A comprehensive analysis of stand-alone ANN, ANN-EP and ANN-PSO is performed to search for the best combination of input features. Based on the results, it can be seen that the ANN-PSO gives the highest regression using two inputs namely *df/dq* and ΔQ. Then the ANN-PSO based islanding detection technique that employs these two input features, was subjected to on and offline tests involving various islanding and non-islanding events. The simulation results vindicate that the proposed technique has the ability to differentiate islanding from non-islanding events such as load increment, load decrement, capacitor switching, generator tripping, starting effect of the induction motor and different types of faults accurately. The detection time of the proposed technique is 120 ms (6 cycles), which is a small fraction of the allowable time of 2 seconds set by the IEEE 1547 standard. The compatibility of the intelligent technique is further authenticated by performing the error analysis. On the basis of error analysis, it has been found that the intelligent technique works proficiently up to 8% of error introduction in both the input parameters. However, the false detection cases increase as the error percentage increases.

It has been observed that both proposed techniques are effective in detecting islanding phenomenon. However, proposed ANN-PSO based intelligent islanding technique is more economical than the proposed passive islanding detection technique.

6.2 Future Work

This thesis has covered an important issue of islanding detection connected with DERs. In order to improve the proposed research, the following are recommendations for future work:

1. The islanded distribution network is reconnected to the grid once the fault that caused the islanding has been identified and removed. This can be accomplished with automatic grid reconnection scheme. In order to perform successful islanding operation of distribution network connected with DER, grid reconnection technique may be applied.

2. This work involves sensitivity analysis of rate of change of different power system parameters. However, sensitivity analysis of the basic power system parameters themselves like voltage, frequency, active power, reactive power and phase angle are not done using different signal processing tools.
3. This research shows that islanding detection is technically a viable option to improve the reliability of the power supply. However, hardware implementation is required in order to validate the significance the proposed techniques.

REFERENCES

61215-2:2005, IEC. (2005). Crystalline silicon terrestrial photovoltaic (PV) modules - Design qualification and type approval (pp. 93): International Electrotechnical Commission.

Abd-Elkader, Ahmad G., Allam, Dalia F., & Tageldin, Elsayed. (2014). Islanding detection method for DFIG wind turbines using artificial neural networks. *International Journal of Electrical Power & Energy Systems, 62*(0), 335-343.

Abdullah, NRH, Musirin, I, & Othman, MM. (2010). Transmission loss minimization using evolutionary programming considering UPFC installation cost. *International Review of Electrical Engineering (IREE), 5*(3), 1189-1203.

Acharya, Naresh, Mahat, Pukar, & Mithulananthan, N. (2006). An analytical approach for DG allocation in primary distribution network. *International Journal of Electrical Power & Energy Systems, 28*(10), 669-678.

Ackermann, T., & Knyazkin, V. (2002). *Interaction between distributed generation and the distribution network: operation aspects.* Paper presented at the Asia Pacific. IEEE/PES Transmission and Distribution Conference and Exhibition 2002.

Afroni, M. J., Sutanto, D., & Stirling, D. (2013). Analysis of Nonstationary Power-Quality Waveforms Using Iterative Hilbert Huang Transform and SAX Algorithm. *IEEE Transactions on Power Delivery, 28*(4), 2134-2144.

Aghamohammadi, Mohammad Reza, & Shahmohammadi, Ali. (2012). Intentional islanding using a new algorithm based on ant search mechanism. *International Journal of Electrical Power & Energy Systems, 35*(1), 138-147.

Aguiar, C. R., Bastos, R. F., Neves, R. V. A., Reis, G. B., & Machado, R. Q. (2013). *Fuzzy positive feedback for islanding mode detection in distributed generation.* Paper presented at the IEEE Power & Energy Society General Meeting.

Alam, M. R., Muttaqi, K. M., & Bouzerdoum, A. (2014). An Approach for Assessing the Effectiveness of Multiple-Feature-Based SVM Method for Islanding Detection of Distributed Generation. *IEEE Transactions on Industry Applications, 50*(4), 2844-2852.

Arachchige, L. W., & Rajapakse, A. (2011). *A pattern recognition approach for detecting power islands using transient signals Part I: Design and implementation.* Paper presented at the IEEE Power and Energy Society General Meeting.

Ayenu-Prah, A. Y., & Attoh-Okine, N. O. (2009). Comparative study of Hilbert–Huang transform, Fourier transform and wavelet transform in pavement profile analysis. *Vehicle System Dynamics, 47*(4), 437-456.

Aziah Khamis, H. Shareef. (2013). An effective islanding detection and classification method using neuro-phase space technique. *World Academy of Science, Engineering and Technology, 7*(6), 2067-2075.

Aziah Khamis, H. Shareef, M.Z.C Wanik. (2010). Pattern recognition of islanding detection using TT-transform. *Journal of Asian Scientific Research, 2*(11), 607-613.

Balaguer-Álvarez, IJ.; Ortiz-Rivera, E.I. (2010). Survey of Distributed Generation Islanding Detection Methods. *IEEE (Revista IEEE America Latina) Latin America Transactions, 8*(5), 565-570.

Barker, P. P., & De Mello, R. W. (2000). *Determining the impact of distributed generation on power systems. I. Radial distribution systems.* Paper presented at the IEEE Power Engineering Society Summer Meeting.

Barsali, Stefano, Ceraolo, M., Pelacchi, P., & Poli, Davide. (2002). *Control techniques of Dispersed Generators to improve the continuity of electricity supply.* Paper presented at the IEEE Power Engineering Society Winter Meeting.

Bayod-Rújula, Angel A. (2009). Future development of the electricity systems with distributed generation. *Energy, 34*(3), 377-383.

Biswal, B., Dash, P. K., & Panigrahi, B. K. (2009). Non-stationary power signal processing for pattern recognition using HS-transform. *Applied Soft Computing, 9*(1), 107-117.

Bitaraf, H., Sheikholeslamzadeh, M., Ranjbar, A. M., & Mozafari, B. (2012). *Neuro-fuzzy islanding detection in distributed generation.* Paper presented at the IEEE PES Innovative Smart Grid Technologies.

Brown, R. A., Lauzon, M. L., & Frayne, R. (2010). A General Description of Linear Time-Frequency Transforms and Formulation of a Fast, Invertible Transform That Samples the Continuous S-Transform Spectrum Nonredundantly. *IEEE Transactions on Signal Processing, 58*(1), 281-290.

Chao, Kuei-Hsiang, Chiu, Chia-Lung, Li, Ching-Ju, & Chang, Yu-Choung. (2011). A novel neural network with simple learning algorithm for islanding phenomenon detection of photovoltaic systems. *Expert Systems with Applications, 38*(10), 12107-12115.

Chen, S. (2005). *Feature selection for identification and classification of power quality disturbances.* Paper presented at the IEEE Power Engineering Society General Meeting.

Chiang, Wen-Jung, Jou, Hurng-Liahng, & Wu, Jinn-Chang. (2012). Active islanding detection method for inverter-based distribution generation power system. *International Journal of Electrical Power & Energy Systems, 42*(1), 158-166.

Chowdhury, S. P., Chowdhury, S., & Crossley, P. A. (2009). Islanding protection of active distribution networks with renewable distributed generators: A comprehensive survey. *Electric Power Systems Research, 79*(6), 984-992.

Chowdhury, S. P., Chowdhury, S., Crossley, P. A., & Chui Fen, Ten. (2008). *UK scenario of islanded operation of active distribution networks: A survey.* Paper presented at the IEEE Power and Energy Society General Meeting - Conversion and Delivery of Electrical Energy in the 21st Century.

Dash, P. K., Padhee, Malhar, & Panigrahi, T. K. (2012). A hybrid time–frequency approach based fuzzy logic system for power island detection in grid connected distributed generation. *International Journal of Electrical Power & Energy Systems, 42*(1), 453-464.

Dash, P. K., Panigrahi, K. B., & Panda, G. (2003). Power quality analysis using S-transform. *IEEE Transactions on Power Delivery, 18*(2), 406-411.

Dash, P. K., Panigrahi, K. B., Sahoo, D. K., & Panda, G. (2003). Power quality disturbance data compression, detection, and classification using integrated spline wavelet and S-transform. *IEEE Transactions on Power Delivery, 18*(2), 595-600.

Daubechies, I. (1990). The wavelet transform, time-frequency localization and signal analysis. *IEEE Transactions on Information Theory, 36*(5), 961-1005.

De Mango, F., Liserre, M., & Aquila, A. D. (2006). *Overview of Anti-Islanding Algorithms for PV Systems. Part II: ActiveMethods.* Paper presented at the 12th International Power Electronics and Motion Control Conference.

De Mango, F., Liserre, M., Aquila, A. D., & Pigazo, A. (2006). *Overview of Anti-Islanding Algorithms for PV Systems. Part I: Passive Methods.* Paper presented at the 12th International Power Electronics and Motion Control Conference.

Dehghani, Muhammad Javed. (2009). Comparison of S-transform and wavelet transform in power quality analysis. *World Academy of Science, Engineering and Technology, 3*(2), 395-398.

del Valle, Y., Venayagamoorthy, G. K., Mohagheghi, S., Hernandez, J. C., & Harley, R. G. (2008). Particle Swarm Optimization: Basic Concepts, Variants and Applications in Power Systems. *IEEE Transactions on Evolutionary Computation, 12*(2), 171-195.

Dias, Fernando Morgado, Antunes, Ana, & Mota, Alexandre Manuel. (2004). Artificial neural networks: a review of commercial hardware. *Engineering Applications of Artificial Intelligence, 17*(8), 945-952.

Ding, X., & Crossley, P. A. (2005). *Islanding detection for distributed generation.* Paper presented at the IEEE Russia Power Tech.

Distributed Generation in Liberalized Electricity Market. (2002) (pp. 124). France.

Dola, H. M., & Chowdhury, B. H. (2006). *Intentional islanding and adaptive load shedding to avoid cascading outages.* Paper presented at the IEEE Power Engineering Society General Meeting.

Donnelly, D. (2006). *The Fast Fourier and Hilbert-Huang Transforms: A Comparison.* Paper presented at the IMACS Multiconference on Computational Engineering in Systems Applications.

Drummond, C. F., & Sutanto, D. (2010). *Classification of Power Quality disturbances using the iterative Hilbert Huang Transform.* Paper presented at the 14th International Conference on Harmonics and Quality of Power.

Dugan, R. C., & McDermott, T. E. (2002). Distributed generation. *IEEE Industry Applications Magazine, 8*(2), 19-25.

El-Arroudi, K., & Joos, G. (2007). Data Mining Approach to Threshold Settings of Islanding Relays in Distributed Generation. *IEEE Transactions on Power Systems, 22*(3), 1112-1119.

El-Arroudi, K., Joos, G., Kamwa, I., & McGillis, D. T. (2007). Intelligent-Based Approach to Islanding Detection in Distributed Generation. *IEEE Transactions on Power Delivery, 22*(2), 828-835.

ElNozahy, M. S., El-Saadany, E. F., & Salama, M. M. A. (2011). *A robust wavelet-ANN based technique for islanding detection.* Paper presented at the IEEE Power and Energy Society General Meeting.

Esram, T., & Chapman, P. L. (2007). Comparison of Photovoltaic Array Maximum Power Point Tracking Techniques. *IEEE Transactions on Energy Conversion, 22*(2), 439-449.

European Union Commission Report. (2015). from https://ec.europa.eu/energy/en/topics/renewable-energy

Faqhruldin, O. N., El-Saadany, E. F., & Zeineldin, H. H. (2014). A Universal Islanding Detection Technique for Distributed Generation Using Pattern Recognition. *IEEE Transactions on Smart Grid, 5*(4), 1985-1992.

Far, H. G., Rodolakis, A. J., & Joos, G. (2012). Synchronous Distributed Generation Islanding Protection Using Intelligent Relays. *IEEE Transactions on Smart Grid,, 3*(4), 1695-1703.

Fayyad, Y., & Osman, A. (2010). *Neuro-wavelet based islanding detection technique.* Paper presented at the IEEE Electric Power and Energy Conference (EPEC).

Frank Delea, Jack Casazza. (2010). *Understanding Electric Power Systems: An Overview of the Technology, the Marketplace, and Government Regulation.* (2nd Edition ed.): Wiley-IEEE Press.

Freitas, W., Wilsun, Xu, Affonso, C. M., & Zhenyu, Huang. (2005). Comparative analysis between ROCOF and vector surge relays for distributed generation applications. *IEEE Transactions on Power Delivery,, 20*(2), 1315-1324.

Fu-Sheng, Pai, & Shyh-Jier, Huang. (2001). A detection algorithm for islanding-prevention of dispersed consumer-owned storage and generating units. *IEEE Transactions on Energy Conversion, 16*(4), 346-351.

Fuangfoo, P., Lee, W. j., & Kuo, M. t. (2006). *Impact Study on Intentional Islanding of Distributed Generation Connected to Radial Subtransmission System in*

Thailand's Electric Power System. Paper presented at the IEEE Industry Applications Conference & Forty-First IAS Annual Meeting.

Ghazi, R., & Lotfi, N. (2010). *A new hybrid intelligent based approach to islanding detection in distributed generation.* Paper presented at the 45th International Universities Power Engineering Conference (UPEC).

Gómez-González, M., López, A., & Jurado, F. (2013). Hybrid discrete PSO and OPF approach for optimization of biomass fueled micro-scale energy system. *Energy Conversion and Management, 65*(0), 539-545.

Gonzalez, S. A., Garcia-Retegui, R., & Benedetti, M. (2007). Harmonic Computation Technique Suitable for Active Power Filters. *IEEE Transactions on Industrial Electronics, 54*(5), 2791-2796.

Gooding, P. A., Makram, E., & Hadidi, R. (2014). Probability analysis of distributed generation for island scenarios utilizing Carolinas data. *Electric Power Systems Research, 107*, 125-132.

Graps, A. (1995). An introduction to wavelets. *Computational Science & Engineering, IEEE, 2*(2), 50-61.

Gsänger, Stefan. (2011). World Wind Outlook: Down But Not Out. 26/09/2014, from http://www.renewableenergyworld.com/rea/news/article/2011/05/world-wind-outlook-down-but-not-out

Gu, Y. H., & Bollen, M. H. J. (2000). Time-frequency and time-scale domain analysis of voltage disturbances. *IEEE Transactions on Power Delivery,, 15*(4), 1279-1284.

Guiliang, Yin. (2005). *A Distributed Generation Islanding Detection Method Based on Artificial Immune System.* Paper presented at the Asia and Pacific, IEEE/PES Transmission and Distribution Conference and Exhibition.

Guo-Kiang, Hung, Chih-Chang, Chang, & Chen, Chern-Lin. (2003). Automatic phase-shift method for islanding detection of grid-connected photovoltaic inverters. *IEEE Transactions on Energy Conversion, 18*(1), 169-173.

Hammerstrom, D. (1993). Neural networks at work. *IEEE Spectrum, 30*(6), 26-32.

Hanif, M., Basu, M., & Gaughan, K. (2012). Development of EN50438 compliant wavelet-based islanding detection technique for three-phase static distributed generation systems. *IET Renewable Power Generation, 6*(4), 289-301.

Hanif, M., Dwivedi, U. D., Basu, M., & Gaughan, K. (2010). *Wavelet based islanding detection of DC-AC inverter interfaced DG systems.* Paper presented at the 45th International Universities Power Engineering Conference (UPEC).

Hashemi, Farid, Ghadimi, Noradin, & Sobhani, Behrooz. (2013). Islanding detection for inverter-based DG coupled with using an adaptive neuro-fuzzy inference system. *International Journal of Electrical Power & Energy Systems, 45*(1), 443-455.

Heidari, Mehrdad, Seifossadat, Ghodratollah, & Razaz, Morteza. (2013). Application of decision tree and discrete wavelet transform for an optimized intelligent-based islanding detection method in distributed systems with distributed generations. *Renewable and Sustainable Energy Reviews, 27*(0), 525-532.

Heidari, Mehrdad, Seifossadat, Ghodratollah, & Razaz, Morteza. (2013). Application of decision tree and discrete wavelet transform for an optimized intelligent-based islanding detection method in distributed systems with distributed generations. *Renewable and Sustainable Energy Reviews, 27*, 525-532.

Hsieh, Cheng-Tao, Lin, Jeu-Min, & Huang, Shyh-Jier. (2008). Enhancement of islanding-detection of distributed generation systems via wavelet transform-based approaches. *International Journal of Electrical Power & Energy Systems, 30*(10), 575-580.

IEEE Guide for Automatic Reclosing of Line Circuit Breakers for AC Distribution and Transmission Lines. (2003). *IEEE Std C37.104-2002*, 1-62.

IEEE Guide for Protective Relaying of Utility-Consumer Interconnections. (2014). *IEEE Std C37.95-2014 (Revision of IEEE Std C37.95-2002)*, 1-70.

IEEE Recommended Practice for Grounding of Industrial and Commercial Power Systems. (2007). *IEEE Std 142-2007 (Revision of IEEE Std 142-1991)*, 1-225.

IEEE Recommended Practice for Protection and Coordination of Industrial and Commercial Power Systems (IEEE Buff Book). (2001). *IEEE Std 242-2001 (Revision of IEEE Std 242-1986) [IEEE Buff Book]*, 1-710.

IEEE Std 929. (2000). IEEE Recommended Practice for Utility Interface of Photovoltaic (PV) Systems. *IEEE Std 929*.

IEEE Std 1547. (2003). IEEE Standard for Interconnecting Distributed Resources With Electric Power Systems. *IEEE Std 1547*.

Illias, Hazlee Azil, Chai, Xin Rui, Abu Bakar, Ab Halim, & Mokhlis, Hazlie. (2015). Transformer Incipient Fault Prediction Using Combined Artificial Neural Network and Various Particle Swarm Optimisation Techniques. *PLoS ONE, 10*(6).

Jacobsen, E., & Lyons, R. (2003). The sliding DFT. *IEEE Signal Processing Magazine, 20*(2), 74-80.

Jae-Hyung, Kim, Jun-Gu, Kim, Young-Hyok, Ji, Yong-Chae, Jung, & Chung-Yuen, Won. (2011). An Islanding Detection Method for a Grid-Connected System Based on the Goertzel Algorithm. *IEEE Transactions on Power Electronics, 26*(4), 1049-1055.

Jia, Ke, Bi, Tianshu, Liu, Bohan, Thomas, David, & Goodman, Andrew. (2014). Advanced islanding detection utilized in distribution systems with DFIG. *International Journal of Electrical Power & Energy Systems, 63*(0), 113-123.

Jiaxin, Ning, & Caisheng, Wang. (2012). *Feature extraction for islanding detection using Wavelet Transform-based Multi-Resolution Analysis.* Paper presented at the IEEE Power and Energy Society General Meeting.

Joshi, K. A., & Pindoriya, N. M. (2013). *Risk assessment of unintentional islanding in a spot network with roof-top photovoltaic system; A case study in India.* Paper presented at the IEEE Innovative Smart Grid Technologies-Asia (ISGT Asia).

Jou, H. L., Chiang, W. J., & Wu, J. C. (2007). Virtual inductor-based islanding detection method for grid-connected power inverter of distributed power generation system. *IET Renewable Power Generation, 1*(3), 175-181.

Jun Yin; Liuchen Chang; Diduch, C. (2004). *Recent developments in islanding detection for distributed power generation*. Paper presented at the Large Engineering systems Conference on Power Engineering.

Jun, Zhang, Dehong, Xu, Guoqiao, Shen, Ye, Zhu, Ning, He, & Jie, Ma. (2013). An Improved Islanding Detection Method for a Grid-Connected Inverter With Intermittent Bilateral Reactive Power Variation. *IEEE Transactions on Power Electronics, 28*(1), 268-278.

K.M. Tsang, W.L. Chan. (2013). Three-level grid-connected photovoltaic inverter with maximum power point tracking. *Energy Conversion and Management, 65*, 221-227.

Kar, S., & Samantaray, S. R. (2014). Data-mining-based intelligent anti-islanding protection relay for distributed generations. *IET Generation, Transmission & Distribution, 8*(4), 629-639.

Karegar, H. Kazemi, & Sobhani, B. (2012). Wavelet transform method for islanding detection of wind turbines. *Renewable Energy, 38*(1), 94-106.

Karimi, H., Yazdani, A., & Iravani, R. (2008). Negative-Sequence Current Injection for Fast Islanding Detection of a Distributed Resource Unit. *IEEE Transactions on Power Electronics, 23*(1), 298-307.

Karimi, M., Mokhtari, H., & Iravani, M. R. (2000). Wavelet based on-line disturbance detection for power quality applications. *IEEE Transactions on Power Delivery, 15*(4), 1212-1220.

Khamis, Aziah, Shareef, Hussain, Bizkevelci, Erdal, & Khatib, Tamer. (2013). A review of islanding detection techniques for renewable distributed generation systems. *Renewable and Sustainable Energy Reviews, 28*(0), 483-493.

Khamis, Aziah, Shareef, Hussain, Mohamed, Azah, & Bizkevelci, Erdal. (2015). Islanding detection in a distributed generation integrated power system using phase space technique and probabilistic neural network. *Neurocomputing, 148*(0), 587-599.

Kim, Il-Song. (2012). Islanding Detection Technique using Grid-Harmonic Parameters in the Photovoltaic System. *Energy Procedia, 14*(0), 137-141.

Kishor, Nand, Saini, R. P., & Singh, S. P. (2007). A review on hydropower plant models and control. *Renewable and Sustainable Energy Reviews, 11*(5), 776-796.

Ku Ahmad, Ku Nurul Edhura, Selvaraj, Jeyraj, & Rahim, Nasrudin Abd. (2013). A review of the islanding detection methods in grid-connected PV inverters. *Renewable and Sustainable Energy Reviews, 21*(0), 756-766.

Kumarswamy, I., Sandipamu, T. K., & Prasanth, V. (2013). *Analysis of Islanding Detection in Distributed Generation Using Fuzzy Logic Technique.* Paper presented at the 7th Asia Modelling Symposium.

Kundur, P. (1994). *Power System Stability and Control*: Mcgraw-Hill.

Laaksonen, H. (2013). Advanced Islanding Detection Functionality for Future Electricity Distribution Networks. *IEEE Transactions on Power Delivery, 28*(4), 2056-2064.

Laghari, J. A., Mokhlis, H., Bakar, A. H. A., & Karimi, M. (2013). A new islanding detection technique for multiple mini hydro based on rate of change of reactive power and load connecting strategy. *Energy Conversion and Management, 76*(0), 215-224.

Laghari, J. A., Mokhlis, H., Karimi, M., Bakar, A. H. A., & Mohamad, Hasmaini. (2014). Computational Intelligence based techniques for islanding detection of distributed generation in distribution network: A review. *Energy Conversion and Management, 88*(0), 139-152.

Li, Canbing, Cao, Chi, Cao, Yijia, Kuang, Yonghong, Zeng, Long, & Fang, Baling. (2014). A review of islanding detection methods for microgrid. *Renewable and Sustainable Energy Reviews, 35*(0), 211-220.

Lidula, N. W. A., & Rajapakse, A. D. (2009). *Fast and reliable detection of power islands using transient signals.* Paper presented at the International Conference on Industrial and Information Systems (ICIIS).

Lidula, N. W. A., & Rajapakse, A. D. (2010). A Pattern Recognition Approach for Detecting Power Islands Using Transient Signals. Part I: Design and Implementation. *IEEE Transactions on Power Delivery, 25*(4), 3070-3077.

Lidula, N. W. A., & Rajapakse, A. D. (2011). Microgrids research: A review of experimental microgrids and test systems. *Renewable and Sustainable Energy Reviews, 15*(1), 186-202.

Lidula, N. W. A., & Rajapakse, A. D. (2012). A Pattern-Recognition Approach for Detecting Power Islands Using Transient Signals. Part II: Performance Evaluation. *IEEE Transactions on Power Delivery, 27*(3), 1071-1080.

Lin, F. J., Huang, Y. S., Tan, K. H., Chiu, J. H., & Chang, Y. R. (2013). Active islanding detection method using d-axis disturbance signal injection with intelligent control. *IET Generation, Transmission & Distribution, 7*(5), 537-550.

Lin, F. J., Kuang-Hsiung, Tan, & Jian-Hsing, Chiu. (2012, 10-15 June 2012). *Active islanding detection method using wavelet fuzzy neural network.* Paper presented at the IEEE International Conference on Fuzzy Systems (FUZZ-IEEE).

Lin, Lu, Qi, Luo, Jun-yong, Liu, & Chuan, Long. (2008). *An improved particle swarm optimization algorithm.* Paper presented at the IEEE International Conference on Granular Computing.

Liu, F., Kang, Y., Zhang, Y., Duan, S., & Lin, X. (2010). Improved SMS islanding detection method for grid-connected converters. *Renewable Power Generation, IET, 4*(1), 36-42.

Liu, Y.H., Luor, T.S., Huang, S.J., & Lin, J.M. (2008). Method and system for detecting stand-alone operation of a distributed generating system: Google Patents.

Londero, R. R., Affonso, C. M., Nunes, M. V. A., & Freitas, W. (2010). *Planned islanding for Brazilian system reliability.* Paper presented at the IEEE PES T&D 2010.

Lopes, J. A. Peças, Hatziargyriou, N., Mutale, J., Djapic, P., & Jenkins, N. (2007). Integrating distributed generation into electric power systems: A review of drivers, challenges and opportunities. *Electric Power Systems Research, 77*(9), 1189-1203.

Lopes, L. A. C., & Huili, Sun. (2006). Performance assessment of active frequency drifting islanding detection methods. *IEEE Transactions on Energy Conversion, 21*(1), 171-180.

Madani, S. S., Abbaspour, A., Beiraghi, M., Dehkordi, P. Z., & Ranjbar, A. M. (2012). *Islanding detection for PV and DFIG using decision tree and AdaBoost algorithm.* Paper presented at the 3rd IEEE PES Innovative Smart Grid Technologies Europe (ISGT Europe).

Mahat, P., Zhe, Chen, & Bak-Jensen, B. (2009). A Hybrid Islanding Detection Technique Using Average Rate of Voltage Change and Real Power Shift. *IEEE Transactions on Power Delivery, 24*(2), 764-771.

Mahat, P., Zhe, Chen, & Bak-Jensen, B. (2011). *Review on islanding operation of distribution system with distributed generation.* Paper presented at the IEEE Power and Energy Society General Meeting.

malaysia explores its renewables options. (2015). from http://www.renewableenergyworld.com/articles/print/volume-14/issue-5/solar-energy/malaysia-explores-its-renewables-options.html

Meng Hui, Wang, Mei-Ling, Huang, & Kang-Jian, Liou. (2015). Islanding detection method for grid connected photovoltaic systems. *Renewable Power Generation, IET, 9*(6), 700-709.

Menon, V., & Nehrir, M. H. (2007). A Hybrid Islanding Detection Technique Using Voltage Unbalance and Frequency Set Point. *IEEE Transactions on Power Systems, 22*(1), 442-448.

Mishra, S., Bhende, C. N., & Panigrahi, K. B. (2008). Detection and Classification of Power Quality Disturbances Using S-Transform and Probabilistic Neural Network. *IEEE Transactions on Power Delivery, 23*(1), 280-287.

Moeini, Ali, Darabi, A., & Karimi, M. (2010). *Clustering governor signal of distributed generation for islanding detection.* Paper presented at the IEEE Region 8 International Conference on Computational Technologies in Electrical and Electronics Engineering (SIBIRCON).

Moeini, Ali, Darabi, Ahmad, Rafiei, S. M. R., & Karimi, Mohsen. (2011). Intelligent islanding detection of a synchronous distributed generation using governor signal clustering. *Electric Power Systems Research, 81*(2), 608-616.

Mohamad, H., & Crossley, P. A. (2009). *Islanded operation of UK radial distribution: Earthing strategy.* Paper presented at the Proceedings of the 44th International Universities Power Engineering Conference (UPEC).

Mohamad, Hasmaini, Mokhlis, Hazlie, Bakar, Ab Halim Abu, & Ping, Hew Wooi. (2011). A review on islanding operation and control for distribution network connected with small hydro power plant. *Renew Sust Energ Rev, 15*(8), 3952-3962.

Mohammadzadeh Niaki, A. H., & Afsharnia, S. (2014). A new passive islanding detection method and its performance evaluation for multi-DG systems. *Electric Power Systems Research, 110*(0), 180-187.

Mohanty, S., Kishor, N., Ray, P., & Catalao, J. (2014). Comparative Study of Advanced Signal Processing Techniques for Islanding Detection in a Hybrid Distributed Generation System. *IEEE Transactions on Sustainable Energy, PP*(99), 1-10.

Mohanty, S. R., Kishor, N., Ray, P. K., & Catalao, J. P. S. (2012). *Islanding detection in a distributed generation based hybrid system using intelligent pattern recognition techniques.* Paper presented at the 3rd IEEE PES International Conference and Exhibition on Innovative Smart Grid Technologies (ISGT Europe).

Mohanty, Soumya R., Ray, Prakash K., Kishor, Nand, & Panigrahi, B. K. (2013). Classification of disturbances in hybrid DG system using modular PNN and SVM. *International Journal of Electrical Power & Energy Systems, 44*(1), 764-777.

Morsi, W. G., Diduch, C. P., & Chang, L. (2010). *A new islanding detection approach using wavelet packet transform for wind-based distributed generation.* Paper presented at the 2nd IEEE International Symposium on Power Electronics for Distributed Generation Systems (PEDG).

Morsi, Walid G., & El-Hawary, M. E. (2010). Novel power quality indices based on wavelet packet transform for non-stationary sinusoidal and non-sinusoidal disturbances. *Electric Power Systems Research, 80*(7), 753-759.

Nantian, Huang, Dianguo, Xu, & Xiaosheng, Liu. (2010). *Power Quality Disturbances Recognition Based on HS-transform.* Paper presented at the First International

Conference on Pervasive Computing Signal Processing and Applications (PCSPA).

O'Kane, P., & Fox, B. (1997). *Loss of mains detection for embedded generation by system impedance monitoring.* Paper presented at the Sixth International Conference on Developments in Power System Protection.

Pahwa, S., Youssef, M., Schumm, P., Scoglio, C., & Schulz, N. (2013). Optimal intentional islanding to enhance the robustness of power grid networks. *Physica A: Statistical Mechanics and its Applications, 392*(17), 3741-3754.

Pai, F. S., & Huang, S. J. (2001). A Detection Algorithm for Islanding-Prevention of Dispersed Consumer-Owned Storage and Generating Units. *IEEE Power Engineering Review, 21*(12), 67-67.

Pan, Tianhong, Xu, Dongliang, Li, Zhengming, Shieh, Shyan-Shu, & Jang, Shi-Shang. (2013). Efficiency improvement of cogeneration system using statistical model. *Energy Conversion and Management, 68*(0), 169-176.

Peng, Z. K., Tse, Peter W., & Chu, F. L. (2005). A comparison study of improved Hilbert–Huang transform and wavelet transform: Application to fault diagnosis for rolling bearing. *Mechanical Systems and Signal Processing, 19*(5), 974-988.

Pepermans, G., Driesen, J., Haeseldonckx, D., Belmans, R., & D'haeseleer, W. (2005). Distributed generation: definition, benefits and issues. *Energy Policy, 33*(6), 787-798.

Pham, J. P., Denboer, N., Lidula, N. W. A., Perera, N., & Rajapakse, A. D. (2011). *Hardware implementation of an islanding detection approach based on current and voltage transients.* Paper presented at the IEEE Electrical Power and Energy Conference (EPEC).

Pigazo, A., Liserre, M., Mastromauro, R. A., Moreno, V. M., & Dell'Aquila, A. (2009). Wavelet-Based Islanding Detection in Grid-Connected PV Systems. *IEEE Transactions on Industrial Electronics, 56*(11), 4445-4455.

Pigazo, A., Moreno, V. M., Liserre, M., & Aquila, A. D. (2007). *Wavelet-Based Islanding Detection Algorithm for Single-Phase Photovoltaic (PV) Distributed Generation Systems.* Paper presented at the IEEE International Symposium on Industrial Electronics.

Pinnegar, C. R., & Mansinha, L. (2003). A method of time–time analysis: The TT-transform. *Digital Signal Processing, 13*(4), 588-603.

Quintero, S. X. Carvajal, Mar, J. D., x00Ed, n, Jim, x00E, nez, & Aramburo, S. Arango. (2012). *Feasibility of intentional islanding operation with small hydropower plants.* Paper presented at the Sixth IEEE/PES Transmission and Distribution: Latin America Conference and Exposition (T&D-LA).

Ray, P. K., Kishor, N., & Mohanty, S. R. (2010). *S-transform based islanding detection in grid-connected distributed generation based power system.* Paper presented at the IEEE International Energy Conference and Exhibition (EnergyCon).

Ray, P. K., Mohanty, S. R., Kishor, N., & Dubeya, H. C. (2010). *Coherency determination in grid-connected distributed generation based hybrid system under islanding scenarios.* Paper presented at the IEEE International Conference on Power and Energy (PECon).

Ray, Prakash K., Mohanty, Soumya R., & Kishor, Nand. (2011). Disturbance detection in grid-connected distributed generation system using wavelet and S-transform. *Electric Power Systems Research, 81*(3), 805-819.

Redfern, M. A., Usta, O., & Fielding, G. (1993). Protection against loss of utility grid supply for a dispersed storage and generation unit. *IEEE Transactions on Power Delivery, 8*(3), 948-954.

Reigosa, D., Briz, F., Blanco, C., Garcia, P., & Manuel Guerrero, J. (2014). Active Islanding Detection for Multiple Parallel-Connected Inverter-Based Distributed Generators Using High-Frequency Signal Injection. *IEEE Transactions on Power Electronics, 29*(3), 1192-1199.

Reigosa, D. D., Briz, F., Charro, C. B., Garcia, P., & Guerrero, J. M. (2012). Active Islanding Detection Using High-Frequency Signal Injection. *IEEE Transactions on Industry Applications, 48*(5), 1588-1597.

Rekik, Mouna, Abdelkafi, Achraf, & Krichen, Lotfi. (2013). A novel control strategy of a distributed generator operating in seven modes for ancillary services under grid faults. *International Journal of Electrical Power & Energy Systems, 47*(0), 100-108.

Rivarolo, M., Greco, A., & Massardo, A. F. (2013). Thermo-economic optimization of the impact of renewable generators on poly-generation smart-grids including hot thermal storage. *Energy Conversion and Management, 65*(0), 75-83.

Rokach, L., & Maimon, O. (2005). Top-down induction of decision trees classifiers - a survey. *IEEE Transactions on Systems, Man, and Cybernetics, Part C (Applications and Reviews), 35*(4), 476-487.

Ropp, M. E., Begovic, M., & Rohatgi, A. (1999). Analysis and performance assessment of the active frequency drift method of islanding prevention.*, IEEE Transactions on Energy Conversion, 14*(3), 810-816.

Roscoe, A. J., Burt, G. M., & Bright, C. G. (2014). Avoiding the Non-Detection Zone of Passive Loss-of-Mains (Islanding) Relays for Synchronous Generation by Using Low Bandwidth Control Loops and Controlled Reactive Power Mismatches. *IEEE Transactions on Smart Grid, 5*(2), 602-611.

Rosolowski Eugeniusz, Arkadiusz Burek, Leszek Jedut. (2007). A new method for islanding detection in distributed generation.

Rovnyak, Yong Sheng ; S. M. (2004). Decision tree-based methodology for high impedance fault detection. *IEEE Transactions on Power Delivery, 19*(2), 533-536.

Salman, S. K., King, D. J., & Weller, G. (2001). *New loss of mains detection algorithm for embedded generation using rate of change of voltage and changes in power factors.* Paper presented at the Seventh International Conference on Developments in Power System Protection.

Samantaray, S. R., El-Arroudi, K., Joos, G., & Kamwa, I. (2010). A Fuzzy Rule-Based Approach for Islanding Detection in Distributed Generation. *IEEE Transactions on Power Delivery, 25*(3), 1427-1433.

Samantaray, S. R., Pujhari, T. M., & Subudhi, B. D. (2009). *A new approach to islanding detection in distributed generations.* Paper presented at the International Conference on Power Systems.

Samantaray, S. R., Samui, A., & Babu, B. C. (2010). *S-transform based cumulative sum detector (CUSUM) for islanding detection in Distributed Generations.* Paper presented at the Joint International Conference on Power Electronics, Drives and Energy Systems (PEDES).

Samui, A., & Samantaray, S. R. (2012). *Performance assessment of wavelet transform based islanding detection relay.* Paper presented at the Annual IEEE India Conference (INDICON).

Samui, A., & Samantaray, S. R. (2013). Wavelet Singular Entropy-Based Islanding Detection in Distributed Generation. *IEEE Transactions on Power Delivery, 28*(1), 411-418.

Santoso, S., Powers, E. J., & Grady, W. M. (1997). Power quality disturbance data compression using wavelet transform methods. *IEEE Transactions on Power Delivery, 12*(3), 1250-1257.

Santoso, S., Powers, E. J., Grady, W. M., & Hofmann, P. (1996). Power quality assessment via wavelet transform analysis. *IEEE Transactions on Power Delivery, 11*(2), 924-930.

Sareen, K., Bhalja, B. R., & Maheshwari, R. P. (2016). Universal islanding detection technique based on rate of change of sequence components of currents for distributed generations. *IET Renewable Power Generation, 10*(2), 228-237.

Shariatinasab, R., & Akbari, M. (2010). *New islanding detection technique for DG using Discrete Wavelet Transform.* Paper presented at the IEEE International Conference on Power and Energy (PECon).

Sharma, R., & Singh, P. (2012). *Islanding detection and control in grid based system using wavelet transform.* Paper presented at the IEEE Fifth Power India Conference.

Shayeghi, H., & Sobhani, B. (2014). Zero NDZ assessment for anti-islanding protection using wavelet analysis and neuro-fuzzy system in inverter based distributed generation. *Energy Conversion and Management, 79*(0), 616-625.

Sheen, Jen-Nan, Tsai, Ming-Tang, & Wu, Szu-Wzi. (2013). A benefits analysis for wind turbine allocation in a power distribution system. *Energy Conversion and Management, 68*(0), 305-312.

Shi, L., & Wu, F. (2013). *An islanding detection algorithm based on fuzzy adaptive phase drift control.* Paper presented at the IEEE International Conference on Information and Automation (ICIA).

Silva, M., Morais, H., & Vale, Z. (2012). An integrated approach for distributed energy resource short-term scheduling in smart grids considering realistic power system simulation. *Energy Conversion and Management, 64*(0), 273-288.

Simon, C., Schimmel, M., & Danobeitia, J. J. (2008). On the TT-Transform and Its Diagonal Elements. *IEEE Transactions on Signal Processing,, 56*(11), 5709-5713.

Singam, B., & Hui, L. Y. (2006). *Assessing SMS and PJD Schemes of Anti-Islanding with Varying Quality Factor.* Paper presented at the IEEE International Power and Energy Conference.

Sozanski, K. P. (2006). *Sliding DFT control algorithm for three-phase active power filter.* Paper presented at the Twenty-First Annual IEEE Applied Power Electronics Conference and Exposition.

Stockwell, R. G., Mansinha, L., & Lowe, R. P. (1996). Localization of the complex spectrum: the S transform. *IEEE Transactions on Signal Processing, 44*(4), 998-1001.

Sumner, M., Palethorpe, B., Thomas, D. W. P., Zanchetta, P., & Di Piazza, M. C. (2002). A technique for power supply harmonic impedance estimation using a controlled voltage disturbance. *IEEE Transactions on Power Electronics,, 17*(2), 207-215.

Sung-Il, Jang, & Kwang-Ho, Kim. (2004). An islanding detection method for distributed generations using voltage unbalance and total harmonic distortion of current. *IEEE Transactions on Power Delivery, 19*(2), 745-752.

Trujillo, C. L., Velasco, D., Figueres, E., & Garcerá, G. (2010). Analysis of active islanding detection methods for grid-connected microinverters for renewable energy processing. *Applied Energy, 87*(11), 3591-3605.

Tuyen, Nguyen Duc, & Fujita, Goro. (2011). *Negative-sequence Current Injection of Dispersed Generation for Islanding Detection and Unbalanced Fault Ride-through.* Paper presented at the 46th International Universities' Power Engineering Conference (UPEC).

UL1741 Inverter, Converter, and Controllers for Use in Independent Power System. (2001).

Urbanetz, Jair, Braun, Priscila, & Rüther, Ricardo. (2012). Power quality analysis of grid-connected solar photovoltaic generators in Brazil. *Energy Conversion and Management, 64*(0), 8-14.

Vahedi, H., & Karrari, M. (2013). Adaptive Fuzzy Sandia Frequency-Shift Method for Islanding Protection of Inverter-Based Distributed Generation. *IEEE Transactions on Power Delivery, 28*(1), 84-92.

Vahedi, H., Noroozian, R., Jalilvand, A., & Gharehpetian, G. B. (2010). *Hybrid SFS and Q-f Islanding Detection Method for inverter-based DG.* Paper presented at the IEEE International Conference on Power and Energy (PECon).

Velasco, D., Trujillo, C., Garcera, G., & Figueres, E. (2011). An Active Anti-Islanding Method Based on Phase-PLL Perturbation. *IEEE Transactions on Power Electronics, 26*(4), 1056-1066.

Velasco, D., Trujillo, C. L., Garcerá, G., & Figueres, E. (2010). Review of anti-islanding techniques in distributed generators. *Renewable and Sustainable Energy Reviews, 14*(6), 1608-1614.

Ventosa, S., Simon, C., Schimmel, M., Danobeitia, J. J., & Manuel, A. (2008). The "S"-Transform From a Wavelet Point of View. *IEEE Transactions on Signal Processing, 56*(7), 2771-2780.

Walling, R. A., & Miller, N. W. (2002). *Distributed generation islanding-implications on power system dynamic performance.* Paper presented at the IEEE Power Engineering Society Summer Meeting.

Wei Yee Teoh, Chee Wei Tan. (2011). An Overview of Islanding Detection Methods in Photovoltaic Systems. *World Academy of Science, Engineering and Technology, 5*(58).

Wen-Yeau, Chang. (2010). *A hybrid islanding detection method for distributed synchronous generators.* Paper presented at the International Power Electronics Conference (IPEC).

Wencong, Wang, Kliber, J., Guibin, Zhang, Wilsun, Xu, Howell, B., & Palladino, T. (2007). A Power Line Signaling Based Scheme for Anti-Islanding Protection of Distributed Generators Part II: Field Test Results. *IEEE Transactions on Power Delivery, 22*(3), 1767-1772.

Wilsun, Xu, Guibin, Zhang, Chun, Li, Wencong, Wang, Guangzhu, Wang, & Kliber, J. (2007). A Power Line Signaling Based Technique for Anti-Islanding Protection of Distributed Generators Part I: Scheme and Analysis. *IEEE Transactions on Power Delivery, 22*(3), 1758-1766.

Xiaolong, Chen, & Yongli, Li. (2014). An Islanding Detection Algorithm for Inverter-Based Distributed Generation Based on Reactive Power Control. *IEEE Transactions on Power Electronics, 29*(9), 4672-4683.

Xuancai, Zhu, Chengrui, Du, Guoqiao, Shen, Min, Chen, & Dehong, Xu. (2009). *Analysis of the Non-detection Zone with Passive Islanding Detection Methods for Current Control DG System.* Paper presented at the Twenty-Fourth Annual IEEE Applied Power Electronics Conference and Exposition.

Yaniktepe, B., Savrun, M. M., & Koroglu, T. Current status of wind energy and wind energy policy in Turkey. *Energy Conversion and Management*.

Yanping, Zhu, Qiuxia, Yang, Junjuan, Wu, Dezhong, Zheng, & Yuexin, Tian. (2008). *A novel islanding detection method of distributed generator based on wavelet transform.* Paper presented at the International Conference on Electrical Machines and Systems.

Ye, Zhu, Dehong, Xu, Ning, He, Jie, Ma, Jun, Zhang, Yangfan, Zhang, . . . Changsheng, Hu. (2013). A Novel RPV (Reactive-Power-Variation) Antiislanding Method Based on Adapted Reactive Power Perturbation. *IEEE Transactions on Power Electronics, 28*(11), 4998-5012.

Yousefi, Moslem, Hooshyar, Danial, Ahmad, Rodina Binti, & Darus, Amer Nordin. (2015). A Practical Review on the Application of Constraint Handling Strategies in Evolutionary Computation from an Engineering Point of View.

Yu, Byunggyu, Matsui, Mikihiko, & Yu, Gwonjong. (2010). A review of current anti-islanding methods for photovoltaic power system. *Solar Energy, 84*(5), 745-754.

Yu, Chen, Zhao, Xu, & Ostergaard, J. (2008). *Frequency analysis for planned islanding operation in the Danish distribution system - Bornholm.* Paper presented at the 43rd International Universities Power Engineering Conference.

Zeineldin, H. H., Abdel-Galil, T., El-Saadany, E. F., & Salama, M. M. A. (2007). Islanding detection of grid connected distributed generators using TLS-ESPRIT. *Electric Power Systems Research, 77*(2), 155-162.

Zeineldin, H. H., & Conti, S. (2011). Sandia frequency shift parameter selection for multi-inverter systems to eliminate non-detection zone. *IET Renewable Power Generation, 5*(2), 175-183.

Zeineldin, H. H., El-Saadany, E. F., & Salama, M. M. A. (2006). Impact of DG interface control on islanding detection and nondetection zones. *IEEE Transactions on Power Delivery, 21*(3), 1515-1523.

Zeineldin, H. H., & Kennedy, S. (2009). Sandia Frequency-Shift Parameter Selection to Eliminate Nondetection Zones. *IEEE Transactions on Power Delivery, 24*(1), 486-487.

Zeineldin, H. H., & Kirtley, J. L. (2009). Performance of the OVP/UVP and OFP/UFP Method With Voltage and Frequency Dependent Loads. *IEEE Transactions on Power Delivery, 24*(2), 772-778.

Zhihong, Ye, Kolwalkar, A., Zhang, Y., Pengwei, Du, & Walling, R. (2004). Evaluation of anti-islanding schemes based on nondetection zone concept. *IEEE Transactions on Power Electronics, 19*(5), 1171-1176.

LIST OF PUBLICATIONS AND PAPERS PRESENTED

1) **S. Raza**, H. Mokhlis, H. Arof, J. A. Laghari, and H. Mohamad, "A Sensitivity Analysis of Different Power System Parameters on Islanding Detection," ***IEEE Transactions on Sustainable Energy**,* vol. 7(2), pp. 461-470, 2016. **[Impact Factor 3.727, Q1]**
2) **S. Raza**, H. Mokhlis, H. Arof, K. Naidu, J. A. Laghari, and A. S. M. Khairuddin, "Minimum-features-based ANN-PSO approach for islanding detection in distribution system," ***IET Renewable Power Generation**,* pp. 1-9, 2016 **[Impact Factor 1.904, Q2]**
3) **S. Raza**, H. Mokhlis, H. Arof, J. A. Laghari, and L. Wang, "Application of signal processing techniques for islanding detection of distributed generation in distribution network: A review," ***Energy Conversion and Management**,* vol. 96, pp. 613-624, 2015 **[Impact Factor 4.801, Q1]**
4) **S. Raza**, H. Arof, H. Mokhlis, H. Mohamad, and H. A. Illias, "Passive islanding detection technique for synchronous generators based on performance ranking of different passive parameters," ***IET Generation Transmission & Distribution**,* 2016 **[Under Review]**

APPENDIX

A.1. df/dq and dq/dt behaviors in proposed intelligent islanding detection technique

The behavior of rate of change of frequency over reactive power (df/dq) and rate of change of reactive power (dq/dt) under non-islanding scenarios are shown below.

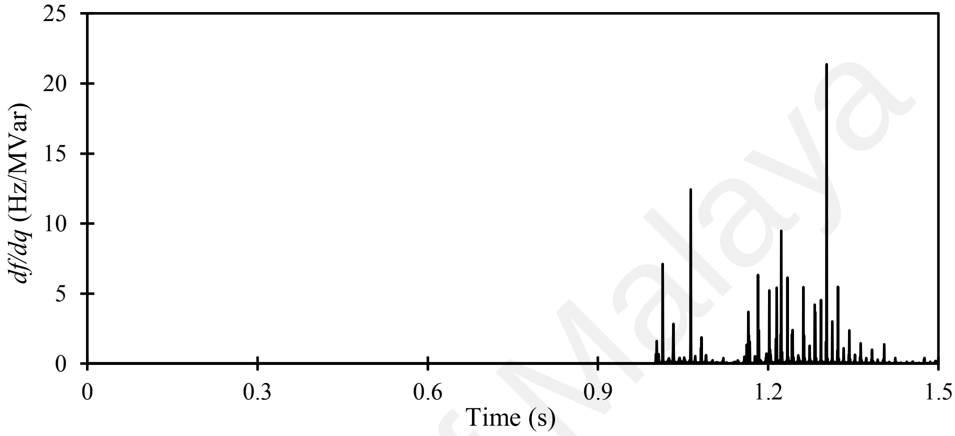

Figure A.1 *df/dq* response at load increment condition

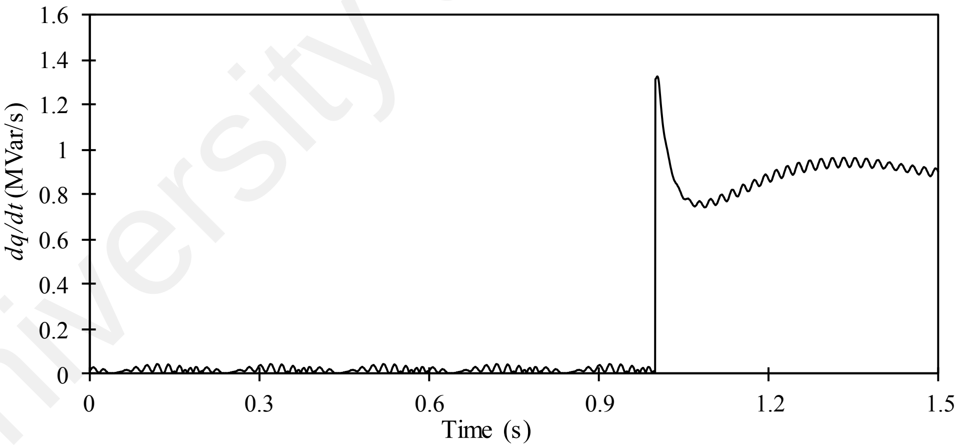

Figure A.2 *dq/dt* response at load increment condition

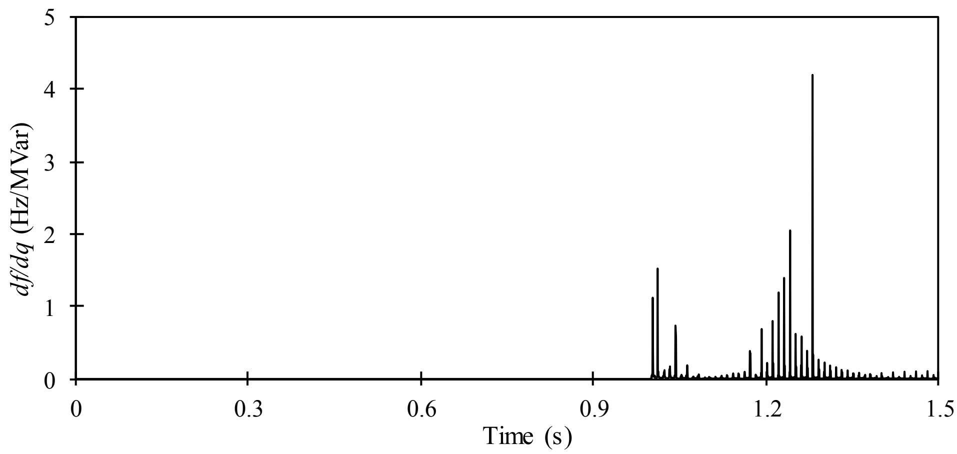

Figure A.3 *df/dq* response at load decrement condition

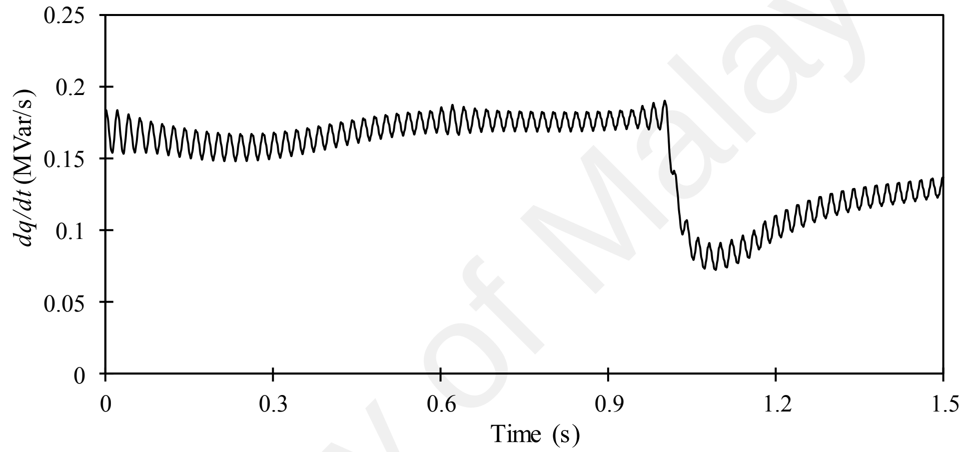

Figure A.4 *dq/dt* response at load decrement condition

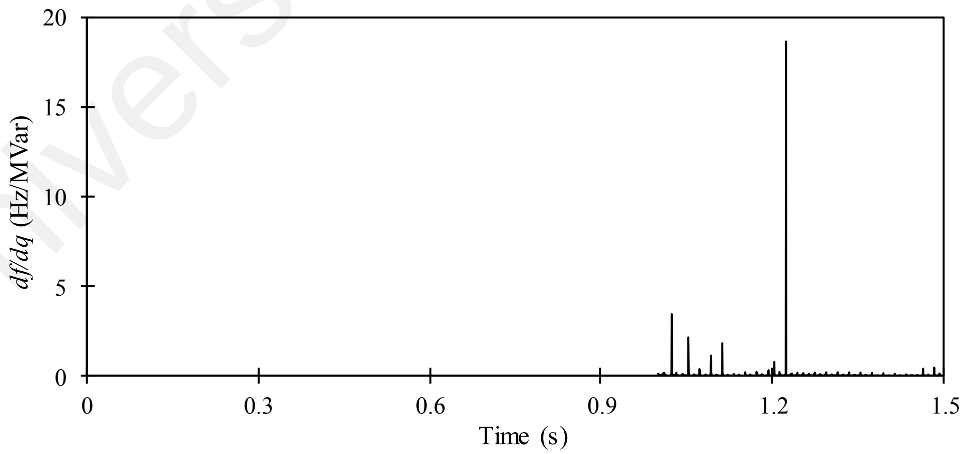

Figure A.5 *df/dq* response at capacitor connection condition

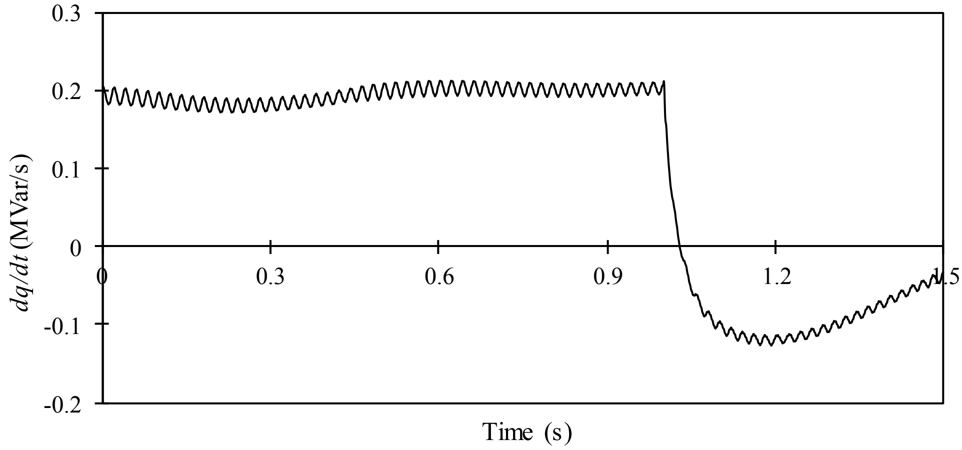

Figure A.6 *dq/dt* response at capacitor connection condition

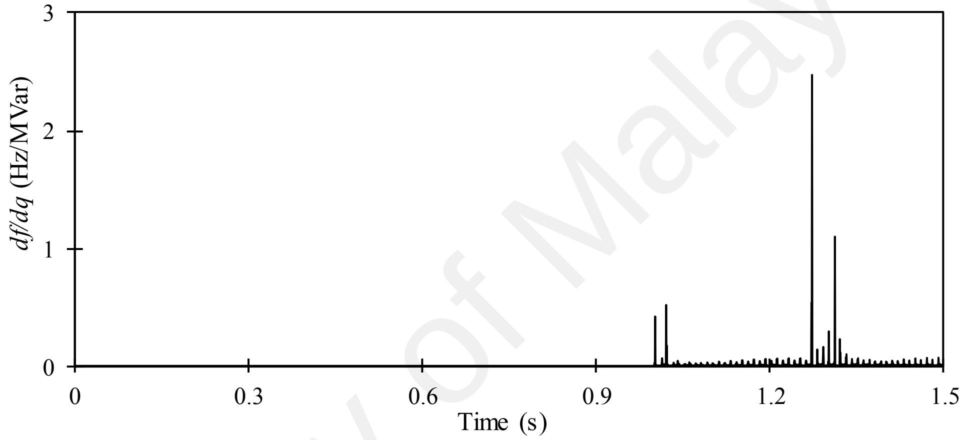

Figure A.7 *df/dq* response at capacitor disconnection condition

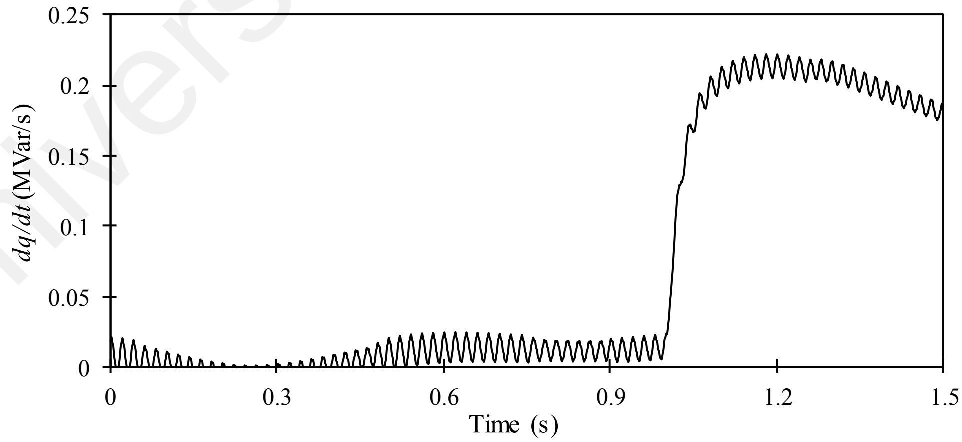

Figure A.8 *dq/dt* response at capacitor disconnection condition

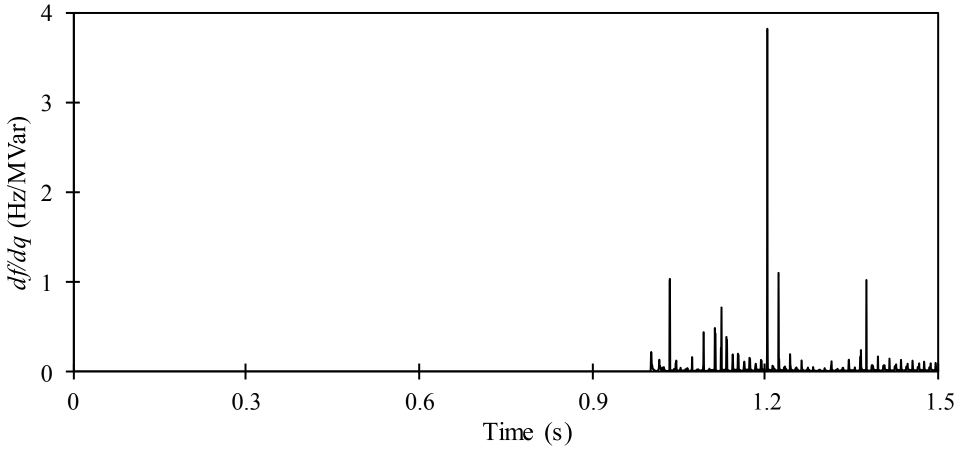

Figure A.9 *df/dq* response at induction motor starting condition

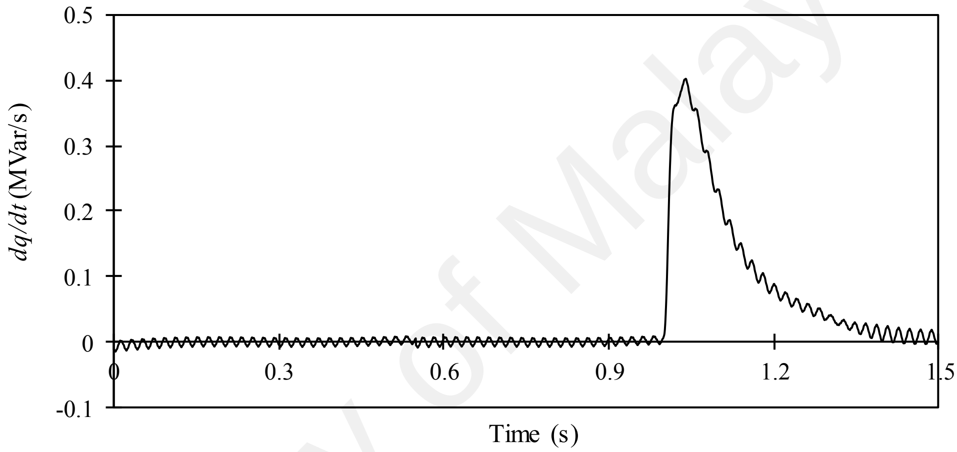

Figure A.10 *dq/dt* response at induction motor starting condition

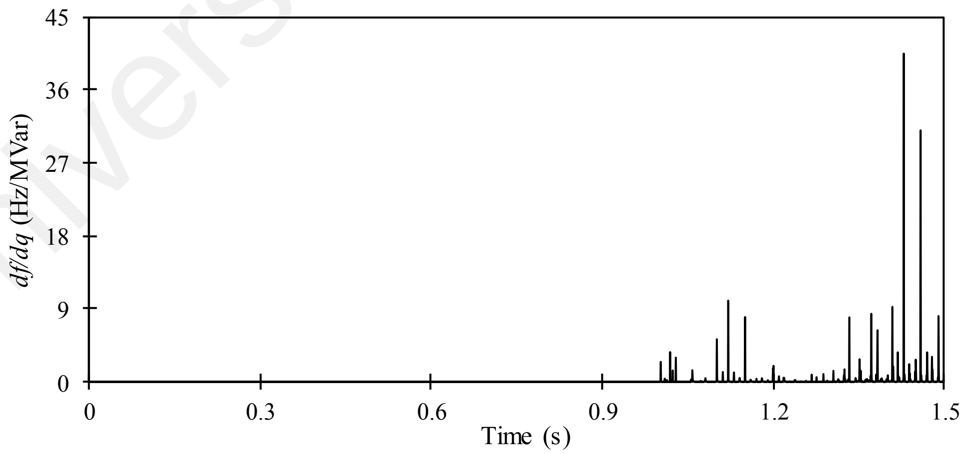

Figure A.11 *df/dq* response at single phase to ground fault condition

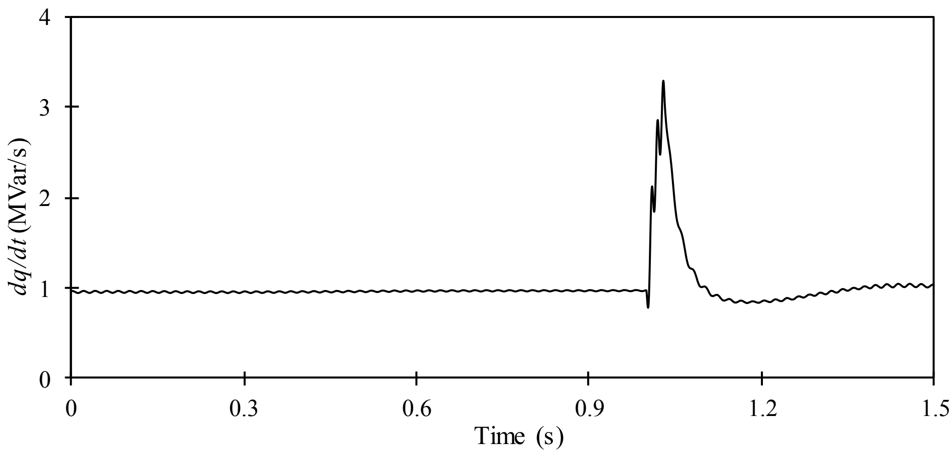

Figure A.12 *dq/dt* response at single phase to ground fault condition

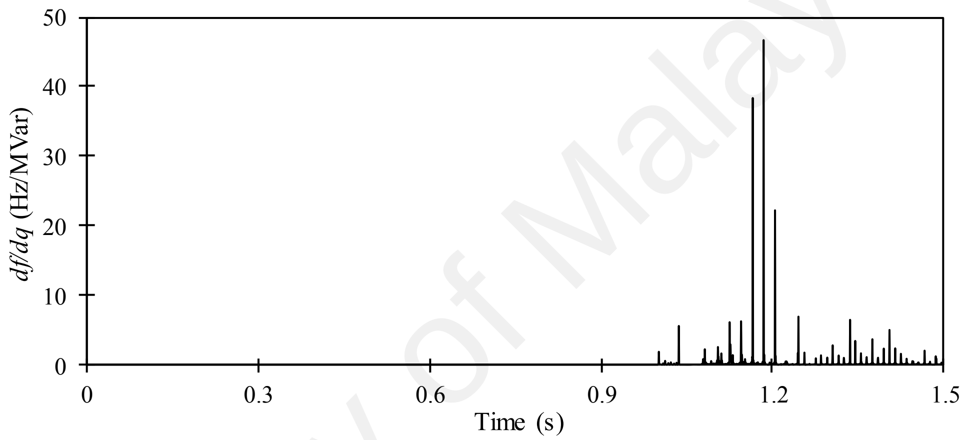

Figure A.13 *df/dq* response at double phase to ground fault condition

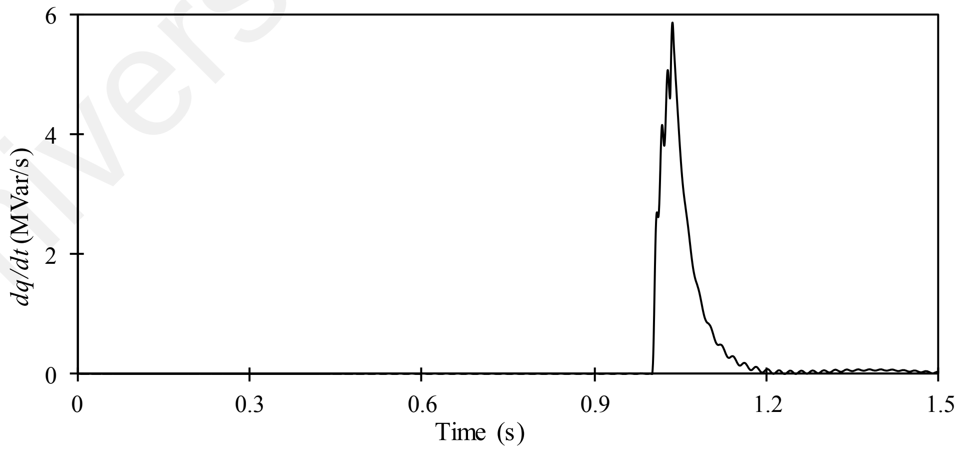

Figure A.14 *dq/dt* response at double phase to ground fault condition

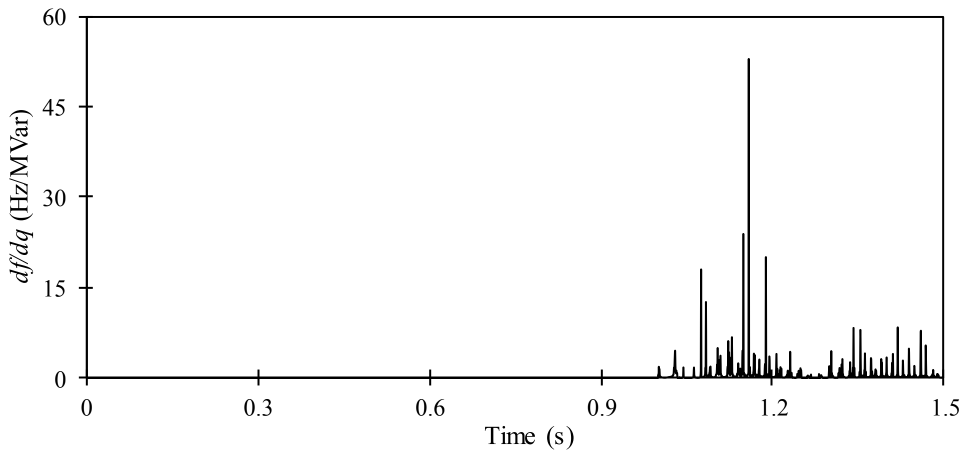

Figure A.15 *df/dq* response at three phase to ground fault condition

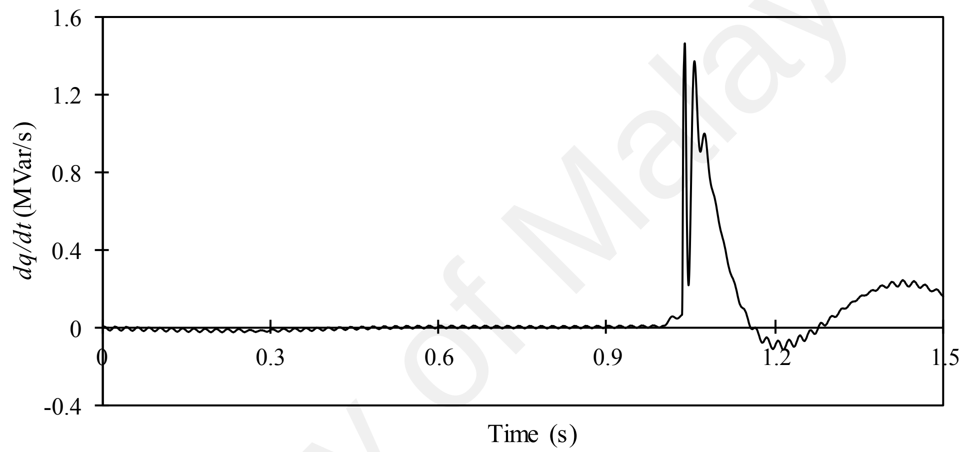

Figure A.16 *dq/dt* response at three phase to ground fault condition

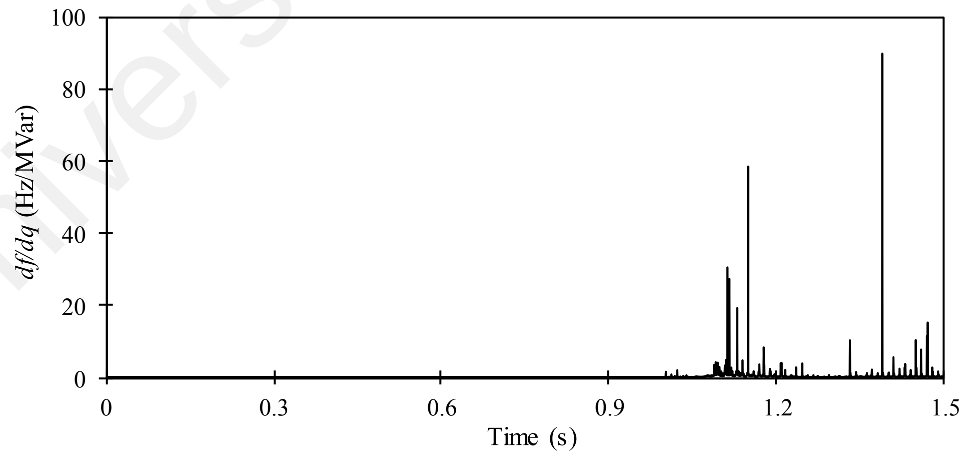

Figure A.17 *df/dq* response at phase to phase fault condition

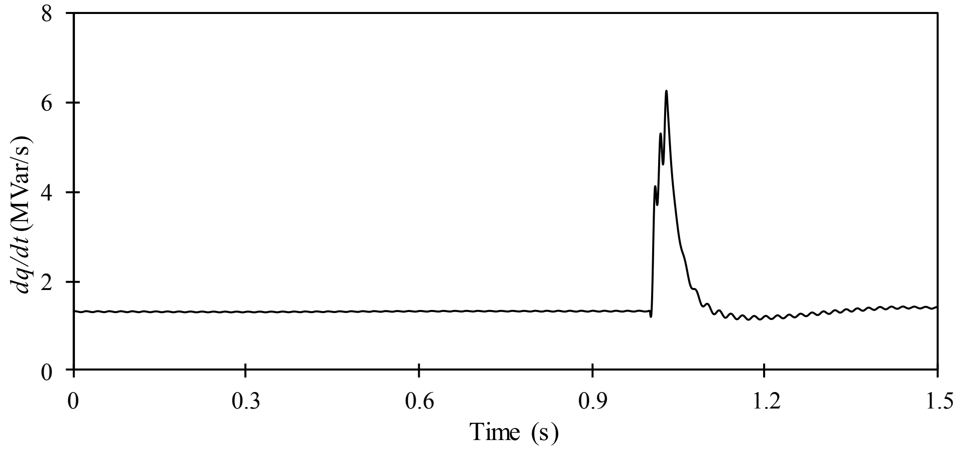

Figure A.18 *dq/dt* response at phase to phase fault condition

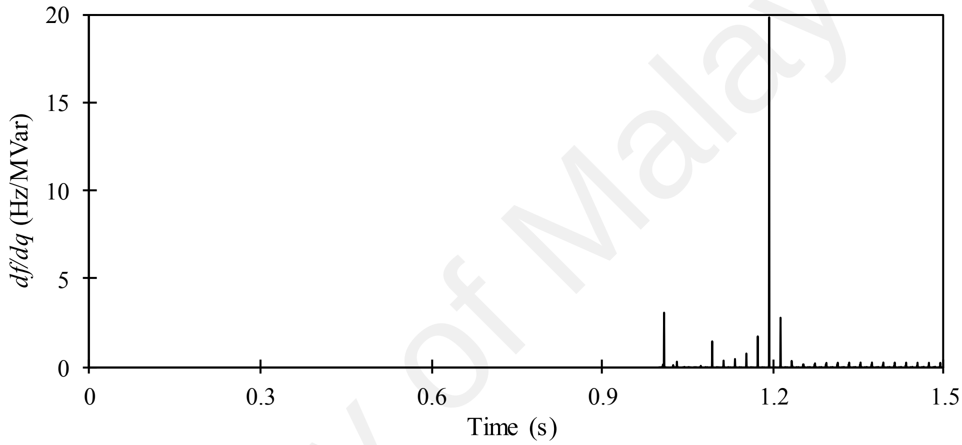

Figure A.19 *df/dq* response at induction generator tripping

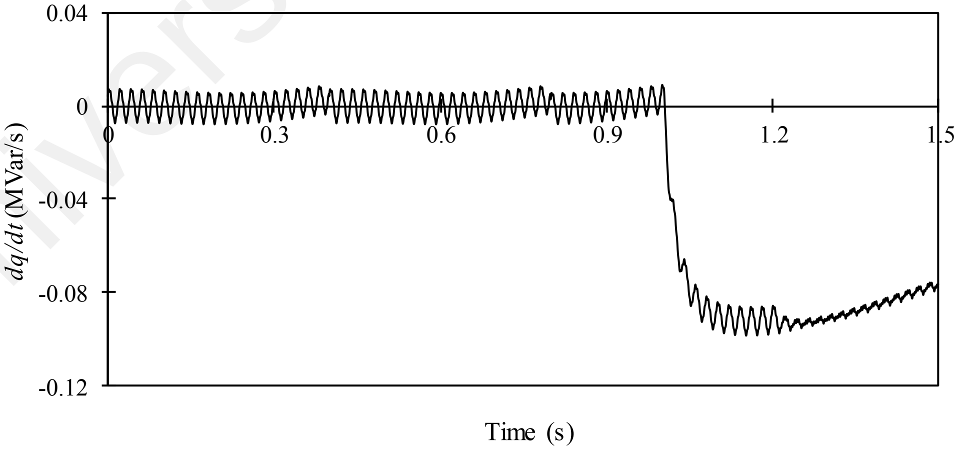

Figure A.20 *dq/dt* response at induction generator tripping